

Department of Biomedical Engineering

**Development of a Mobile Technology System to Measure
Shoulder Range of Motion**

By

Sara Francis Cameron (MSc, BSc)

This thesis is submitted in fulfilment of the requirements for the degree of Master of Philosophy in Biomedical Engineering

Copyright Statement

This thesis is the result of the author's original research. It has been composed by the author and has not been previously submitted for examination which has led to the award of a degree.

The copyright of this thesis belongs to the author under the terms of the United Kingdom Copyright Acts as qualified by University of Strathclyde Regulation 3.50.

Due acknowledgement must always be made of the use of any material contained in, or derived from, this thesis.

Signed:

Date:

Acknowledgements

Thank you to the Department of Biomedical Engineering for giving me the opportunity to learn and develop technical and research skills. I would also like to thank some research and technical staff from the department without whom this thesis would not have been possible. Matthew Banger for taking the time to show me the ropes in the Vicon lab and recording data with me, and to John Mclean for his help in conducting the initial characterisation of my application. Also, thanks to Stevie Murray and John Wilson from the workshop for their continuous support and efforts to manufacture the testing tools. I am extremely grateful to the students and staff who generously volunteered their time to be test subjects in this study.

Like many students, I have faced adversity throughout my studies which has negatively impacted my wellbeing. With new research highlighting the staggering statistics on mental health issues within postgraduate student populations, I am moved to speak up about my own experiences in the hope that others receive the help and support they need. Remember you are not alone: The Advice Hub is an incredible resource for students and can support you in many ways, particularly through supervision and departmental difficulties. I am very thankful to them for helping me to navigate difficult relationships that ultimately disadvantaged the potential of this research. They instilled my belief in myself even when my integrity was being challenged, and I am proud to submit this work as a result of my hard work, determination and perseverance despite the odds.

This journey has been a difficult and often overwhelming one and I am very lucky to have such supportive family and friends that have helped me along the way. Thanks to my mum for always believing in me and my abilities and to my wonderful partner in crime, Callum, who held my hand and made me laugh, even through the tough days.

Abstract

In patients with shoulder movement impairment, assessing and monitoring shoulder range of motion is important for determining the severity of impairments due to disease or injury and evaluating the effects of interventions. Current clinical methods of goniometry and visual estimation require an experienced user and suffer from low inter-rater reliability. More sophisticated techniques such as optical or electromagnetic motion capture exist but are expensive and restricted to a specialised laboratory environment.

Inertial measurement units (IMU), such as those within smartphones and smartwatches, show promise as tools bridge the gap between laboratory and clinical techniques and accurately measure shoulder range of motion during both clinic assessments and in daily life.

This study aims to develop an Android mobile application for both a smartphone and a smartwatch to assess shoulder range of motion.

Initial performance characterisation of the inertial sensing capabilities of both a smartwatch and smartphone running the application was conducted against an industrial inclinometer, free-swinging pendulum and custom-built servo-powered gimbal.

An initial validation study comparing the smartwatch application with a universal goniometer for shoulder ROM assessment was conducted with twenty healthy participants. An impaired condition was simulated by applying kinesiology tape across the participants shoulder girdle.

Agreement, intra and inter-day reliability were assessed in both the healthy and impaired states.

Both the phone and watch performed with acceptable accuracy and repeatability during static (within $\pm 1.1^\circ$) and dynamic conditions where it was strongly correlated to the pendulum and gimbal data (ICC > 0.9). Both devices could perform accurately within optimal responsiveness range of angular velocities compliant with humerus movement during activities of daily living (frequency response of $377^\circ/s$ and $358^\circ/s$ for the phone and watch respectively).

The concurrent agreement between the watch and the goniometer was high in both healthy and impaired states (ICC > 0.8) and between measurement days (ICC > 0.8). The mean absolute difference between the watch and the goniometer were within the accepted minimal clinically important difference for shoulder movement (5.11° to 10.58°).

The results show promise for the use of the developed Android application to be used as a goniometry tool for assessment of shoulder ROM. However, the limits of agreement across all the tests fell out with the acceptable margin and further investigation is required to determine validity. Evaluation of validity in clinical impairment patients is also required to assess the feasibility of the use of the application in clinical practice.

Contents

Copyright Statement	
Abstract.....	ii
Contents	1
Chapter 1.....	9
Introduction.....	9
1 Literature Review	14
1.1 Human Biomechanics	14
1.2 Motion Analysis Techniques	15
1.2.1 Video Techniques	16
1.2.2 Optoelectronic Techniques	17
1.2.3 Electromagnetic Techniques.....	20
1.3 Range of Motion Measurements in a Clinical Setting	22
1.3.1 Goniometer	22
1.3.2 Digital Inclinometers	24
1.3.3 Visual Estimation.....	25
1.3.4 Patient-Reported Questionnaires	25
1.3.5 Limitations of laboratory-based and clinical evaluations of joint range of motion.....	27
1.4 Wearable sensors	28
1.4.1 Accelerometers	29
1.4.2 Gyroscopes	30
1.4.3 Magnetometers	30
1.4.4 Sensor Fusion.....	31
1.5 Mobile technology for kinematic measurements	35
1.5.1 Smartphone goniometry.....	37
1.6 Aims and Objectives	42
Chapter 2.....	45
2 Overview of Shoulder Kinematics and Methods of Describing Joint Range of Motion	45
2.1 Kinematics	45
2.2 Bony Anatomy	46
2.2.1 The Thoracic cage and vertebral column.....	46
2.2.2 The Pectoral Girdle	48
2.2.3 The Humerus.....	50
2.3 Anatomical Coordinate System.....	51

2.3.1	Thorax Anatomical Coordinate System	52
2.3.2	Humerus anatomical coordinate system	53
2.4	Position and Orientation.....	54
2.4.1	Position.....	54
2.4.2	Orientation	55
Chapter 3	73
3	Development of Android Application	73
3.1	Introduction to Smartphone Technology	73
3.1.1	Use of Smartphones	73
3.2	Operating Systems.....	74
3.3	Smartphone Inertial Sensors.....	75
3.3.1	Sensor Coordinate system.....	75
3.3.2	Hardware Sensors	76
3.3.3	Sensor Fusion	77
3.3.4	Software Sensors	78
3.4	Smart Devices used in this work	80
3.5	Development of Android Application	81
3.5.1	Key features of the application.....	81
3.5.2	Development Environment.....	82
3.5.3	Graphical User Interface	82
3.5.4	Sensor Delay Rate	83
3.5.5	Storage of recorded rotation vector data.....	84
3.5.6	Transfer of data to a PC for post-processing.....	86
3.6	Post-processing to obtain 3-dimensional angles from rotation vector data.....	86
Chapter 4: Performance	88
Measure Angular Data	88
4.1	Static Protocol.....	89
4.2	Dynamic movement Protocol	91
4.2.1	Free-Swinging Pendulum	91
4.3	A servo-powered gimbal system	94
4.3.1	Development and design	94
4.3.2	Frequency response	99
4.3.3	Continuous measurements over a 3-hour period.....	99
4.3.4	Post-processing and data analysis	100

4.4 Results	100
4.4.1 Static Measurements.....	100
4.4.2 Free-swinging pendulum	104
4.4.3 Servo-powered gimbal system.....	108
4.5 Discussion	113
4.5.1 Static measurements.....	114
4.5.2 Free-swinging Pendulum	115
4.5.3 Servo-powered Gimbal	116
4.5.4 Continuous Measurement	117
Chapter 5: Concurrent Validity and Repeatability compared to a Universal Goniometer for Clinical Range of Motion Measurements	119
5.1 Introduction.....	120
5.2 Materials and Methods	120
5.2.1 Ethics	120
5.2.2 Subjects.....	120
5.2.3 Materials	122
5.2.4 Planar movements in clinical examination.....	124
5.2.5 Data acquisition and pre-processing.....	127
5.2.6 Sensitivity to change in an impaired condition.....	127
5.3 Data Analysis.....	128
5.3.1 Computation of shoulder goniometric data	129
5.4 Statistical Analysis	131
5.4.1 Concurrent Validity	132
5.4.2 Between day intra-rater reliability	133
5.5 Results	134
5.5.1 Concurrent Validity	134
5.5.2 Reliability.....	136
5.6 Discussion.....	137
Chapter 6.....	141
6 Discussion.....	141
6.1 Methods of Describing Shoulder Kinematics	141
6.2 System Development	142
6.2.1 Devices	142
6.2.2 Validation Protocol	142
6.2.3 Application	147

6.3 Concurrent Validity and Repeatability for Clinical Goniometry	148
6.4 Future Work	151
References.....	154
Appendix 1.....	168
2	173
Appendix 2.....	173
Appendix 3.....	174

List of Figures

Figure 2. 1 Bony Anatomy of the Thorax	46
Figure 2. 2 Bony Anatomy of the Scapula and Clavicle	48
Figure 2. 3 Bony Anatomy of the Humerus	50
Figure 2. 4 Anatomical planes of the human body	52
Figure 2. 5 Anatomical coordinate systems for the thorax and the humerus	52
Figure 2. 6 Position of point p in the global coordinate system, G	55
Figure 2. 7 Orientation of frame A with respect to the global frame, G, showing the direction angles of YA, with respect to the three coordinate axes of the global frame	56
Figure 2. 8 Orientation of frame B with respect to frame A	57
Figure 2. 9 Definition of thoraco-humeral rotations (Wu et al., 2005)	62
Figure 2. 10 Visualisation of spherical coordinate system using altitude (latitude) and azimuth (longitude) to describe the position of a point on the surface of a sphere/globe	68
Figure 2. 11 Relationship between V1 and V2 in terms of Azimuth and Altitude... ..	68
Figure 2. 12 Humerus vector projected onto globe with centre at the centre of rotation of the shoulder in a) The anatomical position and b) 90° abduction	70
Figure 3. 1 Local coordinate system of an Android smartphone	75
Figure 3. 2 World, North-East-Up Coordinate frame	78
Figure 3. 3 a) Sony Xperia Z3 Compact b) Samsung Galaxy SIII	80
Figure 3. 4 LG Urbane Smartwatch	81
Figure 3. 6 Graphical User Interface of Smartwatch Application showing interactions between each screen.	83
Figure 3. 5 Graphical User Interface of Smartphone Application and interactions between each screen.	83
Figure 3. 7 File line format	84
Figure 4. 1 Bosch GAM 270 MFL Professional Angle measurer with smartphone attached in three orientation to measure a) rotation about pitch axis, b) rotation about roll axis, c) rotation about yaw axis	90
Figure 4. 2 Free-swinging pendulum with smartphone attached in three orientations to measure a) rotation about yaw axis, b) rotation about pitch axis, c) rotation about roll axis	92
Figure 4. 3 Calibration curve of low friction potentiometer of varying pendulum arm angular displacement from -90° - +90°.	93
Figure 4. 4 Metal gear servos used. All dimensions in inches. Pictures from HiTec	96
Figure 4. 5 Set up of servo-powered gimbal system	97
Figure 4. 6 Dimensions and design of aluminium frame, tilt table and plastic servo-housing	98
Figure 4. 7 Offset from known zero position reported by each device. Yaw values have been normalised to a 0° reference for interpretation	101

Figure 4. 8 Angles reported by smartphone and smartwatch in 20° steps in a) pitch, b) roll and c) yaw axes. 103

Figure 4. 9 Example from 1 trial of angle (°) recorded by the smartphone compared to the potentiometer during free-swinging pendulum movement in a) orientation A (pitch), b) orientation B (roll), and c) orientation C (yaw) 105

Figure 4. 10 Non-sensitive (roll and yaw) axes during free-swing of pendulum with smartphone in orientation A 107

Figure 4. 11 Frequency response of smartphone in a) pitch axis and b) roll axis... 108

Figure 4. 12 Frequency response of smartphone in a) pitch axis and b) roll axis... 110

Figure 4. 13 Smartphone angular data compared to servo-feedback at 0.68 and 1Hz sinusoidal wave frequency in the a) pitch and b) roll axes at (i) time point 1 and (ii) time point 12. 112

Figure 4. 14 Smartwatch angular data compared to servo-feedback at 0.68 and 1Hz sinusoidal wave frequency in the a) pitch and b) roll axes at (i) time point 1 and (ii) time point 12. 113

List of Tables

Table 2.2 Anatomical reference frame definitions for the thorax and the humerus..	54
Table 4.1 Mean angle and standard deviations of angles (in degrees) reported by each device in a known zero position of the Bosch measurer tool. One-way ANOVA test was used to determine if differed from the Bosch tool reference significantly. *p<0.05	101
Table 4.2 (Mean) Relative orientation in degrees (and standard deviations) reported between each 20° step by each device tested. One-way ANOVA test was used to determine if differed from the Bosch tool reference significantly. *p<0.05	102
Table 4.3 Correlation values between potentiometer and smartphone data for free-swing pendulum movement.	106
Table 4.4 (a) correlation values for non-sensitive axes in orientation A, (b) orientation B, (c) orientation C.	106
Table 4.5 Average amplitude and standard deviations of amplitude (°) recorded by smartphone in pitch and roll axes at each frequency tested.	109
Table 4.6 Average amplitude and standard deviations of amplitude (°) recorded by smartwatch in pitch and roll axes at each frequency tested.	110
Table 4.7 Mean amplitude and standard deviations of smartphone and smartwatch for both frequencies across all 12 sampled time-points.	111
Table 5.1 Subject demographic data	121
Table 5.2 Mean Oxford Shoulder Scores for the study cohort	122
Table 5.3 Alignment of goniometer to anatomical landmarks for each planar movement assessed	126
Table 5.4 Comparison of SW and UG measurements in the Healthy condition	135
Table 5.5 Comparison of SW and UG measurements in impaired condition	136
Table 5.6 Between day reliability for UG and SW measurements	136

Chapter 1: Introduction and Literature Review

Chapter 1

Introduction

The upper limb is an essential appendage of human anatomy: it allows us to carry out many of the tasks of daily living such as feeding, dressing, toileting, grooming and carrying. The shoulder joint is a complex structure which forms the proximal part of the upper limbs kinematic chain and works in coordination with the distal elbow and wrist to position the hand in space. It is the most mobile joint in the body and represents a technical challenge in defining both normal and pathological function. Patients with impairment or restriction of the shoulder joint often encounter problems when interacting with their environment and find it difficult to carry out everyday tasks. This can result in a loss of independence and a decreased quality of life. It is therefore an important clinical goal to restore function as much as possible. Furthermore, in patients with shoulder movement impairment, accurately assessing and monitoring shoulder kinematics is beneficial for determining the useful operational range for assistive devices, the severity of impairments due to disease or injury, and for evaluating the effects of interventions. Determination of range of motion (ROM) is a primary outcome measure for upper limb rehabilitation and is typically measured in a clinical setting by goniometry, visual estimation, or subjective patient questionnaires. Goniometry is the most widely used clinical method of measuring joint ROM (Hayes et al., 2001; Mullaney et al., 2010). Whilst it benefits from being quick and easy to apply, it has been found to suffer from low inter-rater reliability (Riddle et al., 1987), particularly for shoulder measurements (de Winter et al., 2004). Visual estimation is an equipment

free alternative, which when conducted by an experience clinician, shows intra-rater reliability comparable to a mechanical goniometer (Williams and Callaghan,1990). But, reliability of repeated measures is low in some patients groups, particularly those with higher pain and disability severity (Terwee et al., 2005).

Questionnaires such as the Oxford Shoulder Score (Dawson et al., 1996), which evaluate pain and functional ability, have been shown to be useful in diagnostics and in assessing surgical outcomes (Roy et al., 2009). However, this method is limited in that the questionnaires don't allow for comparison between patients since the pain experienced is subjective. They rely largely on the experience and judgment of the clinician and may not be a true representation of the patients everyday joint function. More sophisticated methods such as optical motion capture can be used to measure 3-dimensional shoulder ROM. They can record highly accurate 3D-positional information, with errors of less than 1mm recorded (Merriaux et al., 2017). However, these techniques have many drawbacks including the requirement for expensive, specialised laboratory equipment which isn't readily available in common clinical practice.

There is therefore a need for a method of quantifying shoulder ROM which encompasses qualities of all of the above to create a system that is simple and cost-effective yet accurate, and can be readily applied in both clinical and remote environments.

The advent of miniature inertial sensors such as accelerometers, gyroscopes and magnetometers, has provided a promising alternative to marker-tracker systems for use outside of the dedicated laboratory environment. Such sensors may also open up

the possibility of monitoring individuals in their usual environment with minimal interference (Coley et al., 2007).

Over recent years, the rapid advances in smartphone-based inertial sensing technology have led to the implementation of smartphones as clinical tools for measuring joint kinematics (Milani et al., 2014; Cuesta- Vargas et al., 2016). As well as providing healthcare professionals with an accurate and reliable tool to obtain shoulder ROM measurements, mobile technology applications may facilitate remote monitoring and tele-rehabilitation for patients (Ongvisatepaiboon et al., 2015).

A number of low-cost mobile technology applications which utilise the embedded MEMS inertial sensors have been developed to assess joint goniometry, providing accurate, immediately available and easily interpretable, real-time measurements (Cuesta-Vargas et al., 2016; Vohralik et al., 2015). Such applications exploit the native sensor fusion software to estimate orientation from the physical sensors. Despite the increased interest in the use of smartphones to monitor upper limb ROM, little is known about the performance of these sensor units under conditions representative of upper limb motion. Mourcou et al (2015) reported on the performance of different smartphones and sensor fusion approaches compared to a robotic arm during dynamic movement at different speeds. The performance of the iPhone 4 (Apple Inc., USA) position sensors was evaluated by (Kos et al., 2016) who highlighted the importance of gaining an understanding of the capabilities of individual smartphone parameters for use in human motion analysis.

This showed promise that such mobile technology could be used to address the current lack of objective data describing ROM during daily life. The more recent

evolution of Android Wear technology provides an extension to the handheld mobile device in the form of a smartwatch. Such devices retain many key features of the modern day smartphone including inbuilt inertial sensors, advanced connectivity and user interaction systems. Bluetooth technology facilitates continuous real-time data exchange between the watch and paired smartphone devices. To the best of our knowledge, no studies to date have reported on the use of Wear technology to measure human joint kinematics.

The aim of the work outlined in this thesis, was to develop an Android application for both a smartphone and a smartwatch, that could be implemented in dynamic 3-dimensional goniometry measurements of the shoulder. A characterisation of the accuracy and precision of the mobile and smartwatch sensors under different conditions relating to how the arm is moved in daily life was conducted. This was to investigate whether the application could be used to reliably monitor 3D rotation over a prolonged period, thus serving as an indicator of whether shoulder ROM could be monitored over time in a home environment. Following these tests, an agreement and reliability comparison to a universal goniometer for measuring shoulder ROM was made in twenty healthy participants.

This thesis describes the development and initial testing of a novel mobile system to record shoulder range of motion. Chapter 2 provides a review of the current state of clinical and research laboratory assessment of shoulder kinematics, and an overview of kinematic sensors and mobile technology and their use in human motion measurements. Chapter 3 gives an overview of the theoretical mathematical representation and techniques used to compute 3-dimensional upper limb joint

kinematics and details the mathematical methods used in this thesis. Chapter 4 presents the development of the inertial sensor-based mobile application and Chapter 5 details its preliminary characterisation testing. This is followed in Chapter 6 by findings of the experimental work to compare the output of the mobile application and ‘Gold Standard’ goniometry. Chapter 7 discusses the main findings and recommendations for further work.

1 Literature Review

1.1 Human Biomechanics

Human biomechanics is the study of movement of the human body and has been a subject of interest for centuries. Scientists continuously seek to improve performance of the body and establish methods of diagnosis, rehabilitation and prevention from injury through a better understanding of human movement. Today, motion capture is used across a broad variety of disciplines ranging from digital animation and robotics to biomechanical analysis for sporting performance. One of the most important applications of motion analysis is in a clinical environment where it can be used to quantitatively assess musculoskeletal function and rehabilitation progress to inform clinical decision making and treatment pathways, as well as in the design planning of prosthetics and orthotics (Robertson et al., 2014).

Two branches of biomechanics are commonly studied: kinematics and kinetics. The work in this thesis will focus on the study of kinematics. Kinematics describes the overall motion of the body without consideration of the causes of motion (Wong et al., 2015) and aims to quantify properties of the human joints, such as angular velocity, acceleration and joint angles. Kinematic measurements are widely used by both researchers and clinicians to quantify normal and pathological movements, evaluate the degree of impairment, make clinical decisions and assess the effect of various interventions (Cuesta-Vargas et al., 2010).

This thesis focuses on the use of motion analysis to provide a quantitative measure of function to inform clinical decision making and monitor rehabilitative interventions of the upper limb, specifically the shoulder.

Unlike the cyclic movement pattern of gait, the upper limb is involved in a number of complex movements and a range of different limb trajectories to facilitate the completion of activities of daily living. Quantifying these motions has proven difficult since the upper limb offers many degrees of freedom, movement across multiple joints and a wide range of motion. The shoulder complex in particular presents difficulties in kinematic measurements due to its large range of motion in 3 dimensional planes. In contrast to the hinge-like motion of the knee joint for example, the movement of the shoulder is facilitated largely by the glenohumeral joint, a relatively unstable ball and socket joint capable of smooth and continuous rotation through multiple planes to perform a single movement task. Furthermore, it suffers from ambiguity in movement patterns such as the well-known Codemans Paradox. This refers to a specific pattern of 3D movement of the shoulder in which axial rotation about the longitudinal axis of the arm occurs during two or three sequential humerus rotations that did not involve rotation about the long-axis.

1.2 Motion Analysis Techniques

Various methods have been employed to study upper limb kinematics from simple mechanical techniques such as a goniometer to more complex tracking techniques such as optical motion tracking systems and most recently, wearable inertial sensors. The underlying principles of the motion tracking systems discussed in this work consider the human body to be an assemblage of non-deformable, rigid segments connected by moveable joints. As such, the defined segment embedded coordinate system enables the position and orientation of the segment to be described in relation

to both a global reference frame and to adjacent segments throughout each frame of movement. These principles will be described in relevant detail in chapter 2.

1.2.1 Video Techniques

Stereophotogrammetry video methods involve estimating the 2 or 3-dimensional coordinates of body segments using visual recordings taken from different positions by multiple cameras. Movement can be recorded with or without the use of anatomical landmark markers fixed on the subject's skin. A high contrast between the markers and the capture background must be maintained with this technique as lighting conditions of the environment often lead to errors (Murray et al., 1999). Manual intervention by an operator is commonly required if obstruction of the field of vision of a camera during a series of frames prevents the marker location being recorded, however this is a time-consuming process, particularly for 3D data (Murray, 1999).

Although attractive due to its reduced set-up time and elimination of movement restriction due to marker locations, marker-less video techniques used in clinical assessment and research are generally reported to be less accurate than marker-based techniques. Marker-less motion capture is based entirely on computer algorithms for pattern recognition, which require extensive computational resources (Mundermann et al., 2006).

Limitations of video motion capture include an intensive period of post-processing, preventing its use in real-time analysis. Furthermore, such systems and their associated software require a specialised laboratory environment set-up, preventing their use as a motion capture tool in a day-to-day clinic setting and as a portable tool for monitoring human motion in a natural setting.

Video motion capture has been used in upper limb studies to quantify shoulder and elbow kinetics and kinematics during daily life tasks (Peterson and Palmerud, 1996; Murray and Johnson, 2004) and is one of the main methods currently used in sport biomechanical analysis (Bartlett, 2007). From these studies, it is clear that the complexity of upper limb movements allows redundancy, meaning there is an ability to adopt different kinematic strategies to achieve the same end goal (Buckley et al., 1996). This should be kept in mind when evaluating movement patterns of the upper limb, particularly in impaired populations where completion of a task may be more likely to induce a compensation for restricted movement by an alternative strategy.

1.2.2 Optoelectronic Techniques

Developed as an alternative to photogrammetry, this technique is based on the detection of 3D-body mounted markers by multiple infrared cameras using pulsed-light emitting diodes (LEDs). Markers are attached to relevant body segments and can be either active (light-emitting) or passive (reflective). Individual markers are identified automatically by software pattern recognition or hardware algorithms, similarly to automated digitisation of video techniques.

Stereometric techniques are used to correlate common tracking points on the tracked markers in each image frame, and the marker positions can be determined with knowledge of the calibrated relationship between the capture volume dimensions, camera parameters and the relationship of the cameras to each other. Optoelectronic systems combine sophisticated software packages with the complex camera set up to facilitate the operation of the system. This can include calibration steps, collection of

data and processing of raw image data as well as the 3D reconstruction of landmarks and data filtering and smoothing.

Passive systems (such as the VICON) are characterised by a ring of LEDs around the lens of each camera, coupled with infrared-pass filters placed over the camera lens itself. The LEDs produce a pulsed infrared light emission enabling the cameras to measure the light reflected by the body mounted, reflective markers. The Vicon system (VICON, Oxford) is currently the most widely used system of this kind and is accepted as a practical gold standard optical motion capture system. It requires a minimum of three reflective markers per segment for reconstruction of rigid body movements and its application is relatively quick and easy due to its user-friendly interface and comprehensive software package. The Vicon system has been employed for numerous studies of upper limb kinematics (Haering et al., 2014; Henmi et al., 2006; Rosen et al., 2005) and is often used in validation protocols for newly developed technologies (Luinge et al., 2007; Fernandez y Baena et al., 2012).

Active systems use multiple LED markers that are attached to relevant anatomical landmarks. Each LED marker fire sequential pulses of infrared light at microsecond time intervals such that only one LED is activated in a given time interval. The emitted infrared light is detected by multiple cameras calibrated to the central capture volume. Whilst these systems make marker identification easier, they are very sensitive to light reflections on neighbouring surfaces which can lead to identification and reconstruction errors, and invalid data. The active markers require a constant power supply, tethering the individual and this may cause some restriction in their movement. Modern active systems such as the Optotrak system (Northern Digital Inc., USA) overcome issues of tethering with user-worn, battery-powered

LEDs (Welch and Foxlin, 2002). Such active systems can produce real-time motion analysis and have been used in clinical settings to investigate upper limb kinematics (Levanon et al., 2010; Hebert, 2000; van Andel, 2008).

Whilst Optoelectronic systems can provide very accurate position information (Merriaux et al., 2017), they suffer from some important shortcomings. These include marker occlusion and interference from external light sources which may occur particularly in complex upper limb motion recording where markers can become obscured by other body parts. Reflective materials within the capture space can create so called “ghost-markers”, resulting in the need for manual identification of markers or extrapolation of marker trajectories to calculate marker locations. An intensive post-processing period by a trained operator and a high level of expertise is required to facilitate the complex manipulation of data and interpretation of the results (Wong et al., 2007). Furthermore, they are costly and require a specialised laboratory environment with fixed equipment, impeding their implementation into routine clinical practice to assess a patients functional capabilities for making quick clinical decision and evaluating the effects of interventions. The artificial laboratory environment within which these systems can operate significantly and simulation of tasks, limits understanding of upper limb kinematic patterns during everyday life in a subjects natural or home environment. Typical optical motion capture techniques rely on physical markers placed on the subjects’ skin or clothes. The process of marker placement is both time-consuming and requires experience to ensure proper placement for the most accurate joint centre estimation.

Developments in markerless motion capture systems such as the Kinect (1st and 2nd generation, Microsoft, USA) may avoid some of these issues. The Kinect utilises a

built-in tracking algorithm and a depth camera composed of an infrared laser projector and a regular colour camera to detect a skeleton based on pattern recognition methods (Bonnechère et al., 2014). Whilst developed for the purpose of a gaming interface for consumer use, its motion capture technology has been more cost-effective, easier to set up and takes up less space than conventional systems, thus increasing its overall usability in a clinical setting. Studies comparing the Kinect to conventional motion capture have thus far shown good reliability and potential for clinical applications but show some limitation in accuracy, particularly in sagittal plane movements (Li et al., 2014; Clark et al., 2012; Cancela et al., 2014). The between day reliability of the Kinect 2 (released in 2014), to measure shoulder range of motion was recently investigated (Reither et al., 2018). Absolute range of motion measurements for the Kinect was different from the motion capture system however there was high correlation between patterns of motion detected.

1.2.3 Electromagnetic Techniques

Electromagnetic systems consist of a source that emits an electromagnetic field, which is used to determine the location and orientation of sensors. They operate via the generation of three orthogonal electromagnetic fields from a source transmitter. 3D sensors attached to body segments measure the field strength proportional to the distance of each of the three coils from the field emitter assembly. The 3D-position and orientation of the body-worn sensors can be determined relative to a stationary unit and raw data from the receivers can be used to generate meaningful interpretations using computer software (Jordan et al., 2001). The different models of electromagnetic systems vary in the number of receivers (typically 2-4), range of operation (1.5-3 metres) and update latency. Two major manufacturers are Ascension

Technology (USA) with the Flock of Birds system and Polhemus (USA) with the ISOTRAK and FASTRAK systems.

Such a system has been shown to be highly reliable and accurate (Cuesta-Vargas et al., 2010). These systems don't suffer from the line of sight issues associated with optical systems and are capable of producing dynamic and real-time kinematic information. Although the user-worn sensors are small and unrestrictive to the subjects' movements, they are limited in range and sensitivity to magnetically permeable materials which may be particularly problematic in an uncontrolled clinic setting (Anglin and Wyss, 2000). A similarly high level of expertise as for optical techniques is required for electromagnetic systems. Whilst the requirement of these systems for a consistent computer connection presents benefits such as immediate data storage and retrieval during follow-up sessions, this also presents practicality difficulties for their use in daily clinical practice.

Kinematic assessments of the lumbar spine (van Herp et al., 2000), cervical range of motion (Jordan, 2000) and shoulder complex (Borstad and Ludewig, 2002; Roren et al., 2012) are among various biomechanical investigations using electromagnetic techniques. Namdari et al (2012) found that to successfully perform functional tasks, the range of motion required was significantly less than the anatomical range of motion of the shoulder complex, a finding that is consistent with others (Gates et al., 2015; Magermans et al., 2005). This information may have significant implications for rehabilitation goals and the design of optimal shoulder prosthetics.

1.3 Range of Motion Measurements in a Clinical Setting

Clinical measurement of joint range of motion is a fundamental evaluation procedure in rehabilitation and is the most widely used assessment of function by clinicians and therapists for clinical decision making.

Several methods have been developed to measure joint range of motion in a clinical setting such as visual estimation, goniometry, photography and self-reported questionnaires. Measurements are usually used to assess limitations in range of motion to determine appropriate interventions and document treatment progression (Mullaney et al., 2010). High reproducibility, sensitivity to change and inter-rater reliability are important in assessing the quality of such clinical measurements to produce meaningful, clinically relevant outcomes to assess shoulder function. The methods and types of assessments vary among different clinicians and institutions based on a variety of factors including time available, availability of equipment and the specific movement or pathology being assessed.

1.3.1 Goniometer

Manual goniometry is currently the most widely used clinical method of measuring joint range of motion (Hayes et al., 2001; Mullaney et al., 2010). Goniometers are inexpensive mechanical measurement devices which can be used to manually measure the angle between two body segments. The most basic is a universal goniometer which is commonly used in a clinical setting to measure active or passive joint range of motion. This device consists of a plastic or metal protractor-like device with two arms of varying length. The arms are aligned to the relevant body segments to facilitate joint angle estimation using the central protractor placed approximately over the joint centre. For example, in the measurement of shoulder flexion range of

motion, the goniometer arm could be aligned to the midline between the lateral epicondyle and the middle of the glenoid fossa in the sagittal plane. Numerous studies have investigated the reliability of goniometry for both active and passive range of motion measurements. Boone et al (1978) found the intra-rater and inter-rater reliability of active range of motion taken on the upper extremities in healthy subjects to be high ($r=0.89$ and $r=0.86$ respectively). However, in a study comparing two different sized goniometers to measure passive shoulder range of motion, the inter-rater reliability was variable across different movement planes (0.26-0.89). Intra-rater reliability was high (0.94-0.98) indicating that measurements are reliable when performed by the same therapist or clinician (Riddle et al., 1987).

The degree of error has been shown to increase in shoulders with decreased mobility (de Winter et al., 2004).

Although goniometers are popular due to their portability and low cost, they have several practical limitations associated with their use. They must be attached or placed across a joint to align exactly with the centre of rotation of the joint and the axes of rotation. This is particularly difficult to achieve at ball and socket joints such as the shoulder which have multiple axes of rotation. Measurement requires the assessor to use both hands, making stabilisation of the extremity difficult. It may also be difficult to keep the reference arm of the goniometer stationary whilst the joint is rotated and difficult to read at the end range of motion. Removal of the goniometer from the joint at this stage to read the value may introduce unintended movement of the goniometer and increase the risk of measurement error (Gajdosik and Bohannon, 1987). Tape measures and goniometers provide information in single planes and only for static positions. As such, their assessment cannot contribute to our understanding

of the movement path or velocity of the humerus during elevation or rotation tasks, or be used to assess dynamic movements that occur in a combination of planes.

Electrogoniometers which convert angular motion into an electrical signal, may offer solutions for more than one plane and provide dynamic data. Their use in daily clinical practice however is less feasible than universal goniometers as the devices are anthropometric dependent, meaning different devices are needed for different size limbs. They are therefore primarily used in research applications. Flexible electrogoniometers have been used to measure upper limb motion (Barker et al., 1996; Johnson et al., 2002). These devices are prone to cross talk as a large source of error, i.e. during a pure flexion movement a false abduction signal may appear (Johnson et al., 2002).

1.3.2 Digital Inclinometers

More recently, the clinical use of digital levels for joint measurement has been investigated as a viable alternative to standard goniometry. This technique incorporates the use of gravity as a reference point to assess joint mobility. The assessor is also required to calibrate the inclinometer to an accurate and consistent zero point which can be fixed to the plane of interest. This is an advantage over conventional goniometry for which the reference arm of the goniometer must be manually held in the reference position while the other arm is rotated with the joint being assessed. With digital inclinometry, the digital level can be referenced to a fixed angle, the digital display can be easily read and the value can be locked at the end range of motion, reducing the risk of measurement errors. Digital inclinometers are portable, light and require training similar to that of goniometry but are more

costly than conventional goniometers. Several studies have indicated the interchangeable use of digital inclinometry and goniometry (Mullaney et al., 2010).

1.3.3 Visual Estimation

Goniometry is a very versatile tool, however many don't routinely use it, preferring to rely on visual estimation (Terwee et al., 2005; Hayes et al., 2001). The patient can be seated, standing upright or lying supine dependant on the clinicians preference or the physical capabilities of the patient. From the starting position with the affected arm down by side of the body, the arm is elevated either actively by the patient, or passively by the clinician in the desired plane to the maximum elevation that the patient can comfortably achieve without being limited by pain or weakness. The clinician then visually estimates the resultant angle (in degrees) from the starting to the end position. Whilst this method has benefits in that it doesn't require any equipment and allows a quick evaluation of shoulder function, the reliability of repeated measurements has been shown to be low in some patient groups, especially those with higher pain and disability severity (Terwee et al., 2005). However, when conducted by an experienced clinician with training in goniometry, the intra-rater reliability has been shown by one study to be as reliable as a mechanical goniometer (Williams and Callaghan, 1990).

1.3.4 Patient-Reported Questionnaires

Self-reported questionnaires to measure shoulder function are commonly used in daily practice due to their simplicity, handiness and ease of use. These include subjective questionnaires such as the American Shoulder and Elbow Surgeons

standardised shoulder assessment (ASES), Disabilities of the Arm, Shoulder and Hand (DASH), Simple Shoulder Test (SST), Constant-Murley Shoulder Outcome Score, Oxford Shoulder Score (OSS) and the Shoulder Pain and Disability Index (SPADI). Each of these questionnaires are intended as an outcome measure that reflects the patients shoulder function and range of motion, evaluating disability and pain experienced by the patient in their daily life. In a systematic review of 71 studies investigating the reliability, validity and responsiveness of these questionnaires, it was concluded that their psychometric properties were acceptable for clinical use, with the DASH being the best rated with the lowest measurement error (Roy et al., 2009).

There is currently no gold standard as to which questionnaire should be used to assess shoulder function and no single questionnaire of shoulder function offered superiority in measurement properties (Fayad et al., 2009). This is primarily due to the wide variability in responsiveness between them for different patient populations and interventions and the lack of a single, all-purpose questionnaire. For example, the SPADI has been found to be superior to the SST in terms of reliability and sensitivity to change after rotator cuff surgery (MacDermid et al., 2006), whilst the ASES is superior to the SPADI following shoulder arthroplasty (Angst et al., 2008). For shoulder instabilities, all the questionnaires studied have shown low responsiveness (Kocher et al., 2005; Kirkley et al., 1998).

Whilst such methods are widely utilised, simple, low- cost, can be administered by untrained personnel, and indeed can be completed remotely by the patient, they

suffer from intrinsic limitations relating to language and cultural issues, respondent interpretation and content validity (Pichonnaz et al., 2017). Furthermore, the delineation between objective and subjective is not clearly defined in questionnaire-based assessment and there appears to be discrepancies between questionnaire and objective measurement outcomes (Matsen et al., 2017).

1.3.5 Limitations of laboratory-based and clinical evaluations of joint range of motion

There are a variety of clinical outcome measure tools available each with their own advantages and disadvantages which should be considered with respect to the specific movement and pathology or disorder being presented. Laboratory-based motion analysis such as optoelectronic motion capture can overcome some of the limitations and displays a high accuracy and precision. Despite their growing importance in research, their application in a clinical setting remains unlikely due to cost and operational complexity. There remains a large discrepancy between the currently available clinical systems of motion analysis and those used in the laboratory.

Furthermore, the objective clinical evaluation of range of motion provides only a limited 'snapshot' of the patients maximum range of motion capabilities within the short appointment time frame, for which performance can be influenced by a number of circumstantial factors including current pain levels and time of day. Self-reported questionnaires rely solely on patient recall and perception of functional performance during the past few weeks. Several studies have sought to characterise shoulder kinematics during a variety of common activities of daily living however it is difficult to determine if such laboratory-based simulations characterise typical

movement tasks or if they represent how such tasks would be performed outside of the laboratory environment.

There is a need for performance-based, objective measures that can both describe joint characteristics and complement subjective reports to provide insight on functional capabilities when performing usual tasks in their usual environment throughout daily life for both healthy and pathological populations.

Due to the technical challenges of making accurate 3D measurements, kinematic descriptions of 3D have been limited to laboratory studies of predefined, simulated tasks. Studies using electromagnetic and optical systems have measured motion of simulated tasks such as hair combing, washing, dressing and reaching (Namdari et al., 2012; Gates et al., 2016; Magermans et al., 2005, van Andel et al., 2008).

Without a more general knowledge of upper arm movement in a free-living environment, it is difficult to determine if the laboratory simulations are characterising typical or extreme tasks, or if they represent how the tasks would be performed out with the laboratory setting.

1.4 Wearable sensors

In the last 20 years, research advances have pointed to the use of small, low-powered, portable electromechanical sensors to bridge the gap between large laboratory-constrained systems and clinical systems (Luinge, 2002, 2007; Luinge and Veltrik, 2004). In contrast to the current laboratory-based and vision systems, wearable sensors offer greater flexibility without the spatial constraints of the systems previously discussed. Developments in wearable technologies such as miniaturised inertial motion capture are enabling continuous capture of biomechanics beyond the typical laboratory setting. These sensors use technologies such as

accelerometers, gyroscopes and magnetometers, to provide high accuracy dynamic 3D-motion analysis in a free-living environment (Cutti et al., 2008; Galinski et al. 2012; Picerno et al., 2008).

1.4.1 Accelerometers

3D-Accelerometer sensors provide information on linear acceleration and acceleration due to gravity along each of the sensors three orthogonal axes (Schutz et al., 2001). Direct measurement of human movement by accelerometry was first suggested in the 1970s (Morris et al., 1973). Direct accelerometry has been extensively used for ambulatory measurements of gross movement classification during daily life such as physical activity behaviour, step count and postural changes (Bouten et al., 1997; Mathie et al., 2003; Veltink et al., 1996; Godfrey et al., 2003; Uswatte et al, 2005). A simple uni-axial accelerometer was attached bilaterally to the wrist of stroke survivor inpatients to quantify the number of hours per day of recovering arm use (Lang et al., 2007) and this measure was found to be correlated to standard clinical outcome measures and could be used to supplement usual practice and evaluate recovery over time.

Tri-axial accelerometers-based methods have been suggested as a useful means to evaluate humerus position and activity intensity out with a clinical setting (Bernmark et al., 2002; Faber et al., 2006; Hurd et al., 2014).

As well as the advantages of being small, lightweight and inexpensive, modern accelerometers operate with a low energy consumption, allowing them to record data for long periods of time out with a laboratory setting. However, the integration of data from these sensors can only be used for inclination measurements under quasi-static conditions (O'Donovan et al., 2007), and without providing information on

movement around the vertical axis (Luinige et al., 2007). Inclination estimates are only truly reliable for static postures or slowly executed movements since the linear acceleration must be sufficiently small in comparison to gravity (Luinige and Veltrik, 2004). Movement around the vertical axis cannot be estimated as the output vector remains constant if the sensor is rotated around the gravitational vector (Luinige et al., 2002). Furthermore, the integration of acceleration data to obtain orientation is prone to accumulative error over time, thus the integrated data is only considered to be reliable over short periods of a few seconds (Giansanti et al., 2003).

1.4.2 Gyroscopes

3D-gyroscopes are sensitive to angular change about each axis and by signal integration can estimate 3D-orientation. Gyroscopes are not sensitive to linear acceleration and are uninfluenced by gravity, thus the output is the same regardless of the sensors physical placement along the length of the limb segment (Aminian et al., 2002). Whilst using gyroscopes to directly measure segment inclination has been shown to be feasible in some cases (Mayagoitia et al., 2002), they present some significant limitations. Gyroscopes are subject to the accumulation of drift errors when angular velocity data is integrated to obtain angular information (Luinige et al., 2005) and fluctuating offsets if no external reference system for error correction is available (Zhou and Hu, 2007). Thus direct measurement with gyroscopes may not be suitable for accurate ambulatory monitoring.

1.4.3 Magnetometers

Magnetometers measure the direction and intensity of the local earth magnetic field vector (Zheng et al., 2005), and thus can detect magnetic north. Therefore, these

sensors can be a source of information for orientation around the vertical axis, assuming the absence of ferro-magnetic elements in the close environment, that may cause interference (Roetenberg et al., 2005).

1.4.4 Sensor Fusion

Combining acceleration and angular velocity information can considerably reduce the drift effects of gyroscopes and improve accuracy (Roetenberg et al., 2007; Martin-Schepers et al., 2010; Picerno et al., 2008; Mayagoitia et al., 2002; Zhou et al., 2008; Cutti et al., 2008). However, some studies have shown that measurements of orientation around the vertical axis remain inaccurate (Luinge et al., 2007; Schiefer et al., 2014). Much research has highlighted the benefits of combining the magnetometer to overcome the drawbacks of accelerometers and gyroscopes, and most modern inertial measurement unit (IMU) sensors incorporate readings from all three sensors to estimate 3D-orientation (Roetenberg et al., 2005; Schiefer et al., 2014). The concept underlying the function of IMU sensors is the combination of these three types of sensors through sensor fusion algorithms (Bachmann et al., 2001; Perez et al., 2010, Foxlin 1996; Luinge and Veltrik, 2004; Zhu and Zhou, 2004; Roetenberg et al., 2007). Complementary filters can be used to combine two measurements with different noise properties to produce a single, more accurate output. For example, combining measurements of both a low frequency accelerometer signal and a high frequency gyroscope signal (Liu et al., 2009). The 3D orientation of a sensor is represented by a technical coordinate system, expressed with respect to the defined global coordinate system (Bachmann et al., 2001; Cutti et al., 2008). The global coordinate system is defined using gravity and the magnetic north reference vectors and is thus common to all of the IMUs referenced to it. The

relative motion between two consecutive body segments can be calculated by attaching a sensor to each segment and applying appropriate sensor-to-segment calibration to give anatomical signification (De Vries et al., 2010). For description of relative orientation of consecutive body segments, the distance of the attached sensor to the joint centre is irrelevant (el-Zayat et al., 2011).

With technological advances in micro-machined inertial sensors, and automated data processing, this method has been greatly refined within the last 20 years and has led to the establishment of some commercial systems such as Xsens (Xsens Technologies, The Netherlands). Products can include a customised 3D-sensor apparatus and software package available with cable or wireless Bluetooth connection. Some systems contain an embedded processor within the IMU sensors to calculate absolute orientation, acceleration, angular velocity and magnetic North in real-time. The accuracy, reliability and validity of inertial sensor-based motion analysis was investigated in a systematic review by Cuesta-Vargas et al (2010), which reviewed applications that had been directly compared to gold standard motion capture (e.g. electromagnetic systems, optoelectronic systems, goniometry). It was concluded that inertial sensors can be accurately and reliably applied to many body regions, however to which degree is site specific and within the context of the systems proposed use. Errors associated with upper limb kinematic measurements were found to be more consistent (2.3° - 4.83°) compared to other body areas such as the lower limb (0.49° - 8.3°), (Cuesta-Vargas et al., 2010).

A recent review by Wong et al (2015), gives a comprehensive overview of the versatile applications of wearable inertial sensors to the real-time study of human

biomechanics, such as for gait analysis, subtle movement capture in Parkinson's patients, stroke rehabilitation and sporting performance. IMU sensors have been used as either single sensors or a combination of sensors in a number of applications to measure upper limb kinematics, including scapular motions during activities of daily living (Roetenberg et al., 2016; Cutti et al., 2008; Perez et al., 2010; Zhou et al., 2004; Wong et al., 2007; Roldan-Jimenez et al., 2015; van den Noort et al., 2014). A number of novel rehabilitation applications employing IMU technology have been developed to quantify upper limb movement during the intervention for a number of impairment conditions (Zhou et al., 2006; Zhou and Hu, 2008; Perez et al., 2013; Bai et al., 2012).

Perez et al (2013) developed an upper limb monitoring system using 4 IMU sensors mounted in a specifically designed garment worn by the subject. Data from the sensors was transferred to a PC by USB connection and during post-processing 3D-joint angles were estimated for the shoulder, elbow and wrist. The resultant data was highly correlated with that of an optoelectronic system and the system was proposed to undergo further development as a portable rehabilitation tool for brain injury recovery. An Xsens MT9-B system was integrated into a stroke tele-rehabilitation to track upper limb movement. The wireless system allowed for real-time transmission of motion pattern data to a remote therapist location. The system showed a good degree of accuracy when compared to a standard method of motion analysis (Zhou et al., 2006).

Inertial sensor-based systems have been increasingly used to monitor ambulatory upper limb motion during daily life. Much of this research has focused on arm usage

and the duration of movement cycles. A novel application consisting of a 3D-gyroscope was developed to recognise arm movement and the velocity and frequency of these movements over an 8-hour period in a free-living environment (Coley et al., 2009).

Tri-axial angular velocities were classified as flexion/extension, abduction/adduction and external/internal rotation using an algorithm validated with lab-based motion capture. All 31 healthy subjects also wore an IMU on their chest to classify posture. This study found that the frequency of arm movements increased from sitting to standing and from standing to walking postures. Interestingly, no significant differences between dominant and non-dominant arm movements were found. In previous research, Colley et al (2008) used a similar IMU system to estimate arm dominance in healthy subjects during an 8-hour ambulatory measurement period. Humerus angular velocity and acceleration was evaluated in activity envelopes of 5 seconds. The more dominant arm was found to be more active whilst standing but similar to the non-dominant arm during periods of walking. The combined results of these two studies suggest that arm dominance is not determined solely by the frequency of humerus movement and that postural classification also needs to be considered. Arm usage and velocity of humerus movements at home was further investigated in rotator cuff patients and a control group (Duc et al., 2013). The quantity and quality of movement was correlated to pre- and post-operative disease-specific questionnaires. They found that speed of movement was related to clinical scores and thus may be related to disease status. The system requires a trained operator to attach and programme the devices and therefore its use may not be suitable for everyday clinical practice.

More recently, the feasibility of wearable inertial sensors to track shoulder joint angles during daily life was investigated in 5 healthy participants for 4 hours in the workplace and 4 hours of recreational time (Kirking et al., 2016). Using an algorithm previously validated (El-Gohary et al., 2012), they demonstrated an accuracy of 2° in relative upper arm angles from the IMU data. Wearable, inertial sensor systems have brought continuous kinematic analysis of daily life closer to reality.

1.5 Mobile technology for kinematic measurements

Mobile technology has advanced rapidly in the past 20 years with most modern smartphones now having advanced computational and sensing capabilities. Such devices are widely available and have become an everyday asset in modern life.

Smartphone use has become ubiquitous over the years growing from 52% in 2012 to 87% in 2018 (Deloitte, 2018). The number of users is expected to exceed 2.5 billion worldwide by 2019 (Statistica, 2018). In the UK alone, the number of active smartphone users in 2015 was 41.09 million, over 63% of the population and this is forecast to increase by over 12 million users by 2020. As they are becoming increasingly affordable and have a number of high-performance sensors, it is now possible to easily acquire a handheld smartphone which has many of the computational and connectivity capabilities of a computer. Similar to IMU sensors, smartphones have inbuilt kinematic sensors, (tri-axial accelerometers, gyroscopes and in some models, magnetometers), which allow detection and monitoring of angular movements. Smartphones also contain additional features such as Global Positioning Sensors (GPS), Wi-Fi and Bluetooth ® connectivity, self-contained

battery power, a camera and a microphone, screen display, an audio system and a tactile feedback system for user interaction.

More recently, miniaturised wearable technology such as smartwatches have become commercially available to the mainstream market. In addition to functioning as a timekeeping device, a smartwatch is a wrist-worn “general purpose, networked computer with an array of sensors (Rawassizadeh et al., 2015). Whilst early models were designed to do basic tasks such as calculations, digital time and date display and simple game playing, the current state of the art hardware can sync to a smartphone via Bluetooth communication, have comparable sensing capabilities to a smartphone, and can function effectively as wearable computers. For everyday use, information and notifications from the smartphone can be displayed on the watch on the users’ wrist and manipulated using voice recognition or haptic input. Similarly to smartphones, they contain inbuilt inertial sensor units and connectivity functionality, and their smaller physical size and wearable design makes them an attractive platform for monitoring human movement. Users can wear the device throughout the day and this unique characteristic enables a wide range of possible healthcare applications including joint angle estimations. Rawassizadeh et al. (2015) cite market research that predicts growth of smart watch demand to 214 million units in the year 2018 with financially feasible prices of around £100 per unit.

In the field of biomechanics, these technological advances offer the opportunity to adopt new tools that can improve patient kinematic assessments, follow-ups and ultimately lead to improved clinical outcomes. Due to their relatively low cost and ubiquitous nature, smartphones and wearable technology has inadvertently addressed

the issue of hardware and software costs, and availability associated with current wearable sensor systems. Furthermore, compliance limitations are minimised with smartphones as most users carry their device with them as an integral part of daily life.

Research thus far has focused on the exploitation of smartphones inbuilt sensors to monitor physical activity and patterns of human gross movements both in daily life (Del Rosario et al., 2015; He and Li, 2013; Antos et al., 2014) and in sport (Mitchell et al., 2013), and more recently to measure kinematic patterns of individual joints. Less research can be found in the literature on the use of smartwatches however a limited number of studies have shown their potential integration in general health monitoring (Phan et al., 2015), physiotherapy compliance (Micallef et al., 2016), posture tracking (Mortazavi et al., 2015) and in monitoring specific disease characteristics such as hand tremor in Parkinson's (Zheng et al., 2017).

1.5.1 Smartphone goniometry

A variety of applications which exploit the goniometry capabilities of smartphones have been developed and validated for measuring joint angles. The two leading platforms are Apple and Android and they have many commercially available goniometer applications between them. Two approaches to measuring joint angles with smartphone technology are described in the literature; image-based or inertial-sensor based.

The image-based approach employs the camera features of the device. The 'DrGoniometer' application (CDM S.r.L, Milano, Italy), first released to the market in 2011, is one such photographic application. It has been validated for both elbow and knee joint angle measurements with good agreement to a standard universal

goniometer (Ferriero et al., 2013). Image-based applications facilitate measurements to be taken after the initial assessment (post-production and independent of the patients' location) and allow images to be saved, printed or filed in the patients' medical records for comparison during subsequent visits. Furthermore, they could be advantageous for use in operating theatre where sterile medical instrumentation is normally required due to contact of a goniometer device on the patient's skin. There are some limitations to image-based applications which should be considered, such as pictures that are taken short of the maximal ROM or if the photography is mistimed altogether (Mejia-Hernandez et al., 2017). Care is required when measuring angles under investigation in photographs, especially in placing virtual markers on the desired anatomical landmarks.

Inertial sensor-based goniometry using the inbuilt sensors of the device, requires the smartphone to be attached to the relevant segment distal to the joint of interest. The majority of such applications primarily utilise the accelerometer to estimate inclination. An accelerometer-based application, Angle (Smudge Apps), showed a significant correlation with a navigation system typically used in total knee arthroplasty, as well as good to excellent intra- and inter-rater reliability (0.81 and 0.79 respectively) for passive knee flexion measurements (Jenny et al., 2013).

Using an armband to fix a smartphone to the ventral aspect of the wrist, the commercially available Clinometer (Plaincode Software Solutions, Stephanskirchen, Germany) has been validated compared to a standard double-arm goniometer for shoulder range of motion measurements (Shin et al., 2012). With the smartphone attached to the distal portion of the forearm, the resultant shoulder range of motion

measurements assume that the elbow joint remains fixed throughout the movement, which could introduce errors in compensatory movements of the elbow were introduced. Nonetheless, the intraclass correlation coefficient (ICC) values were good (>0.7) for all movement axes apart from internal rotation at 90° abduction where the ICC range was 0.63-0.68. Clinometer was further compared to visual estimation and a standard goniometer in a study with 15 shoulder pain patients (Werner et al., 2014). 5 observers of varying levels of experience (a sports orthopaedic surgeon, a sports orthopaedic fellow, a resident physician, a physician's assistant and a medical student), measured flexion, abduction and internal/external rotation in both the patients and the control subjects. For the patient group, the intra-rater reliability ICC was excellent at greater than 0.8 and the inter-rater reliability ICC was greater than 0.6 for all subjects.

It was concluded that the application had good to excellent agreement with gold standard goniometry techniques and that its use is validated for clinical angle measurements. Furthermore, this study highlights that the application can easily and reliably be used by healthcare providers of different levels of experience. This is important as clinicians and allied health professionals may employ these smartphone applications with the confidence that they will provide consistent results.

GetMyROM (Interactive Medical Productions LLC, USA) is another application that has been compared to standard goniometry with promising results in measuring shoulder range of motion (Mitchell et al., 2014). Oihenart et al (2012) used a custom application called iShould (Instrumented Shoulder Test) with iPhone 4 or iPod Touch devices (Apple, Cupertino, USA). iShould quantifies the shoulder movement

based on angular velocities, and P score, which is based on the power of shoulder movement, directly from inertial signal sensors. The application was compared with another 3D kinematics sensors composed 3D gyroscopes and accelerometers. Both the phone and a reference IMU sensor were attached to the anterior humerus with an armband whilst the subjects performed active movements in 3 planes. The mean difference between the iShould and the IMU measurements for 5 participants was 1.09% for angular velocity and 0.6% for the P score. The authors concluded that the use of a specific Smartphone application for the active angle measurement of shoulder range of motion was acceptable.

Mejia-Hernandez et al (2018) assessed the reliability and validity of two different smartphone applications (GetMyROM, DrGoniometer) for measuring both passive and active shoulder range of motion across a spectrum of shoulder disease patients compared to conventional techniques. Both applications were found to be comparable to the clinical methods, with excellent inter-rater reliability, independent of pathology diagnosis and it was concluded that clinicians could confidently employ these newer tools to measure shoulder range of motion of patients.

Some limitations exist in using inclinometer applications for shoulder ROM measurements. For example, the position of the measurement device is important in achieving consistent results and vigilance of the assessor is required when attaching the mobile device to the relevant segment and ensuring its fixed position throughout the movement.

There are several other applications developed for the purpose of measuring joint range of motion using a smartphone (Johnson et al., 2015; Mitchell et al., 2014; Mourcou et al., 2015; Shin et al., 2012; Werner et al., 2014; Stenneberg et al., 2018)

and numerous studies have investigated their validity as clinical tools (Mourcou et al., 2015). There is overall agreement that smartphone-based goniometry has accuracy and reliability comparable to some gold standard systems (Milani et al., 2014; Oihenart et al., 2012). Compared to the variable reliability of universal goniometers (Riddle et al., 1987; Hayes et al., 2001; Mullaney et al., 2010), smartphone applications appear to be just as, if not more reliable (Cuesta-Vargas et al., 2016; Jenny 2013; Pichonnaz et al., 2015; Shin et al., 2012; Werner et al., 2014). There are certain advantages to adopting these new technologies. They allow fast, reliable measurements of shoulder ROM, are widely available and cost-effective, given the prevalence of smartphone ownership in the general population. They are available not only to physicians but also to allied health professionals and patients. As well as being used in a clinical setting, the smartphone applications allow patient self-measurement (Ferrierio et al., 2013), and can provide real-time feedback for exercise completed at home. This may be of particular benefit to those with limited access to health care because of rural location or disability, for whom some assessment may be performed by a combination of telephone, tele-link or email. Moreover, the clinician-patient interaction may potentially be enhanced by demonstrating the patients' progress in ROM remotely over time (Ferrierio et al., 2013; Milani et al., 2014).

Smartphone goniometry has also been incorporated into systems designed to improve patient compliance to a physiotherapy programme after surgical intervention of the knee (Vaish et al., 2017). The patient was required to attach the smartphone to the medial aspect of the tibia on the affected leg whilst the application ran to record knee ROM during the physiotherapy exercises. The results from this pilot study were

encouraging and demonstrate the relative ease of incorporating smartphone technology to improve patient compliance and remote monitoring by the therapist. To date, the majority of studies have focused on the development and validation of smartphone applications that are interchangeable with conventional goniometry. That is, that they are capable of estimating the maximum ROM of a joint when the movement is held statically at the end of the subjects range. Capturing transient ROM throughout a movement or daily task would be beneficial according to clinician feedback (Lee et al., 2014). During dynamic assessments, the subject would not be required to sustain the maximum angle achievable, which can be particularly challenging in pathological conditions.

3-dimensional shoulder kinematics were measured in healthy participants during flexion and abduction movements with an iPhone4 (Roldan-Jimenez et al., 2015). The descriptive results of this study support the feasibility of using a mobile phone as a device to analyse upper-limb kinematics and to facilitate the dynamic evaluation of patients. However this study was only conducted using one participant and only one plane of movement. A system capable of dynamically measuring 3D shoulder kinematics is required but remains to be developed.

1.6 Aims and Objectives

This thesis focuses on the use of mobile technology in the clinical environment to provide a quantitative and objective measure of 3-dimensional shoulder range of motion to inform clinical decision making.

The first aim is to develop a mobile application based on inertial sensor technology for the measurement of 3D shoulder range of not which can be applied within a

clinical setting. The application is required to be simple to use, provide accurate measurements and be cost effective to maximise potential clinical uptake.

Secondly, the accuracy of the application for measuring 3D orientations will be investigated under varying conditions relating to how the shoulder range of motion can be measured both in the clinic and in a home setting. The third aim of this study is to determine the effectiveness of the mobile application as a tool for clinical upper limb functional assessment by comparison of goniometry data with simultaneously recorded values from the “gold standard” universal goniometer.

Chapter 2: Overview of Shoulder Kinematics and Methods of Describing Joint Range of Motion

Chapter 2

2 Overview of Shoulder Kinematics and Methods of Describing Joint Range of Motion

2.1 Kinematics

As mentioned in the literature review, Kinematics is the study of body motion in space, without reference to the forces which cause the motion. It provides a quantitative description of movement which can be clinically useful for the diagnosis, treatment and evaluation of patients with pathological movement conditions.

In order to mathematically describe the relative rotations between body segments, each segment is assumed to be a rigid body based on the underlying bony structures, and a Cartesian coordinate system is specified for each segment. The definitions of these bone-embedded coordinate systems are based on the location of anatomical landmarks. In order to define the coordinate systems for the thorax and upper arm, a brief description of the upper limb bony anatomy is required.

Different mathematical methods to represent 3D-orientation of a rigid body segment have been developed and will be defined and discussed in this chapter.

2.2 Bony Anatomy

2.2.1 The Thoracic cage and vertebral column

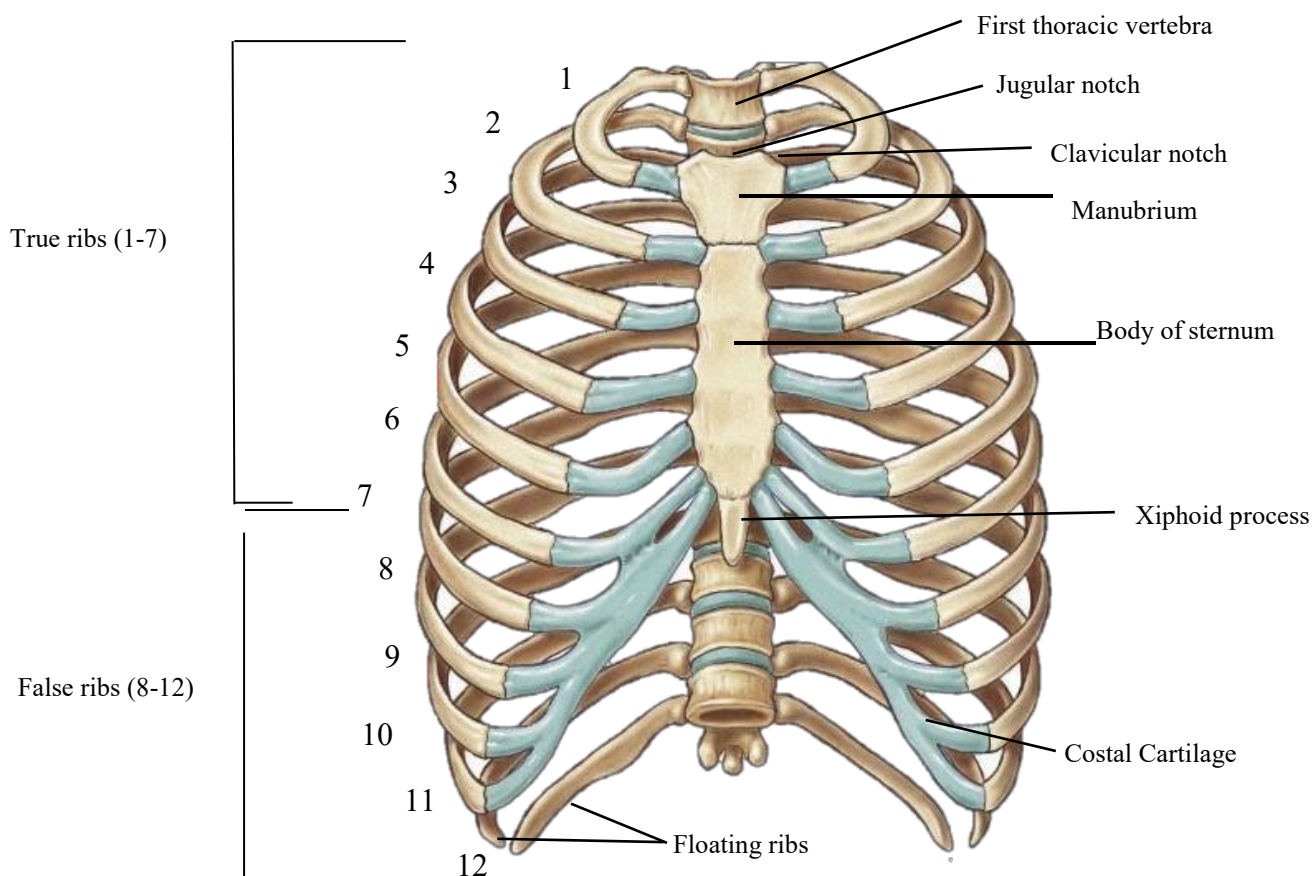


Figure 2. 1 Bony Anatomy of the Thorax

The thoracic cage consists of the thoracic vertebrae, the ribs and the sternum (figure 2.1). It provides a point of attachment for the muscles involved in pectoral girdle and upper limb movement as well as a protection for the internal chest organs. The anterior midline of the thoracic wall is formed by the sternum, an elongated bony structure which has three components: the manubrium, the central body and the xiphoid process. Its most superior and widest portion is the manubrium, which has a

shallow indentation on the superior surface of the manubrium called the jugular notch, which can be palpated between the clavicular articulations on either side of the manubrium at the

sternoclavicular joints. The central portion of the sternum is the central body and the inferior tip is a small structure called the xiphoid process.

The twelve thoracic vertebrae form the posterior of the thoracic wall and articulate with twelve pairs of thoracic ribs. Each rib is a curved, flattened bone that makes a significant contribution to the wall of the thorax. The first seven pairs also articulate with the sternum via costal cartilages and are commonly referred to as the 'true ribs', with the five free ribs referred to as 'false ribs'. Superior to the thoracic vertebrae are seven cervical vertebrae, which constitute the neck region. The first cervical vertebra is called the atlas (C1) which supports the skull, and the second cervical vertebrae is called the axis (C2) whose structure provides a point of pivot allowing for rotation of the skull. Inferior to the thoracic vertebrae are five lumbar vertebrae that form the concave lower back region and carry the majority of the weight of the upper body whilst providing flexibility and movement to the trunk region. The fifth lumbar vertebra articulates inferiorly with the five fused vertebra of the sacrum, which in turn articulates with the similarly fused coccyx.

2.2.2 The Pectoral Girdle

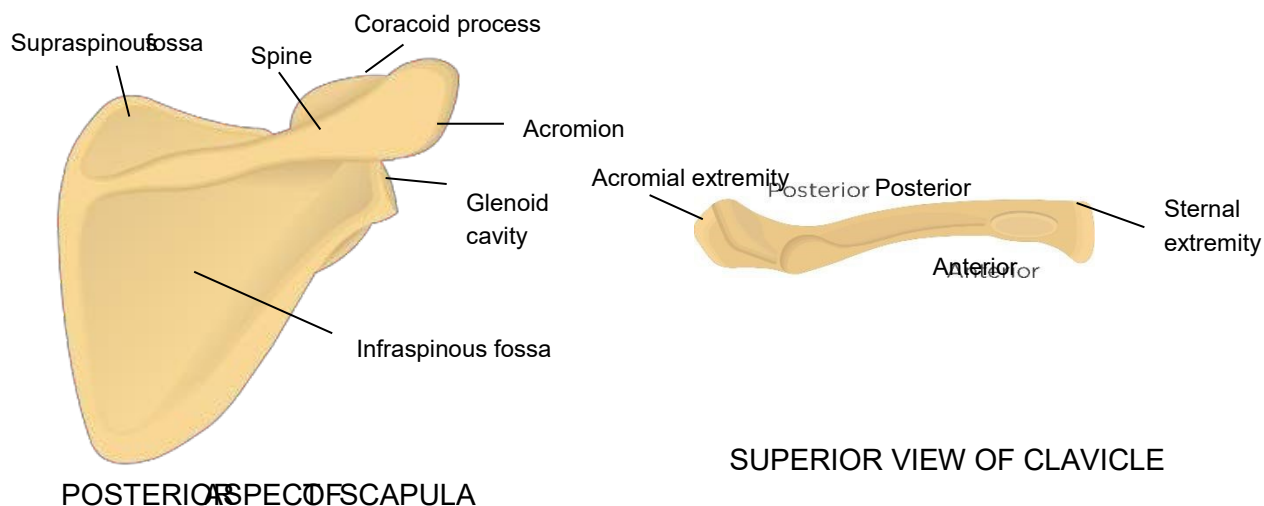


Figure 2. 2 Bony Anatomy of the Scapula and Clavicle

The pectoral girdle is a set of bones in the appendicular skeleton which anchor the upper appendages to the axial skeleton. The pectoral girdle which is comprised of the scapula and the clavicle (figure 2.2). These bones contribute to the formation of the shoulder joint and provide points of attachment for the muscles that support the joint and facilitate movements of the upper arm.

The scapula is a broad, flat, triangular-shaped bone that lies on the posterior thoracic wall between the levels of the second and eighth ribs. It has no direct bony articulations or ligamentous attachments with the thoracic cage and is supported in position solely by skeletal muscle, permitting great mobility of the shoulder complex. These muscles attach along the edges of the superior, medial, and the

lateral borders. The superior and inferior and lateral borders form the three corners of a bony triangle with the lateral border broadening to form the shallow glenoid fossa. This is the site of articulation with the head of the humerus to form the primary joint of the shoulder, a ball and socket joint known as the glenohumeral joint.

The smooth, rounded articular head of the humerus is several times the diameter of the glenoid fossa, resulting in inherent instability of the joint. Congruency between the humerus and the glenoid fossa is improved by both fibrous and soft tissue supporting structures.

The scapula has a prominent ridge, referred to as the spine, running across its posterior surface which divides the bone into two concave fossae which give attachment to intrinsic and extrinsic muscles of the pectoral girdle. The ridge extends laterally, superior to the head of the humerus to form the acromion which articulates with the lateral end of the clavicle. Overhanging the glenoid fossa is a hook like projection, the coracoid process.

The clavicle is an anteriorly located, S-shaped bone. It attaches medially to the manubrium of the sternum of the axial skeleton, and laterally to the acromion of the scapula at the acromioclavicular joint. As such, the clavicle provides the only true articulation between the pectoral girdle and the axial skeleton.

2.2.3 The Humerus

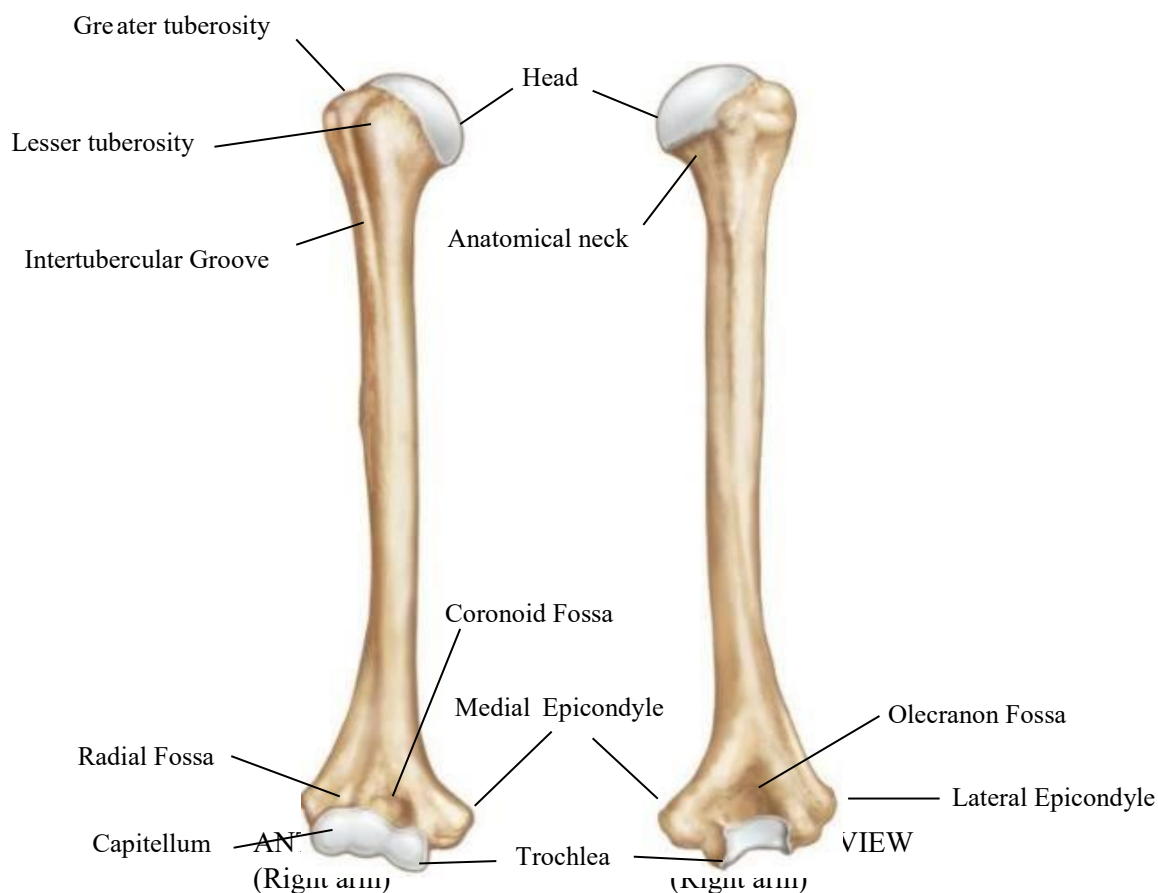


Figure 2.3 Bony Anatomy of the Humerus

The upper arm is formed by a single long bone called the humerus which extends from the scapula to the elbow (figure 2.3). The proximal rounded head of the humerus articulates with the glenoid fossa of the scapula to form the glenohumeral joint as described in section 2.2.2. Immediately inferior to the head lies the narrow anatomical neck and then the greater and lesser tuberosities lying on the antero-lateral and anterior surface respectively. These rounded projections form muscle attachment sites and are separated by the definitive intertubercular groove which accommodates the long tendon of the biceps muscle. The humerus has a narrow

neck which broadens to form the middle section of the humerus is referred to as the shaft, which expands at the distal end to form the medial and lateral epicondyles, the non-articular projections of the distal humerus. The humerus articulates distally with the bones of the forearm at the articular condyle of the humerus at two distinct regions known as the trochlea and capitellum. The trochlea forms the medial surface of the condyle and articulates with the ulna and the capitellum lies laterally, articulating with the radius. Superior to the anterior aspect of the trochlea is a depression known as the coronoid fossa which accommodates the coronoid process of the ulna during elbow flexion. The olecranon fossa also lies immediately superior the trochlea on its posterior aspect and accommodates the olecranon process of the ulna when the elbow is extended. The shallow radial fossa is located superior to the anterior aspect of the capitellum and accommodates the radial head during elbow flexion.

2.3 Anatomical Coordinate System

The anatomical coordinate system for the trunk and upper arm segments are defined using bony landmarks in accordance with the International Society of Biomechanics (ISB) recommended standards (Wu et al., 2005). This is shown in figure 2.5. The following definitions are descriptive of a subject with Right Hand dominance. For left-handed subjects, the raw position data were mirrored in the sagittal plane (i.e $z = -z$). The anatomical planes are defined as shown in figure 2.4.

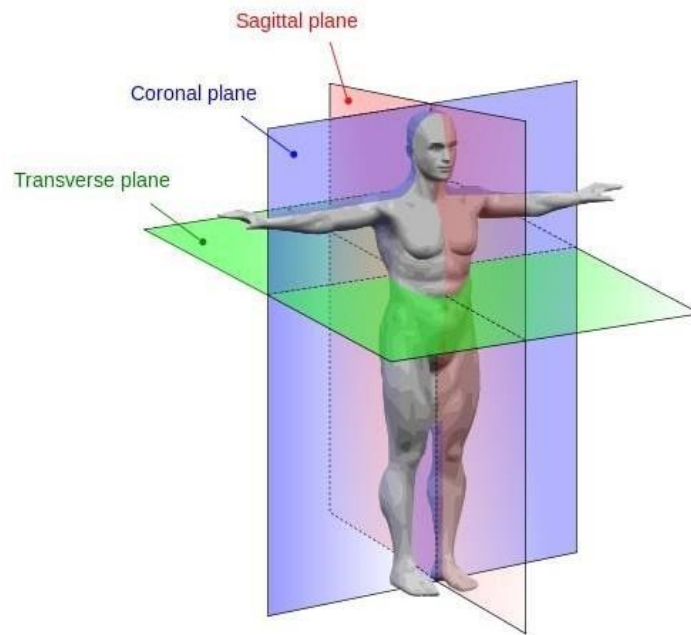


Figure 2. 4 Anatomical planes of the human body

2.3.1 Thorax Anatomical Coordinate System

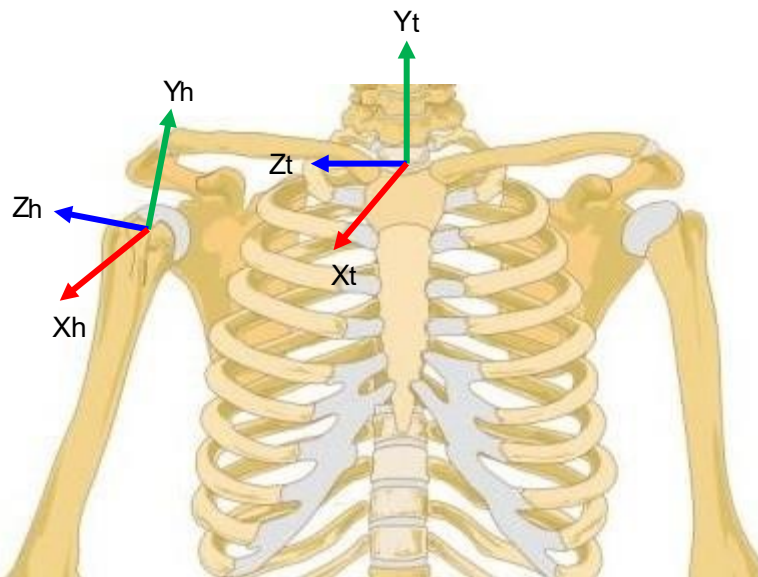


Figure 2. 5 Anatomical coordinate systems for the thorax and the humerus

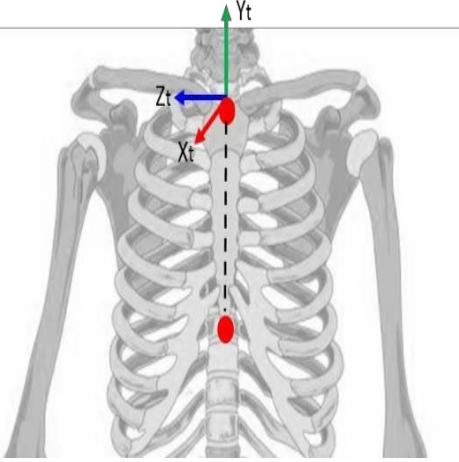
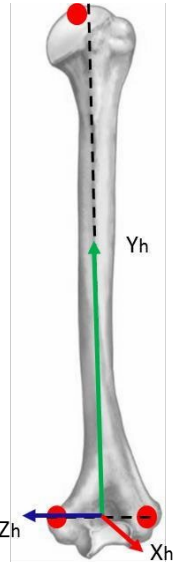
The bony landmarks used to define the anatomical coordinate system of the thorax are the spinous processes of both the 7th cervical vertebra (C7) and the 8th thoracic vertebra (T8), and the caudal tip of the xiphoid process (XP) and the deepest part of the jugular notch of the sternum (JN). The location of these landmarks were shown previously in figure 2.1. The coordinate system is described in table 2.2 below.

2.3.2 Humerus anatomical coordinate system

The anatomical landmarks that are recommended for the definition of the humerus coordinate system are the most distal points of the medial and lateral epicondyles of the humerus (EM and EL), and the glenohumeral joint centre (GH). The GH is not a bony landmark but it is used to estimate the long axis of the humerus. It is not possible to manually locate the humeral head joint centre, and different regression or motion recording methods for its reliable estimation have been suggested and recommended by the ISB (Stokdijk et al., 2000; Veeger et al., 2000). In this study, the GH was estimated by regression as according to Wang (1998), based on its position relative to the acromio-clavicular (AC) joint, whilst the upper arm is in a neutral, resting position. In this position, it was estimated the GH was located 37mm inferior, 14mm lateral and 8mm anterior to the AC joint. The location of these landmarks were shown previously in figures 2.2 and 2.3.

The following definition is in accordance with the first option of the ISB standardisation (Wu et al., 2005) for the thorax and humerus coordinate systems:

Table 2.1 Anatomical reference frame definitions for the thorax and the humerus

	<p>O_t Coincident with JN</p> <p>Y_t The Y_t-axis is formed by the line connecting the midpoint between the XP and T8 and the midpoint between JN and C7, pointing upwards.</p> <p>Z_t The Z_t-axis is perpendicular to the Y_t-axis described above and the plane formed by connecting JN and C7, pointing to the right.</p> <p>X_t The X_t-axis corresponds to the common line that is perpendicular to both the Y_t-axis and Z_t-axis, pointing forwards.</p>
	<p>O_h Coincident with the GH</p> <p>Y_h The Y_h-axis is formed by the line connecting GH to the midpoint between EM and EL, pointing towards GH.</p> <p>X_h The X_h-axis is the line perpendicular to the Y_h-axis plane formed by EM, EL and GH, pointing forward.</p> <p>Z_h The Z_h-axis is the common line perpendicular to the Y_h and X_h-axes, pointing laterally right from the body.</p>

2.4 Position and Orientation

2.4.1 Position

A single point in space can be described with respect to a global coordinate system

as:

$${}^G\mathbf{p} = [p_i \ p_j \ p_k] \quad (1)$$

here ${}^G\mathbf{p}$ is the position vector of point p in the global frame, G .

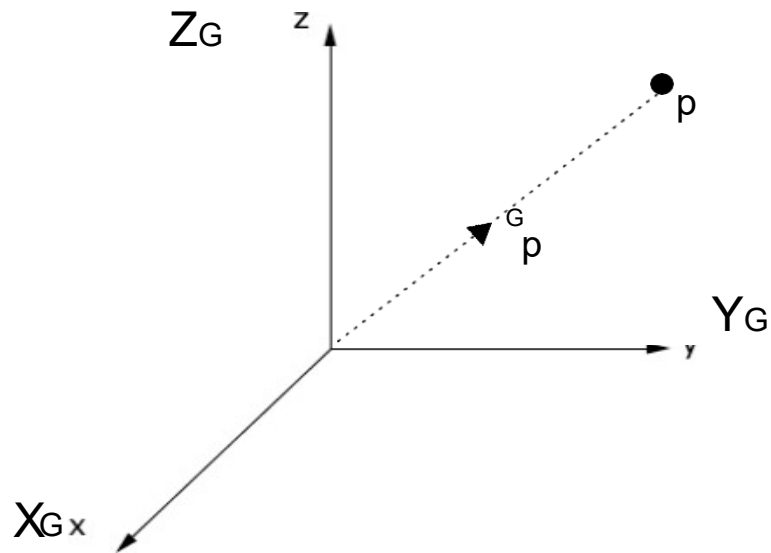


Figure 2. 6 Position of point p in the global coordinate system, G

2.4.2 Orientation

2.4.2.1 Rotation Matrices

The orientation of a local coordinate system with respect to a global coordinate system can be mathematically described by a 3x3 rotation matrix:

$${}^G_R_A = \begin{bmatrix} r_{11} & r_{12} & r_{13} \\ r_{21} & r_{22} & r_{23} \\ r_{31} & r_{32} & r_{33} \end{bmatrix} = \begin{bmatrix} i \cdot I & i \cdot J & i \cdot K \\ j \cdot I & j \cdot J & j \cdot K \\ k \cdot I & k \cdot J & k \cdot K \end{bmatrix} \quad (2)$$

Where G_R_A describes the orientation of frame A relative to the global frame, G , and i , j , k and I , J , K are the unit vectors of frame A and frame G respectively. The rotation matrix, G_R_A , is also termed the direction cosine matrix because each of its nine

components are the cosines of the direction angles between the unit vector coordinate axes of frame A, and those of the global frame, G.

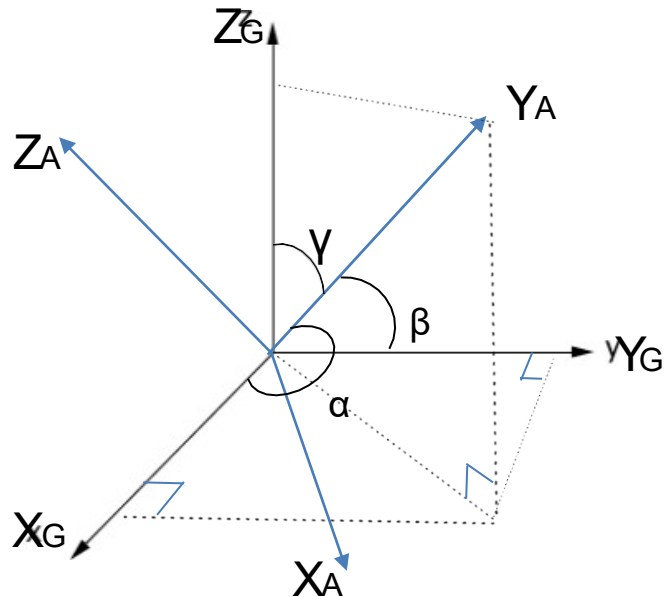


Figure 2.7 Orientation of frame A with respect to the global frame, G, showing the direction angles of Y_A , with respect to the three coordinate axes of the global frame

The above rotation matrix allows the position of any point in system A, ${}^A p$, to be mathematically represented as a point in the global system, ${}^G p$ by the following transformation:

$${}^G p = {}^G R \cdot {}^A p + {}^G O \quad (3)$$

Where ${}^G O$ is the origin of the embedded frame A, as expressed in the global system.

Conversely, any point in the global system, can be represented as a point in system

A:

$${}^A p = {}^A R^{-1} \cdot ({}^G p - {}^G O) \quad (4)$$

The rotation matrix can also be used to describe a rotation of one local coordinate frame orientation to another. This facilitates the mathematical description of the

relative orientation of a distal body segment, to a proximal body segment, when both segments are defined with embedded, local coordinate frames within a global reference system.

The description of the orientation of any local frame relative to another is given as:

$${}^A R_B = {}^G R_B \cdot {}^G R_A^{-1} \quad (5)$$

Where ${}^A R_B$ is the orientation of frame B relative to frame A.

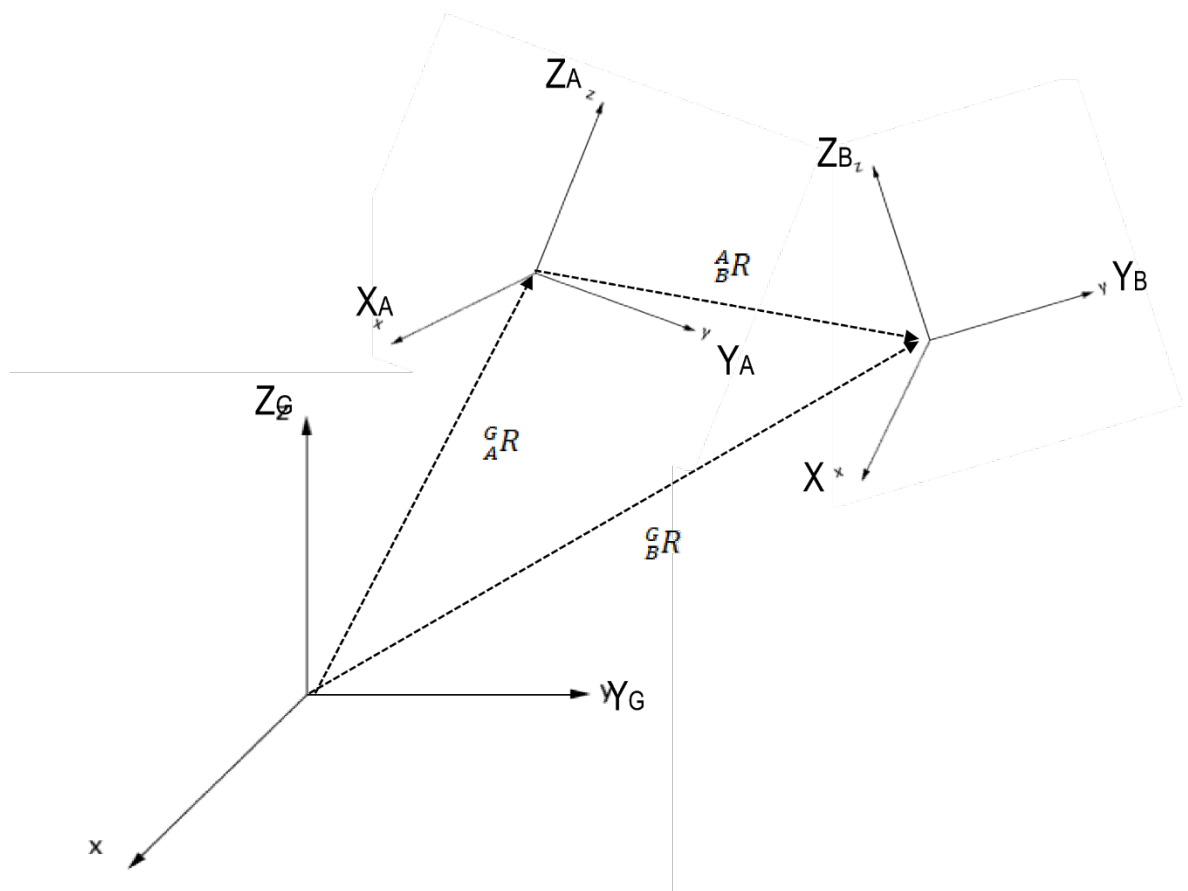


Figure 2. 8 Orientation of frame B with respect to frame A

A 3x3 rotation matrix as described above, represents a motion with three degrees of freedom. This can further be described as three sequential rotations about defined axes.

If α , β and γ represent angular rotation about the axes X, Y and Z respectively, then three independent rotation matrices, R_α , R_β , R_γ can be defined to describe the rotation of the local coordinate system to the world coordinate system or to another local coordinate system with the global reference frame.

For a rotation through α about the X-axis:

$$R_\alpha = \begin{bmatrix} 1 & 0 & 0 \\ 0 & \cos\alpha & \sin\alpha \\ 0 & -\sin\alpha & \cos\alpha \end{bmatrix} \quad (6)$$

Rotation of angle β about the Y-Axis:

$$R_\beta = \begin{bmatrix} \cos\beta & 0 & -\sin\beta \\ 0 & 1 & 0 \\ \sin\beta & 0 & \cos\beta \end{bmatrix} \quad (7)$$

Rotation of angle γ about the Z-Axis:

$$R_\gamma = \begin{bmatrix} \cos\gamma & \sin\gamma & 0 \\ -\sin\gamma & \cos\gamma & 0 \\ 0 & 0 & 1 \end{bmatrix} \quad (8)$$

Rotations can be in the global system, occurring about the three axes of the fixed global coordinate system, or body-fixed rotations, occurring about the three axes of the segment-embedded, local frame. For a sequence of three rotations, the resulting transformation is sequence-dependent. In other words, the result will differ according to the defined axes and the order in which the rotations occur.

Two commonly used techniques to describe 3-Dimensional joint rotations are the Cardan and Euler angle method, described in the following section.

2.4.2.2 Cardan and Euler Angles

The three independent rotation matrices R_α , R_β and R_γ can be combined as a sequence of three successive and ordered rotations ordered rotations to obtain a single rotation matrix, ${}^G_L R$, that can wholly describe the rotation of an embedded frame from one orientation to another. For example:

$${}^G_L R = R_\gamma R_\beta R_\alpha \quad (9)$$

$${}^G_L R = \begin{bmatrix} \cos\beta\cos\gamma & \sin\alpha\sin\beta\cos\gamma + \cos\alpha\sin\gamma & -\cos\alpha\sin\beta\cos\gamma + \sin\alpha\sin\gamma \\ -\cos\beta\sin\gamma & -\sin\alpha\sin\beta\sin\gamma + \cos\alpha\cos\gamma & \cos\alpha\sin\beta\sin\gamma + \sin\alpha\cos\gamma \\ \sin\beta & -\sin\alpha\cos\beta & \cos\alpha\cos\beta \end{bmatrix} \quad (10)$$

These successive, ordered rotations are referred to as sequence-dependant Cardan or Euler angles. Cardan or Euler angles are the most common and recommended method for mathematical estimation of 3-dimensional joint motion (Wu et al., 2002, 2005). They can be used to define the relative orientation of a distal segment to a proximal segment as a set of sequential rotations about three anatomical axes (Wei et al., 1993). This provides a relatively easier clinical interpretation of joint motion than other methods such as helical angles (Woltring, 1991, 1994).

Matrix multiplication is non-commutative and hence the resulting rotation matrix,

${}^G_L R$, is sequence dependant and a different form of ${}^G_L R$ will be obtained according to the angle rotation sequence chosen. There are 12 possible combinations of angle sequences. Cardan angles involve sequential rotations around all three coordinate axes (e.g. α - β - γ), whereas sequences in which the first and third rotations occur around the same axis (e.g. α - β - α), are termed Euler angles.

As an example, through decomposition of the resultant matrix in equation 10, we can extract the three successive and ordered rotations as the Cardan angle sequence, $xy'z''$.

First, we determine:

$$\beta = \sin^{-1}(r_{31}) \quad (11)$$

We can then use this to calculate α :

$$\alpha = \cos^{-1}\left(\frac{r_{33}}{\cos\beta}\right) \quad (12)$$

and γ :

$$\gamma = \cos^{-1}\left(\frac{\cos\beta}{r_{11}}\right) \quad (13)$$

The resultant α , β and γ describe the rotation around the X, Y and Z-axis respectively.

Cardan and Euler sequences are limited to a description of an angular orientation, rather than the actual path of motion from the start through to the maximum range of the movement (Woltring, 1991). The joint orientations obtained from matrix calculations cannot be linearly added or subtracted to estimate the trajectory. However, the difference between the final and initial orientation is commonly used to describe the range and direction of motion (van Andel et al., 2008; Bourne et al., 2007; Ludewig et al., 2009). It is important to note, that the same physical change in 3-dimensional orientation can be represented in various mathematical forms

dependant on the sequence of rotations and thus it is imperative to use a sequence which can best reflect anatomical movement patterns.

The sequence dependency of the three rotations creates a disadvantage to the use of these angles. Gimbal lock is an inherent mathematical problem which occurs due to the loss of one degree of freedom in a 3-dimensional system. In an $xy'z''$ cardan sequence, it results when the first (α) and third (γ) rotation axes are driven into an indeterminate configuration when the second rotation (β) is equal to $\pm 90^\circ$ forcing the system into a degenerate 2-dimensional space. When gimbal lock occurs, unreliable and inconsistent changes are observed in the angle values with the largest changes occurring for rotations around the first and third axes. As a result, none of the three successive rotations can be accepted during gimbal lock.

Whilst gimbal lock is difficult to avoid in some joints such as the shoulder, its effects can be minimised by an appropriate choice of local coordinate system and rotation order (de Groot, 1997). The International Society of Biomechanics (ISB) has thus proposed recommended standardised sequences for describing the motion of specific human joints. The recommended sequences are typically based on avoidance of singular positions within the normal range of motion whilst allowing clinical interpretation of motion (Karduna et al., 2000; Wu et al., 2005).

2.4.2.3 3-Dimensional angles applied to humero-thoracic joint angle

The large range of motion of the shoulder complex in particular presents complications to 3-dimensional kinematic analyse using rotation matrices and sequential angles. Despite the proposed standardised recommendation for motion description (Wu et al.,

2005), there remains a lack of agreement over which rotation sequence could better describe the joint motion and as to how to prevent gimbal lock occurrence in particular motions. In fact, no single sequence satisfies the criterion to describe all humero-thoracic motions across all available ranges accurately, without singularity (Senk and Cheze, 2005).

The standardised rotation sequence recommended for motion of the humerus relative to the thorax is the Euler Y-X-Y sequence, which describes the plane of elevation, elevation angle and axial rotation:

α : The axis fixed to the thorax and coincident with the Y_t -axis of the thorax coordinate system. Rotation (γ_h): Plane of elevation, 0° is abduction, 90° is forward flexion.

β : The axis fixed to the humerus and coincident with the X_h -axis of the humerus coordinate system. Rotation (β_h): elevation (negative). γ : Axial rotation around the Y_h -axis. Rotation (γ_h): axial rotation, internal rotation (positive) and external-rotation (negative).

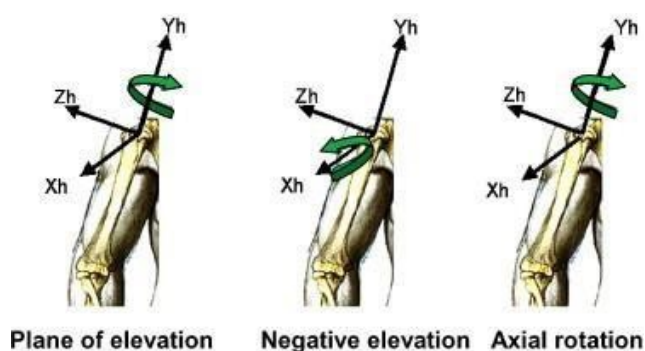


Figure 2. 9 Definition of thoraco-humeral rotations (Wu et al., 2005)

This sequence allows the second rotation (β , elevation) to pass through 90° without singularity. However, singular positions will occur at and approaching 0° and 180° (within 20°) of humeral elevation (Doorenbosch et al., 2003). Hence the assessment of the plane of elevation and axial rotation (1st and 3rd rotations) are mathematically inaccurate in these humeral elevation orientations. Furthermore, the Y-X-Y rotation sequence cannot feasibly evaluate humeral axial rotation with the arm at the side (Rundquist et al., 2003).

Alternative sequences have been proposed such as XZ'Y'' (Levasseur et al., 2007; Ludewig et al., 2000). This sequence describes the angle of elevation, angle of horizontal adduction/abduction and axial rotation and has the advantage of describing motion with 3 separate non-repeating axes. It has been recommended as the best sequence for evaluating elevation motions (Phadke et al., 2011). Senk and Cheze (2006) also evaluated the XZ'Y'' sequence and compared it to the YX'Y'' and YX'Z'' orders. Twelve anatomical plane shoulder movements were described by each sequence. Whilst the YXY sequence produced coherent results when movements avoided singularity positions, and the XZY sequence appeared to best describe anatomical abduction, none of the rotation sequences were found to be satisfactory for all movement variations. Thus, in order to obtain a complete clinical interpretation of shoulder movement, the aim of the individual assessment should be taken into consideration when selecting an appropriate rotation sequence.

2.4.2.4 Quaternions

Quaternions provide an alternative measurement technique that does not suffer from gimbal lock singularity issues. They are less intuitive than Euler angles but more

compact (facilitating faster computations) than matrices, however they are mathematically more complex (Deibel 2006, Hanson 2006, Herda et al., 2003). This section will cover the mathematical concepts relating to the use of quaternions to represent orientation attitude.

First devised by William Rowan Hamilton, an Irish mathematician in 1843, quaternions are defined as an extension to complex numbers that describes the quotient of two 3-dimensional vectors. A quaternion is a 4-tuple, concise representation of the form:

$$q_0 + q_1\mathbf{i} + q_2\mathbf{j} + q_3\mathbf{k} \quad (14)$$

where q_0 , q_1 , q_2 and q_3 are real numbers, and \mathbf{i} , \mathbf{j} , and \mathbf{k} are the fundamental quaternion units. This is commonly simply denoted as:

$$q = (q_w \ q_x \ q_y \ q_z) \quad (15)$$

A quaternion of this form can be viewed as the sum of a real number q_w (the real or scalar part of the quaternion) and a 3D-vector, $(q_x \ q_y \ q_z)$ in R^3 (the imaginary, or vector part). In its unit form, it can be used to encode any rotation in a 3D coordinate system. The scalar part specifies the amount of rotation that should be performed about the vector part. Specifically, if θ is the angle of rotation and the vector $(v_x \ v_y \ v_z)$ is a unit vector representing the axis of rotation, then the quaternion elements are defined as:

$$\begin{pmatrix} q_w \\ q_x \\ q_y \\ q_z \end{pmatrix} = \begin{pmatrix} \cos(0.5\theta) \\ v_x \sin(0.5\theta) \\ v_y \sin(0.5\theta) \\ v_z \sin(0.5\theta) \end{pmatrix} \quad (16)$$

Quaternions therefore represent a rotation of a certain number of radians around a three-dimensional vector (axis) so that the orientation of the object is transformed from the initial orientation to the final orientation. By selecting the correct axis and angle, any change of 3D-orientation of an object can be achieved.

In this work, orientation is represented as the 3D-rotation of the local frame to the global frame.

Let q_G^A be defined as the unit-quaternion representing a rotation of frame A relative to the global frame, G.

$$q_G^A = (q_w \ q_x \ q_y \ q_z)^T \quad (17)$$

Where T is the vector transpose operator. The unit quaternion, q_G^A , can be used to rotate an arbitrary 3D-vector (v_G) from the global frame to frame A:

$$v_A = q_G^A \begin{pmatrix} 0 \\ v_G \end{pmatrix} (q_G^A)^{-1} \quad (18)$$

As such, the vector v_G can be rotated by treating it like a quaternion with a zero real part and multiplying it by the unit quaternion and its inverse. The inverse of a unit quaternion is equivalent to its transpose, thus the vector elements $q_x \ q_y \ q_z$ are negated.

This operation requires quaternion multiplication which has its own, non-commutative definition as follows. The product of two quaternions

$q_1 = (q_{1_w} \ q_{1_x} \ q_{1_y} \ q_{1_z})$ and $q_2 = (q_{2_w} \ q_{2_x} \ q_{2_y} \ q_{2_z})$ is given by:

$$q_1 q_2 = \begin{pmatrix} q_{1_w} q_{2_w} - q_{1_x} q_{2_x} - q_{1_y} q_{2_y} - q_{1_z} q_{2_z} \\ q_{1_w} q_{2_x} + q_{1_x} q_{2_w} + q_{1_y} q_{2_z} - q_{1_z} q_{2_y} \\ q_{1_w} q_{2_y} - q_{1_x} q_{2_z} + q_{1_y} q_{2_w} + q_{1_z} q_{2_x} \\ q_{1_w} q_{2_z} + q_{1_x} q_{2_y} - q_{1_y} q_{2_x} + q_{1_z} q_{2_w} \end{pmatrix} \quad (19)$$

Alternatively, a unit quaternion can be used to construct a 3x3 rotation matrix to perform rotation in a single matrix multiplication operation (Baker, 2017). The resultant rotation matrix from the global frame, G, to the local frame, A using quaternion elements is defined as:

$$R_G^A(q_G^A) = \begin{pmatrix} 1 - 2q_y^2 - 2q_z^2 & 2q_x q_y - 2q_w q_z & 2q_x q_z + 2q_w q_y \\ 2q_x q_y + 2q_w q_z & 1 - 2q_x^2 - 2q_z^2 & 2q_y q_z - 2q_w q_x \\ 2q_x q_z - 2q_w q_y & 2q_y q_z + 2q_w q_x & 1 - 2q_x^2 - 2q_y^2 \end{pmatrix} \quad (20)$$

2.4.2.5 Converting Quaternions to Cardan/Euler Angles

The conversion from a quaternion to a Cardan/Euler angle representation utilises a mediatory rotation matrix as in equation 20. Similar to the definition of obtaining 3 sequential angles from a conventional 3x3 rotation matrix, the exact equations depends on the chosen order of rotations. For example, the Cardan angle sequence 'xy'z'' would result in the following equations:

$$\alpha = \arctan2 \left(\frac{2(q_w q_x + q_y q_z)}{1 - 2(q_x^2 + q_y^2)} \right) \quad (21)$$

$$\beta = \arcsin(2(q_w q_y - q_x q_z)) \quad (22)$$

$$\gamma = \arctan2\left(\frac{2(q_w q_x + q_y q_z)}{1 - 2(q_y^2 + q_z^2)}\right) \quad (23)$$

It should be noted that when converting quaternions to an angle representation, the *atan2* function should be used to generate all four-quadrant orientations (Baker, 2017). In addition, the gimbal lock problem still manifests in the resulting angles and is unavoidable when using Cardan/Euler angles, regardless of their derivation.

2.4.2.6 Expressing the orientation of a vector in a spherical coordinate system

As previously discussed, the Cardan/Euler angle representation of humero-thoracic joint orientation is problematic during certain movement ranges. A quaternion representation, whilst avoiding these issues, is non-intuitive and lacks clinical meaning. One method of describing the relative orientation of the humerus to the thorax in a meaningful way is to use a spherical coordinate-based system. These are also called spherical polar coordinates and are a system of curvilinear coordinates to describe positions on the surface of a sphere or a globe. The location on the globe is expressed in terms of altitude (or latitude) and azimuth (or longitude).

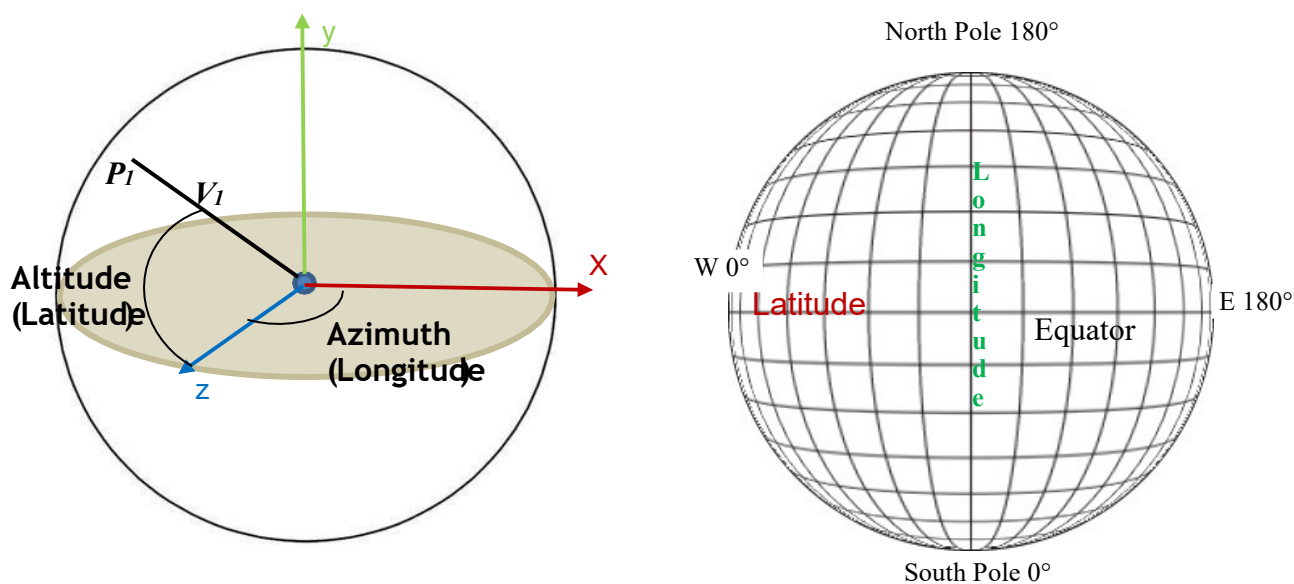


Figure 2. 10 Visualisation of spherical coordinate system using altitude (latitude) and azimuth (longitude) to describe the position of a point on the surface of a sphere/globe

The vector V_1 originates at the midpoint of the globe and is projected along the y-axis (figure 2.10).

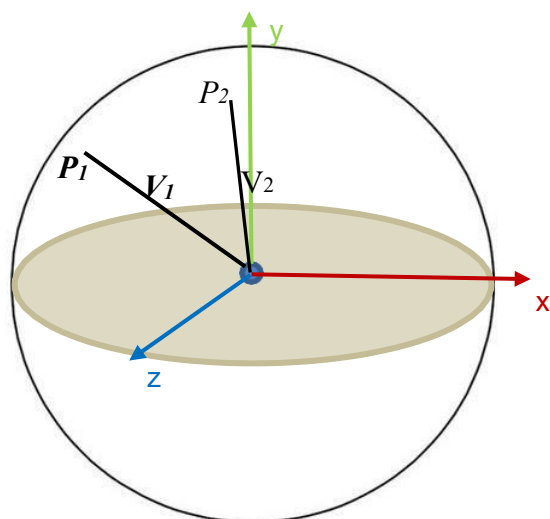


Figure 2. 101 Relationship between V_1 and V_2 in terms of Azimuth and Altitude.

With θ as the azimuth (longitude) angle in the x-z plane, and ϕ as the altitude (latitude) angle, the position of point p_1 , can be described on the surface of the globe and thus the orientation of the vector v_1 can be represented.

Using the operations in section 2.4.2.4, equation 18, we can rotate a 3D-vector by a unit quaternion. Applying a quaternion rotation to V_1 will produce a new vector orientation (V_2) with the new point p_2 projected on the surface of the globe (figure 2.11).

$$V_2 = x_2 y_2 z_2 \quad (24)$$

The coordinates of V_2 can be used to calculate the altitude (latitude) and Azimuth (longitude) of the new point, p_2 from the initial point p_1 :

$$\text{Azimuth } (\theta) = \arctan2(y_2, x_2) \quad (25)$$

$$\text{Altitude } (\phi) = \arctan2(z_2, \sqrt{(x_2)^2 + (y_2)^2}) \quad (26)$$

To visualise this method of describing the relative 3D-orientation of the humerus to the thorax, the globe is projected around the shoulder (figure 2.12), with its midpoint on the assumed centre of rotation about the shoulder and the coordinate axes are aligned with the predefined anatomical axes described in detail in the previous sections. In the anatomical position, with the arm down by the side, the humerus is represented by 3D-vector originating at the origin and projecting along the negative y-axis. Therefore, the altitude of the humerus vector in this position would be 0° , whilst with the humerus raised to directly above the shoulders centre of rotation it

would become 180° . The system is also defined such that the abduction plane corresponds to 0° azimuth whilst the plane of pure flexion is 90° and the plane of pure extension is -90° .

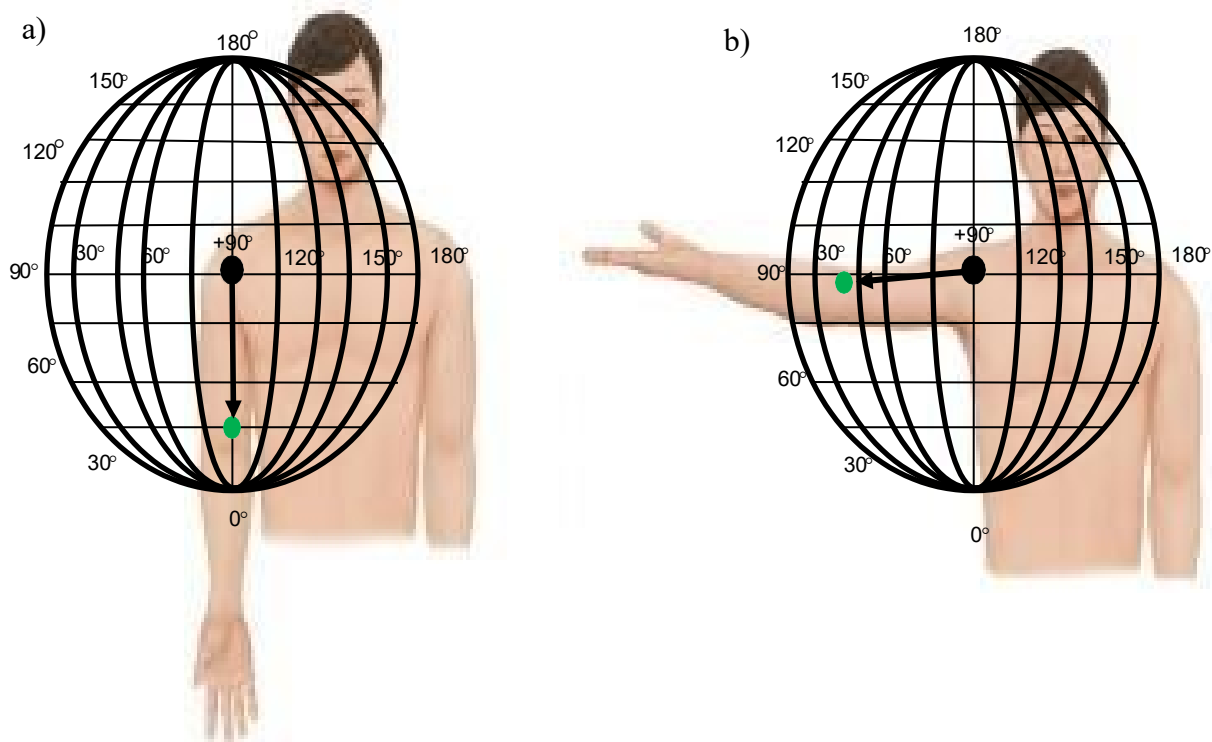


Figure 2.12 Humerus vector projected onto globe with centre at the centre of rotation of the shoulder in a) The anatomical position and b) 90° abduction

This method gives a coherent and meaningful means of describing the orientation of the humerus relative to the thorax during different movement tasks. The resultant altitude (latitude) represents the degree of elevation of the humerus from the anatomical position whilst the resultant azimuth (longitude) describes the plane in which the elevation occurs in. This method is free from the problems of gimbal lock and is more intuitive than a quaternion interpretation. The degree of axial rotation of

the humerus is not defined by either altitude or azimuth and the use of Cardan/Euler angles remains the most convenient way to obtain this information. In other words, while the polar method can describe the polar location of the humerus relative to the trunk, it does not inform us of the rotation of the forearm or the hand.

Chapter 3: Development of Android Application

Chapter 3

3 Development of Android Application

In this chapter, the development of a smartphone-based, wearable system intended to be used for shoulder joint angle measurements is described. An overview of the devices employed and a description of their sensing capabilities for determining spatial orientation will be given. In depth description of the application development will follow.

3.1 Introduction to Smartphone Technology

3.1.1 Use of Smartphones

In recent years, the rapid advances in mobile technology have led to the implementation of smartphones for clinical research and practice. Such devices are widely available and has become an essential everyday asset in modern life. The number of users is expected to exceed 2.5 billion worldwide by 2019 (Statistica, 2018). In the UK alone, the number of active smartphone users in 2015 was 41.09 million, over 63% of the population and this is forecast to increase by over 12 million users by 2020. As they are becoming increasingly affordable and have a number of high-performance sensors, it is now possible to easily acquire a handheld smartphone which has many of the computational and connectivity capabilities of a computer.

In the past few years, wearable smartwatch technology has grown in popularity and affordability (Statistica, 2018). Whilst early models were designed to do basis tasks such as calculations, digital time and date display and simple game playing, the current state of the art hardware can sync to a smartphone via Bluetooth

communication, have comparable sensing capabilities to a smartphone, and can function effectively as wearable computers. For everyday use, information and notifications from the smartphone can be displayed on the watch on the users' wrist and manipulated using voice recognition or haptic input. Users can wear the device throughout the day and this unique characteristic enables a wide range of possible healthcare applications including joint angle estimations.

3.2 Operating Systems

The two leading mobile operating systems on the market are Apple iOS and Google Android OS, accounting for 99% in all smart-device sales (Moontechnolabs, 2017). Android has consistently dominated the market by a significant percentage and Android run devices are cheaper compared to Apple devices and prices are continuing to fall year by year (Statistica, 2017).

An application can be developed natively for specific platforms or as a multi-platform application through web development. The application used in this project was developed specifically for the Android OS since devices running this OS are the cheapest and most used smartphones. Android is an open platform meaning that developed applications can be adapted for any device, including compatible tablets, smart-TVs and smartwatches. It is also open source, and code for existing applications is readily available and there are currently no approval processes for new applications to be freely released and uploaded for use in markets such as Google Play. This is in contrast to development and release of iOS applications which require a paid license from Apple.

3.3 Smartphone Inertial Sensors

3.3.1 Sensor Coordinate system

All of the above hardware sensors use the standard sensor coordinate system described below.

The coordinate system is defined as relative to the screen of the phone in a vertical position with the screen facing the user. In this description it is assumed that the axes are not transformed when the screen's physical orientation is changed and that the origin is central to the screen display of the device.

The positive X axis is horizontal to the screen and points to the right of the device when looking at the device screen, the positive Y axis is perpendicular to the X axis and points vertically upwards and the positive Z axis is formed from the cross product of the X and Y axis such that it points directly out of the front face of the screen. The axes x, y and z are commonly referred to as Pitch, Roll and Yaw, respectively (figure 3.1).

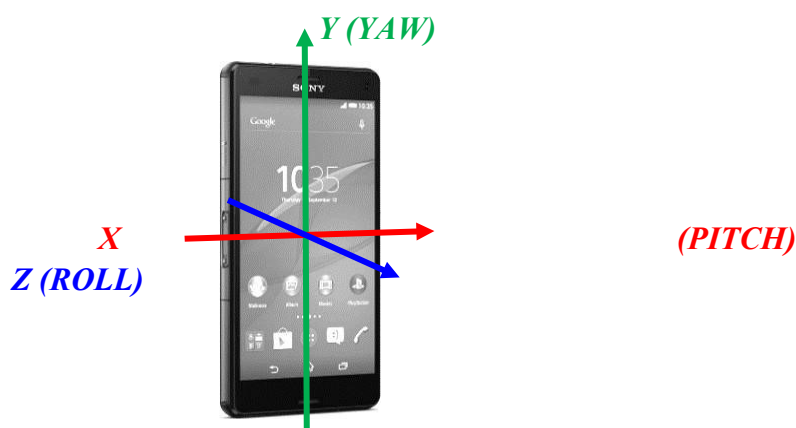


Figure 3. 1 Local coordinate system of an Android smartphone

3.3.2 Hardware Sensors

Most modern Android smartphones and some smartwatches contain the following inbuilt hardware sensors and are described in the Android API as:

- Tri-axial Accelerometer
- Tri-axial Gyroscope
- Magnetometer

The following sensor descriptions are used by the native Android API and apply in the resultant application.

The accelerometer sensor reports the acceleration of the device along the 3 sensor axes by measuring the total acceleration of the phone that typically results from compounding the gravity acceleration and the phone acceleration with respect to an earth-based frame of reference. For example, with the smartphone lying flat on the table and the screen towards the sky, the acceleration value along the z axis is -9.81ms^{-2} , This corresponds to the acceleration of the device (0ms^{-2}) minus the force of gravity (-9.81ms^{-2}), In this same position, applying a force to its left side towards the right will result in a positive acceleration value in the x axis. Accelerometer readings are calibrated using temperature compensation, online bias compensation and online scale calibration.

The magnetic-field sensor senses stability of the 3-dimensional plane by measuring the environmental magnetic field force along the 3 sensor axes in micro- Tesla (uT). The readings are calibrated using temperature compensation, online hard-iron calibration and factory (or online, real-time) soft-iron calibration to counter distortions of the earth's magnetic field by external magnetic influences. Hard-iron distortion is produced by materials that exhibit a constant, additive field to the output

of each of the magnetometer axes, for example, a speaker magnet. In contrast, soft-iron distortion is the result of material that influences a magnetic field but does not necessarily generate a magnetic field itself for example, iron and nickel.

The rate of rotation around the 3 sensor axes is measured with the gyroscope sensor. Rotation is positive in the counterclockwise direction and all values are in radians per second (rads^{-1}). Gyroscope readings are calibrated using the same methods as for the accelerometer and in this case, online bias calibration is used to remove drift in which the drift (bias) and noise are monitored and compensated for using information from the accelerometer and magnetometer.

3.3.3 Sensor Fusion

Each of the above mentioned sensors cannot reliably be used in isolation to estimate the position and orientation of a device due to their individual inherent errors. Accelerometer data lacks precision if the device is static and not placed on a solid surface as the sensors lack the ability to differentiate between dynamic acceleration and gravity. Furthermore, when the device is flat on a table, the accelerometer is unable to distinguish the different horizontal orientations. There is an inherent lack of reliability due to the requirement of positional information, which is a double integral of acceleration and hence even small errors in acceleration cumulate to give large errors in the position. Magnetometer sensors are susceptible to error due to magnetic interference in the environment and require time to settle (Roetenberg et al., 2009). The gyroscope (if present) can be integrated to obtain a more accurate representation of the phone orientation however they can also be prone to drift and noise accumulation over time and suffer the same lack of reliability as accelerometers through integration of the signal.

Sensor fusion aims to derive accurate data by deriving it from a combination of sensors, improving the quality of the measurements of each individual sensor through continuous calibration procedures. Within the Android API, software sensors use native software algorithms to perform sensor fusion and derive their data from one or more hardware sensors with the aim of optimising the quality of individual sensor measurements.

3.3.4 Software Sensors

The Android API implements fusion as a variety of software-based sensors which combines data from the underlying physical sensors. One such sensor is the Orientation Sensor (`SENSOR_TYPE_ORIENTATION`) which reports the orientation of the device in degrees around the X, Y and Z axis using the accelerometer, gyroscope (if available) and magnetometer. The orientation sensor was deprecated in API level 8 and replaced with the Rotation Vector Sensor.

(`SENSOR_TYPE_ROTATION_VECTOR`) - This software sensor is the most frequently used sensor for motion detection and monitoring due to its versatility in monitoring angular changes for different functions such as camera stabilisation or augmented reality applications. The Rotation Vector Sensor uses the gyroscope as the main orientation change input and integrates the accelerometer and magnetometer input to compensate for gyroscope drift.

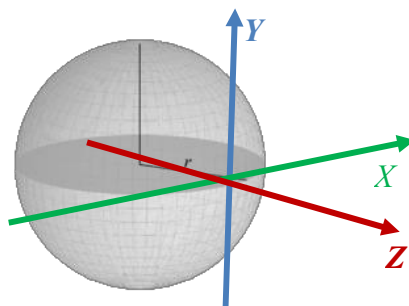


Figure 3. 2 World, North-East-Up Coordinate frame

Orientation of the device is estimated by the rotation vector as relative to the North-East-Up world coordinate frame. This system is defined as a direct orthonormal basis where X points East and is tangential to the ground, Y is tangential to the ground, perpendicular to X and points North, and Z is perpendicular to the ground and points towards the sky (figure 3.2). This coordinate system is always fixed independently of the orientation of the device. The orientation is described as the rotation necessary to align the World coordinate frame with the devices embedded reference frame (XYZ to xyz). By rotating the phone by an angle θ around an axis to go from the reference (East-North-Up aligned) orientation to the current phone orientation, the rotation can be described as a unit quaternion composed of four unit-less components, x, y, z and w. This can be represented as 4 sensor events:

$$\text{sensors_event_t.data}[0] = \text{rot_axis.x} * \sin(\theta/2)$$

$$\text{sensors_event_t.data}[1] = \text{rot_axis.y} * \sin(\theta/2)$$

$$\text{sensors_event_t.data}[2] = \text{rot_axis.z} * \sin(\theta/2)$$

$$\text{sensors_event_t.data}[3] = \cos(\theta/2) \quad (27)$$

Where rot_axis.x , rot_axis.y and rot_axis.z are the world coordinates of a unit vector which represents the rotation axis and θ is the rotation angle.

The Rotation Vector quaternion can alternatively be expressed in the form of a 3x3 rotation matrix and as a Euler Angles representation. The formulas for converting between each of these representations are described in chapter 2.

3.4 Smart Devices used in this work

In this study, two smartphone models were used: the Sony Xperia Z3 Compact (Sony Corp., Japan) and the Samsung Galaxy SIII (Samsung, South Korea). The Sony smartphone is a commercially available Android device with sensor specifications that meet the requirements to enable this study, including hardware triaxial accelerometer, gyroscope and magnetometer sensors. The Samsung Galaxy SIII is also a commercial Android smartphone with similar specifications to the Sony model.



Figure 3. 3 a) Sony Xperia Z3 Compact b) Samsung Galaxy SIII

The smartwatch used in this research was the LG Watch Urbane (LG, Japan), a commercially available device with specifications compatible with the requirements of this study including hardware triaxial accelerometer and gyroscope sensors. Full specifications of all models can be found on www.gsmarena.com (accessed October, 2018).



Figure 3. 4 LG Urbane Smartwatch

3.5 Development of Android Application

3.5.1 Key features of the application

Both an android smartphone application and an Android Wear application were developed that could be employed to a smartphone and a smartwatch respectively. The main aim of the developed applications was to record the orientation of a device as reported by the Rotation Vector Sensor of the Android OS. The resultant applications therefore had the following key features:

- (i) A cross-platform application suitable as a stand-alone application for both a smartphone and a smartwatch.
- (ii) Sensor listener service to return the Rotation Vector Sensor (software sensor) readout for sensor data extraction
- (iii) Storage of extracted data in the form of a timestamped unit quaternion in .csv format in the internal storage of the device
- (iv) Bluetooth connectivity between the smartphone and smartwatch to allow for
 - a. Timestamped synchronisation of the data captured by each device
 - b. Transfer of stored data from the watch to the phone, to facilitate the transfer of smartphone and smartwatch data to a PC for post-processing.

- (v) Minimum data sampling rate of 60Hz. This was determined by review of the literature using sensors to measure upper limb movement in which this sample rate is generally accepted as within the acceptable range (Roetenberg, 2006; Perez et al., 2010; Xsens, Netherlands). This is required to allow adequate comparison of the developed application to Gold Standard measurement tools as described in chapter 4 and 6.

The next sections will give a detailed description of the development of the application. The programming scripts can be found in full in Appendix A.

3.5.2 Development Environment

The application was developed in Visual Studio 2015. Visual Studio is an integrated development environment from Microsoft (USA) that can be used to build native Android and Android Wear applications using C# and Xamarin (Microsoft, USA), whilst making all of the native Android API functionalities available to the programmer. The applications were initially simulated on an Android emulator which provides a comparable performance to an actual device allowing the programmer to test applications for any Android platform, screen resolution and other hardware properties before deployment to a physical device.

3.5.3 Graphical User Interface

The graphical user interface was developed in Visual Studio as axml files. The axml version used was 1.0 and the encoding was “utf-8”. Different layout templates provided by the Android namespace can be used for different screen specifications of various devices. Figures 3.5 and 3.6 show the graphical user interface of the phone and smartwatch applications respectively in a wireframe representation.

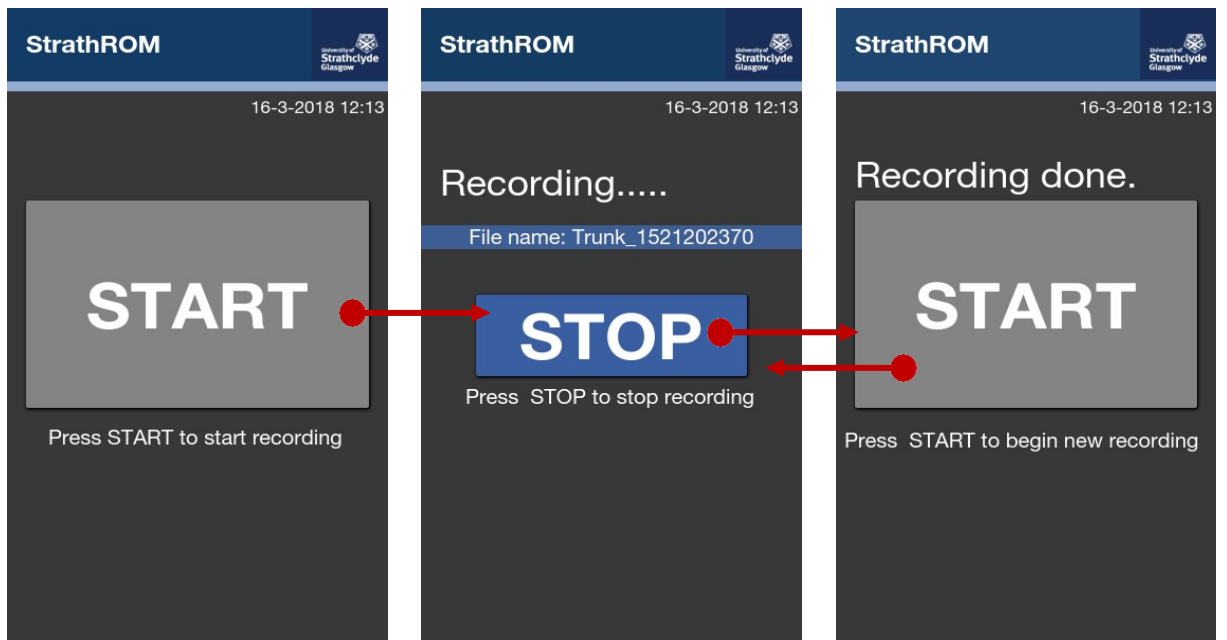


Figure 3. 6 Graphical User Interface of Smartphone Application and interactions between each screen.



Figure 3. 5 Graphical User Interface of Smartwatch Application showing interactions between each screen.

3.5.4 Sensor Delay Rate

The data delay controls the interval at which sensor events are sent to the application.

The sensor delay rate used in the application is the *fastest* speed, as specified by the Android API. To tests how many samples are collected from a sensor with this setting, the data from the rotation vector was saved to .csv file with the correspondent timestamp in nanoseconds. Using the following calculation, the average sample rate can be estimated:

$$[1000/(((Last\ timestamp\ point - First\ timestamp\ point) / \Sigma points) / 1,000,000)]$$

For smooth movements, the smartphone used (Sony Xperia Z3 Compact) collected data at a frequency of 125Hz and the smartwatch used (LG Urbane) at a frequency of 198Hz. The sensor delay rate is limited by factors such as the intrinsic sample rate of the individual hardware sensors, which may vary between devices, as well as the rate at which the application samples the rotation vector sensor. It should be noted that the sample rate is non-uniform, however and the sample frequencies calculated are based on the estimated average sample rate. On closer investigation of the absolute sample frequency, the number of samples per second differed by 2-3 samples over a measurement period of 30 seconds continuous smooth movement, indicating that the calculated average sample frequency was adequate for this application and would not result in loss of data.

3.5.5 Storage of recorded rotation vector data

The unit quaternion representing the event values of the rotation vector sensor is saved to a .csv file in the internal storage of the device itself. When the user presses the ‘ON’ button on the user interface, the application begins recording the rotation vector sensor data, line by line, to the file created. The file line format is shown in figure 3.7.

UnixTimestamp	Qx	Qy	Qz	Qw
----------------------	-----------	-----------	-----------	-----------

Figure 3. 7 File line format

Conversely when the user presses the ‘OFF’ button on the user interface, the application ceases to record the sensor data and the file is closed and saved to the

internal storage of the device. A block diagram of the Android application is shown below.

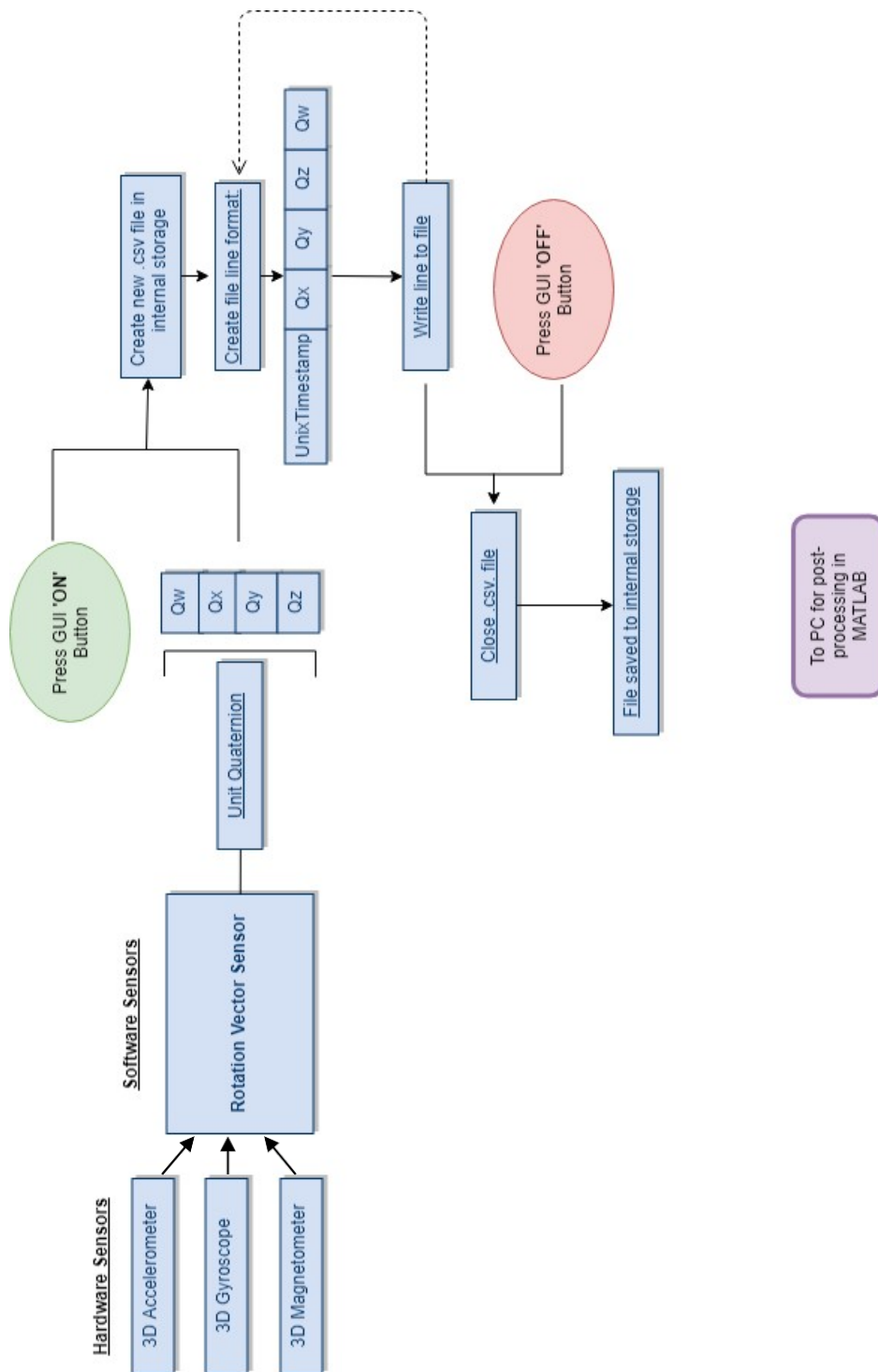


Figure 3. 8 Block diagram of Android application

3.5.6 Transfer of data to a PC for post-processing

The LG Urbane smartwatch has integrated functionality to be easily connected to a compatible Android smartphone via Bluetooth® 4.1 Low Energy with no additional programming required to establish a connection. With the Bluetooth activated on both the smartphone and the smartwatch, the Android Wear application on the phone should be opened and the user should tap on the watch's name as it appears. This will generate a pairing code on both devices. If the codes match, the user should tap "Pair" on the smartphone to initiate the pairing process. After a few minutes the connection will be ready and this will be indicated in the Android Wear application on the smartphone.

To facilitate the transfer of data files from the smartwatch via Bluetooth to the smartphone, a File Manager application that is compatible with Android Wear was employed (*File Manager for Android Wear v1.0.7, John Li, China, 2015. Available on GooglePlayServices*). The data was transferred to an allocated file directory within the internal storage of the smartphone.

Data from the smartphone was then transferred to a PC or laptop via USB connection.

3.6 Post-processing to obtain 3-dimensional angles from rotation vector data

Post-processing of the raw data was conducted in MATLAB (Mathworks, USA) and involved converting the unit quaternion (q_w, q_x, q_y, q_z) into three sequential Cardan angles, which give a more intuitive representation of the degree of rotation about

each of the three axes in the global coordinate system as described in Chapter 2, section 2.4.2.5.

Further system architecture of the developed Android application as a tool to measure human shoulder range of motion is described in detail in chapter 4.

Chapter 4: Performance Characterisation of the Android Application to Measure Angular Data

Chapter 4

4 Performance Characterisation of the Android Application to Measure Angular Data

Preliminary characterisation of the resultant application was carried out to evaluate:

- (1) The offset, accuracy and precision of the device to estimate static angular orientations and the repeatability of these measurements
- (2) The accuracy, precision, frequency response and repeatability of the device during dynamic movement compared to a free-swinging pendulum and a servo-powered gimbal system.

4.1 Static Protocol

5 Sony Xperia Z3 handhelds and 1 Samsung Galaxy SIII handheld were tested under the same conditions. The static protocol was tested on multiple Sony devices as well as one Samsung device to evaluate any offset in the orientations reported by each individual device and model for the same known absolute and relative angles. The LG Urbane smartwatch was also tested using the same protocol.

A Bosch GAM 270 MFL Professional Angle measurer (Bosch-Professional GmbH, Germany, accuracy $\pm 0.1^\circ$) was used to evaluate the accuracy and precision of the smartphone sensors and software under static measurement conditions (figure 4.1).



Figure 4. 1 Bosch GAM 270 MFL Professional Angle measurer with smartphone attached in three orientation to measure a) rotation about pitch axis, b) rotation about roll axis, c) rotation about yaw axis

All tested devices were fixed using an adjustable elasticated strap on the arm of the Bosch angle measurer that was placed on a flat, horizontal surface. Horizontal orientation of the reference arm was verified by the Bosch measurer itself. The devices were fixed in different orientations on the arm to evaluate each of the three axes, Pitch, Roll and Yaw. The GAM 270 MFL arm was used to reproduce known angular positions from 0° to 180° in steps of 20° , with a stop of ten seconds at each position. For the Yaw axis, the start angle was altered to 20° , due to the difficulties of rotation sensors calibration, discussed in the section 3.3.2. This was repeated three times for each axis. All tested were performed in stable conditions (20°C , absence of

vibration, minimal magnetic interference). Data from all devices was processed in MATLAB to obtain angle data as described in chapter 2, section 2.4.2.5.

4.2 Dynamic movement Protocol

4.2.1 Free-Swinging Pendulum

A pendulum that had previously been designed and manufactured (Chan, 2014) was used. The pendulum has a low friction potentiometer (Vishay Spectrol 157) securely attached to the rear of its solid upright to measure angular displacement of the pendulum arm, and was connected to a 5V power supply. A Genuino MEGA 2560 board (Arduino, Italy) was used for 8bit analogue-to-digital conversion at a sampling frequency of 60Hz, and connected to a laptop for data collection and storage. The zero position was measured with the pendulum arm at rest and the pointer attached to the top of the arm pointing vertically upwards. A 360° protractor mounted to the solid upright, and centralised to the fulcrum of the pendulum arm was used to visually verify the zero position. The pendulum was calibrated over a range of angles from $\pm 90^\circ$.

One Sony Xperia Z3 Compact was validated using the free-swinging pendulum. The smartphone was attached to the pendulum arm using a thick Velcro strap, ensuring the posterior side of the smartphone was flush against the pendulum arm. It was attached in three different orientations to record rotations around each of the three local axes of the smartphone (figure 4.2). At the beginning of each trial, the pendulum arm was manually rotated from the rest position to 90° before being released to swing freely.

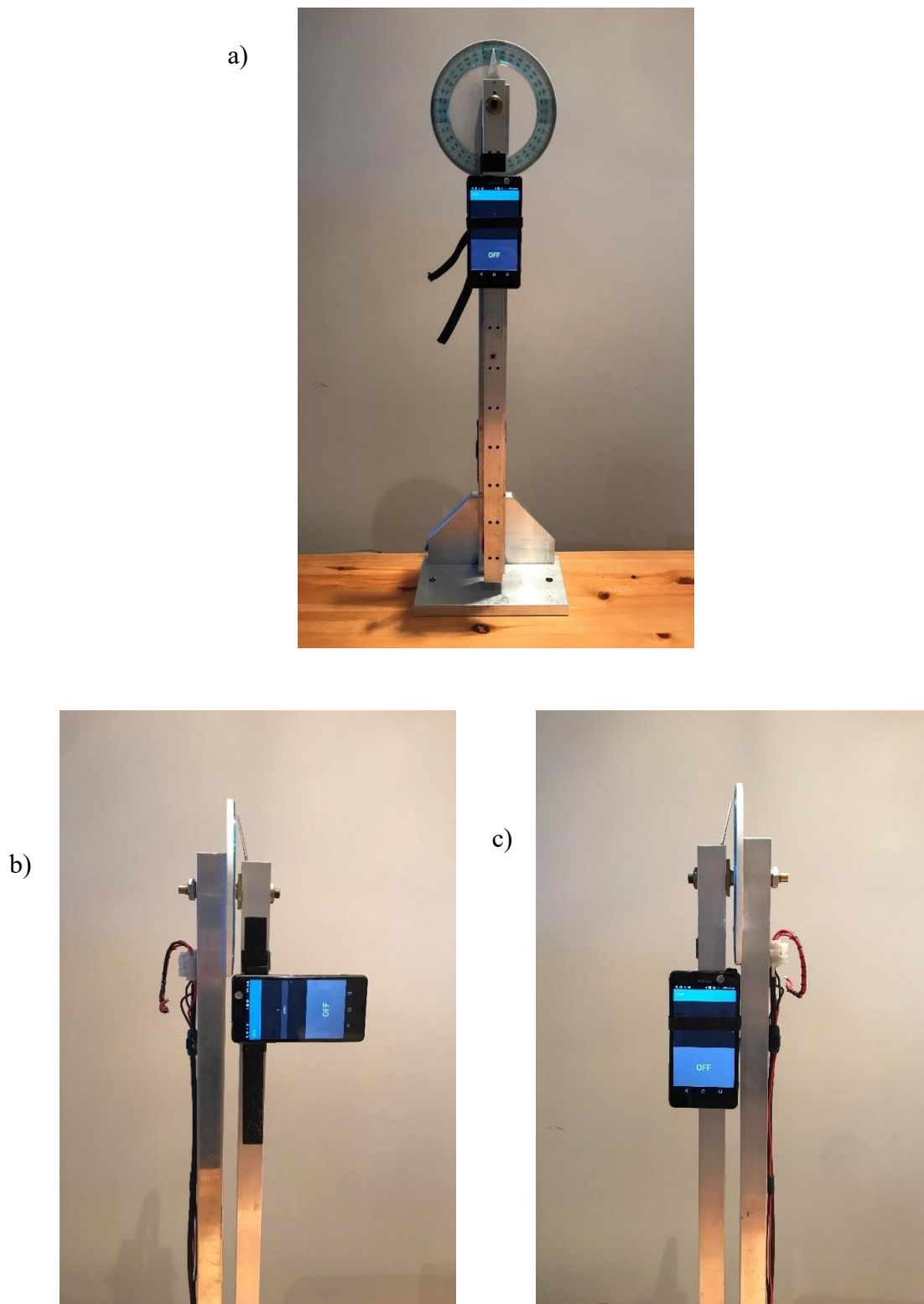


Figure 4. 2 Free-swinging pendulum with smartphone attached in three orientations to measure a) rotation about yaw axis, b) rotation about pitch axis, c) rotation about roll axis

4.2.1.1 Potentiometer calibration

To determine the relationship between the angle of rotation of the pendulum arm and the corresponding potentiometer voltage output, the calibration method as described by Chan, 2014 was conducted. For this, the pendulum arm was manually displaced in increments of 10° from -90° to $+90^\circ$ (relative to the zero position), and the corresponding potentiometer voltage at each increment recorded. The potentiometer voltage output was plotted against the angular rotation of the pendulum (Figure 4.3), and a straight line was fitted to the curve and the mean R-squared value was calculated to ensure that there was a linear response. The repeatability of the potentiometer measurements had already been verified with a linear response of 5 trials mean R-squared value of $0.999 (\pm 2.48 \times 10^{-5})$, (Chan, 2014). This indicates that the potentiometer would provide a sufficiently accurate angle measurement with which to validate the smartphone system data in this study.

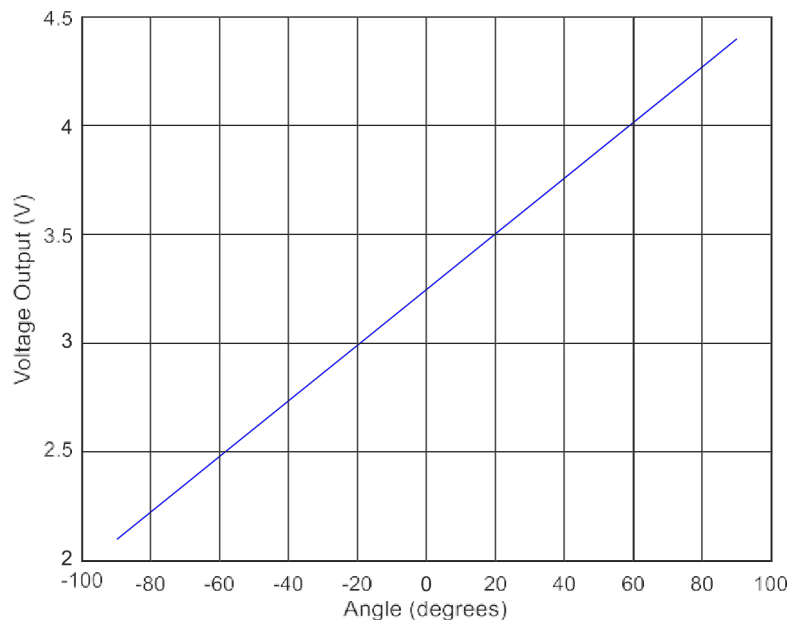


Figure 4. 3 Calibration curve of low friction potentiometer of varying pendulum arm angular displacement from -90° - $+90^\circ$.

4.2.1.2 Accuracy and repeatability

In each orientation (figure 4.2), the smartphone was secured to the arm with its midpoint 100mm distal to the fulcrum. The pendulum was allowed to swing freely until rest during each trial. Five trials were recorded for each orientation.

4.2.1.3 Sensitivity to out-of-plane rotation

During each of the above trials, the orientation data from each of the smartphone axes was observed to assess for any potential crosstalk between the axes during single plane rotation.

4.2.1.4 Post-processing and data analysis

Potentiometer data recorded during each trial was recorded and stored directly to the connected laptop. Smartphone data was processed in MATLAB to obtain 3-dimensional angle data as described in chapter 2, section 2.4.2.5 Smartphone data was resampled to 60Hz in MATLAB and compared to the potentiometer data in Excel.

4.3 A servo-powered gimbal system

4.3.1 Development and design

A servo-powered gimbal system was designed and manufactured with dimensions as shown in figure 4.4 to figure 4.6 to investigate the frequency response of the Sony Xperia Z3 and LG Urbane smartwatch during controlled movements in multiple axes. To facilitate this, the system was designed to incorporate two, motor-powered tilting frames with orthogonal pivot axes.

The system was therefore comprised of the following key features:

- (i) An aluminum frame composed of 12 aluminium profiles (KJN, UK) with an outer and an inner frame secured to a wooden base by two of the

profiles. The outer frame provides structure and stability to the system and two attachment points for the rectangular-shaped inner frame. The inner aluminium frame attaches to the outer frame via two points. The first point of attachment is central to one side of the rectangular frame directly by a low friction bearing to allow free planar rotation of the inner frame relative to the fixed outer frame. The second point of attachment is to the centre of the opposing side of the rectangle via a servo, housed within a custom-designed plastic casing. Plastic casing was designed in Rhinoceros and printed in PLA using an Ultimaker 3D. The casing is firmly attached to both the outer and inner frames by 6mm screws, to facilitate the secure fixation of the servo body to the outer frame and of the servo arm to the inner frame. This architecture allows the inner frame to pivot in a single plane orthogonal to the outer frame, controlled by the servo motor.

- (ii) A central custom-fit plastic mount was designed in Rhino and 3D-printed in 1.75mm PLA material using an Ultimaker2⁺ 3D printer (Ultimaker, The Netherlands). The mount formed the innermost part of the system. It was attached to the inner aluminium frame similarly as the attachment of the inner frame to the outer frame via a low friction bearing. The points of attachment on the inner frame for the central mount were on the two sides of the rectangular frame free attachment to the outer attachment. Plastic casing for the second, smaller servo was fixed to the inner frame and the arm of the servo attaches directly to the central mount via an attachment point incorporated into the design of the mount.

- (iii) Two metal-gear servos (HS-5765MH and HS-85mg, Hi-Tec, RCD USA, Inc.), connected to a 6V power supply and Maestro (Pololu, USA)) servo driver controlled the movement of the gimbal frame axes. Both servos had a maximum angular velocity of of $375^\circ/s$, which. The servos were housed in custom-3D-printed housing, which were attached to the aluminium frames as described above. The plastic housings were attached to the centre of the relevant side of the frames such that the servo could be similarly fixed to the centre of relevant side of the next inner portion of the system. The servos were securely attached attached using long metal 6mm screws to ensure no relative movement between the servo and the tilt frame.
- (iv) An Arduino Mega controller (Arduino, Italy) was used to control the Maestro driver and collect timestamped feedback on the angular position of each servo. Figure 4.4 a) HS-5765MH metal gear servo and dimensions, b) HS- 85mg metal gear servo and dimensions.

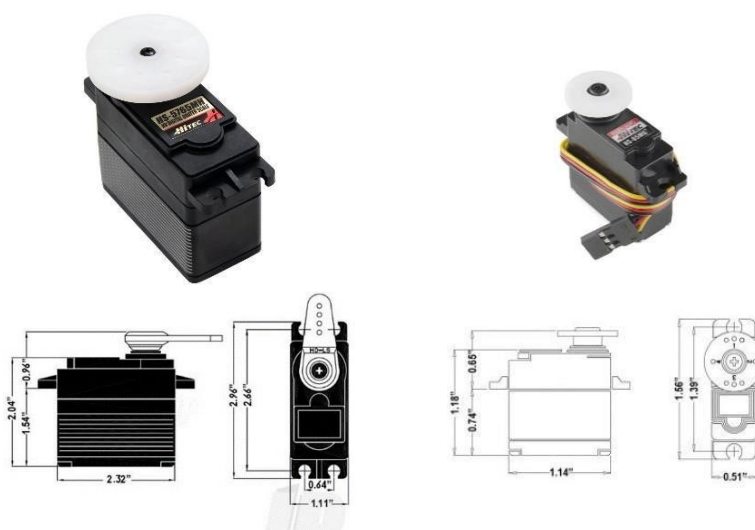


Figure 4. 4 Metal gear servos used. All dimensions in inches. Pictures from HiTec

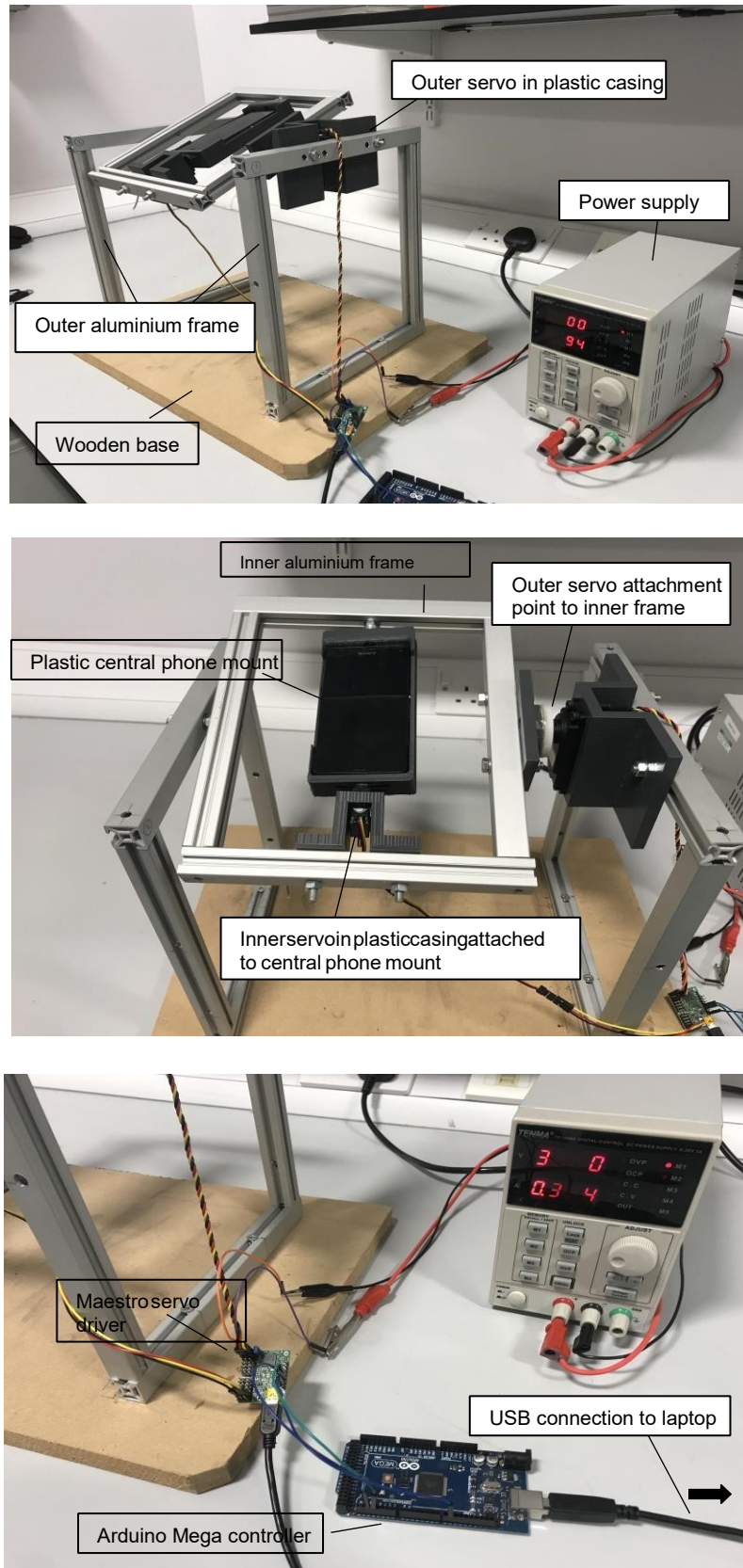


Figure 4. 5 Set up of servo-powered gimbal system

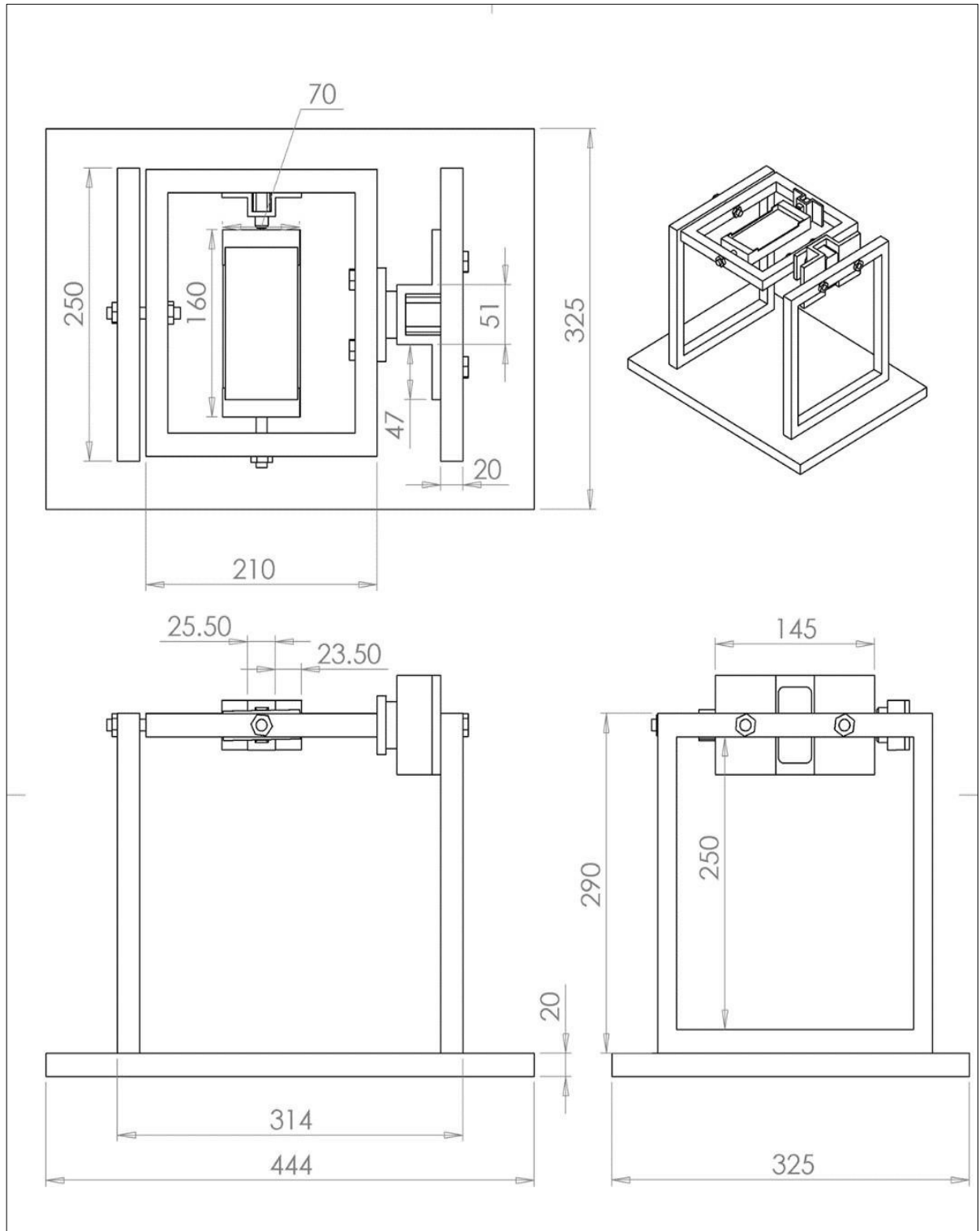


Figure 4. 6 Dimensions and design of aluminium frame, tilt table and plastic servo-housing

4.3.2 Frequency response

A repetitive oscillation was generated using a sinusoidal wave at a range of amplitudes and frequencies within the constraints of the servo specifications. An amplitude of 10° was used, allowing a maximum frequency of the sinusoidal wave of 6.8Hz, equivalent to an angular velocity of $375^\circ/\text{s}$ of rotation. The frequency range used was 0.1Hz to 6.8Hz. 10 periods per frequency were recorded with a stop of 5 seconds between each frequency per trial.

This protocol was carried out 5 times for each axis in a single day and once a day for 5 consecutive days in the same stable, controlled conditions as the static protocol.

The system was operated on a flat, horizontal surface and the orientation reported by the phone was recorded before each trial to account for any offset presented by the system.

4.3.3 Continuous measurements over a 3-hour period

Two frequencies within the optimal range identified in the frequency response trials (0.68Hz and 1Hz) were used to create a repetitive oscillation in the pitch and roll axes for a 3-hour period. A Sony Xperia Z3 and the LG Urbane smartwatch were tested under these conditions. Data was continuously recorded by each device for the entirety of the 3-hour test period. The first 10 periods of each frequency in each axis at 15 minute intervals was extracted for post processing (12 time-point samples). Comparisons of the mean amplitude and the time-phase relationship to the servo data was conducted between each of the time-points sampled.

4.3.4 Post-processing and data analysis

All smartphone and smartwatch data were resampled to 60Hz and post-processed to obtain angular data as in MATLAB 2017b (The MathWorks Inc, USA). The mean amplitude recorded at each frequency was used to compute a logarithmic ratio for frequency response estimation.

4.4 Results

4.4.1 Static Measurements

4.4.1.1 Absolute orientation

Figure 4.7 shows the angle reported by the processed smartphone data when placed in a known, absolute zero position on the Bosch angle measurer in each orientation. A one-way ANOVA test found a statistically significant difference between the device data and the Bosch tool in each orientation was found for all of the devices tested ($p < 0.05$) as shown in table 4.1. Furthermore, the angle reported by each device when placed in the same known physical orientation differed between devices. The low standard deviation values between repeated measures with each device indicates that this difference is repeatable. This suggests that characterisation of angular data reported by a device should be done at an individual device level rather than at a manufacturer and model level, to account for any offset from the known, absolute orientation.

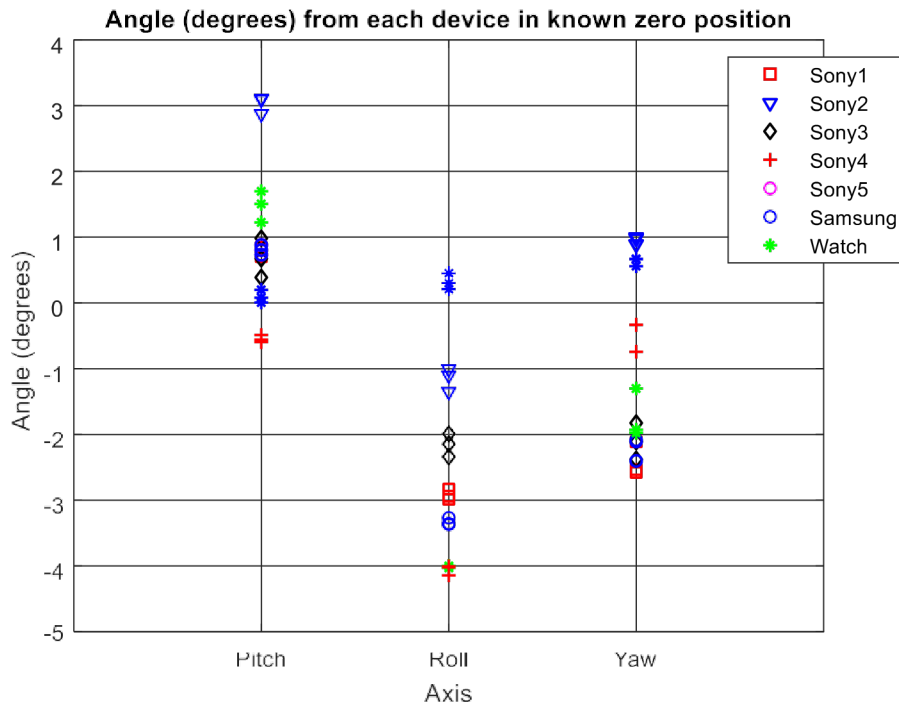


Figure 4. 7 Offset from known zero position reported by each device. Yaw values have been normalised to a 0° reference for interpretation

Table 4. 1 Mean angle and standard deviations of angles (in degrees) reported by each device in a known zero position of the Bosch measurer tool. One-way ANOVA test was used to determine if differed from the Bosch tool reference significantly. *p<0.05

Device		Pitch	Roll	Yaw
Bosch		0	0	0.000
Samsung	Mean	3.0268*	1.155*	0.959*
	SD	0.132	0.176	0.057
Sony 1	Mean	1.4758*	1.36*	1.249*
	SD	0.238	0.199	3.894
Sony 2	Mean	0.805*	3.329*	2.199*
	SD	0.074	0.055	0.176
Sony 3	Mean	0.547*	0.541*	2.368
	SD	0.054	0.075	2.509
Sony 4	Mean	0.68*	0.684*	0.976*
	SD	0.298	0.421	1.928
Sony 5	Mean	0.792*	0.767*	1.002*
	SD	0.077	0.089	2.591
SD Smartwatch	Mean	0.094	0.102*	0.325*
	SD	0.097	0.136	0.180

4.4.1.2 Relative orientation

Table 4.2 shows the mean angle difference reported by the devices between each known 20° step (0° to 180°) in each attachment orientation to the Bosch angle measurer arm. Although statistically significant differences were found for three of the Sony Xperia devices in the roll axis and one in the yaw axis, each device was able to accurately estimate the change in angle in all three axis within $\pm 1.1^\circ$. The low standard deviation values also indicate the repeatability of the smart device measurements when compared to the Bosch tool.

Table 4. 2 (Mean) Relative orientation in degrees (and standard deviations) reported between each 20° step by each device tested. One-way ANOVA test was used to determine if differed from the Bosch tool reference significantly. * $p < 0.05$

Axis	PITCH	ROLL	YAW
Sams	19.76±0.88	19.87±1.68	19.55±1.31
Sony 1	19.88±1.07	21.04±1.11*	19.53±1.125
Sony 2	19.87±1	20.65±0.81*	19.77±0.65
Sony 3	19.89±0.65	19.06 ±0.58*	19.48±1.02
Sony 4	19.83±0.61	19.73±1.08	19.36±0.67*
Sony 5	19.75±0.6	20±1.63	20.25±0.66
Watch	19.93±0.74	20.08±0.56	20.24±0.94

Figure 4.8 shows graphs of the mean angle (°) reported by one Sony Xperia Z3 and the LG Urbane smartwatch against the known angle reported by the Bosch tool for each axis. The graphs shows a strong, positive linear association between both devices and the Bosch tool. When evaluating the angular difference between steps in the yaw axis, the initial position was 20°. This approach was taken as it is known that the algorithm used to calibrate the rotation sensors works on assumptions of gravity (chapter 3, section 3.3.3). When the local coordinate system of the embedded sensors

of the device is aligned to the world axes, the yaw axis of the device lies parallel to the vector of gravity. This prevents the inertial sensors from obtaining a reference for calibration from the angle around the yaw axis. It is apparent in figure 4.8(c), that the initial angle reported by the smartphone and the smartwatch differs substantially from both the known angle (20°) and each other (68° and 158° respectively), given the difficulties in obtaining a reference ‘zero’ position. However, the relative orientation between successive 20° steps showed strong agreement between the devices (table 4.2).

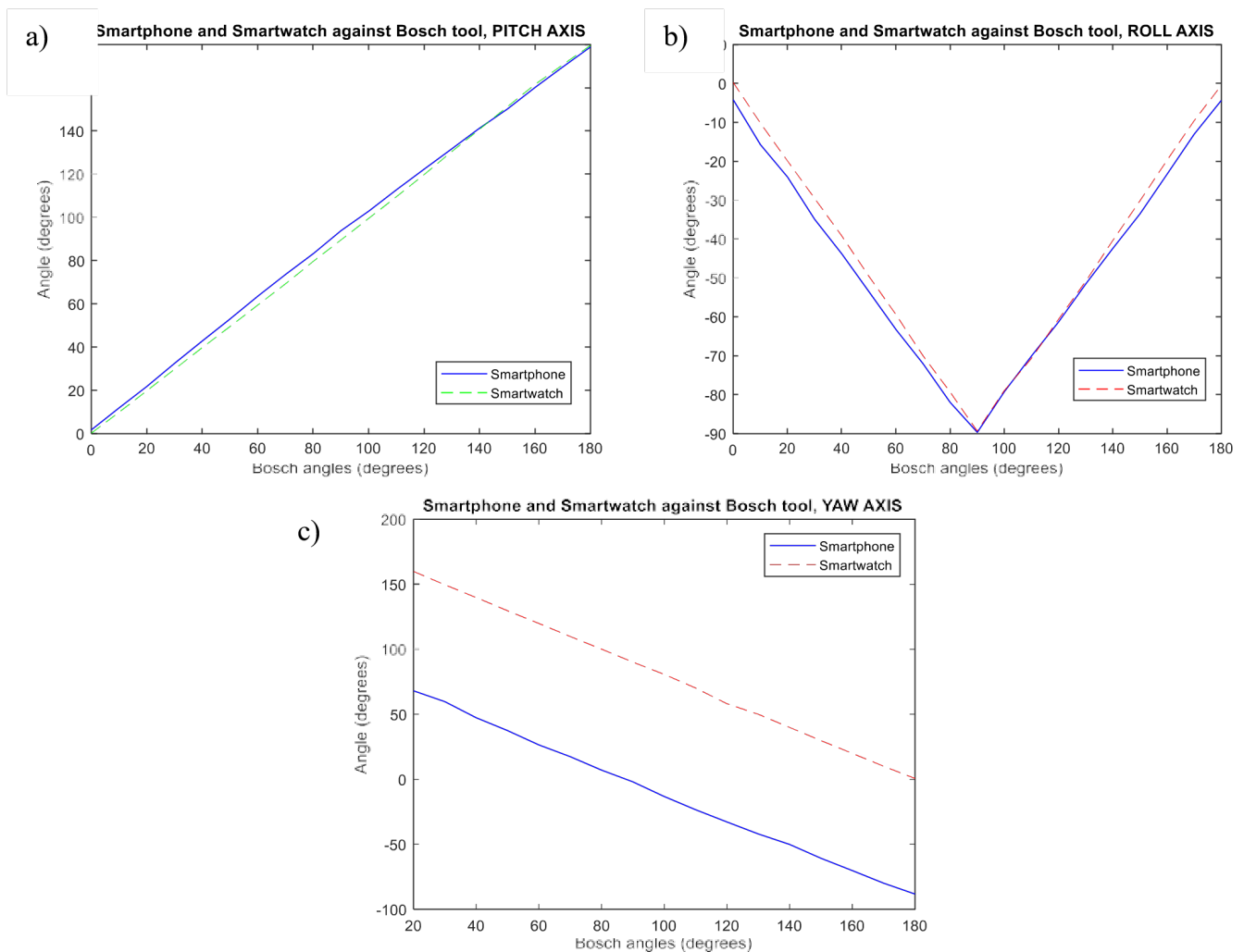
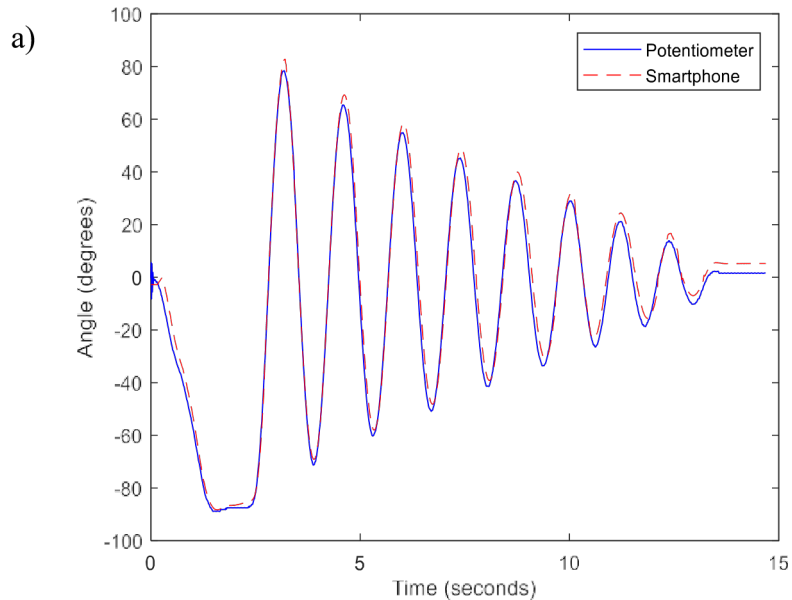


Figure 4. 8 Angles reported by smartphone and smartwatch in 20° steps in a) pitch, b) roll and c) yaw axes.

4.4.2 Free-swinging pendulum

4.4.2.1 Accuracy and repeatability

Figure 4.9 shows a graph of angle ($^{\circ}$) plotted against time (seconds) for the processed smartphone output and the potentiometer output in orientation A, B and C, 100mm from the fulcrum of the pendulum during free swing movement. The graphs shows that for this condition, the orientation recorded by the phone closely follows that recorded by the potentiometer in each of the three axes tested. The smartphone data appears to be accurate in both time-phase and amplitude when compared to the potentiometer. From the potentiometer calibration protocol validated by Chan (2014), it is indicated that the potentiometer data is accurate and reliable, and therefore the result graphs indicate that the smartphone data is also accurate.



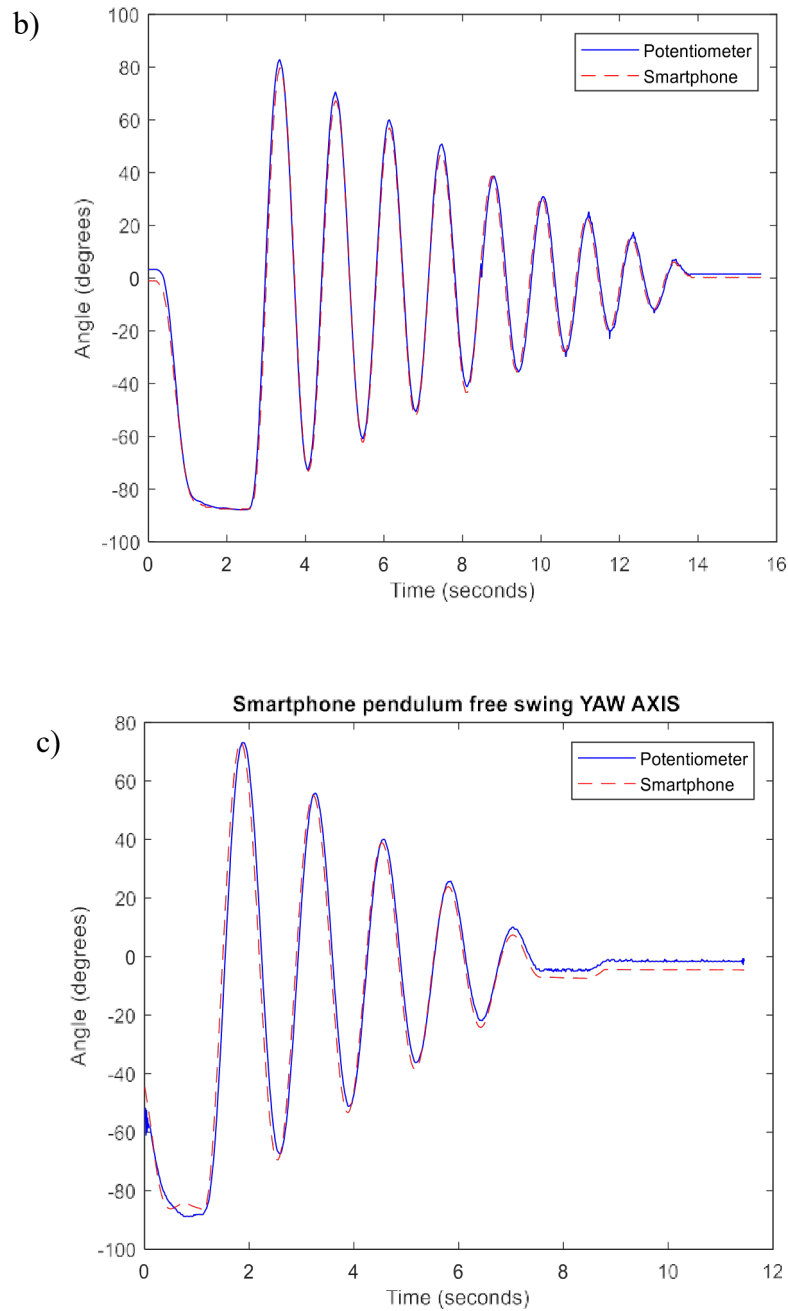


Figure 4. 9 Example from 1 trial of angle ($^{\circ}$) recorded by the smartphone compared to the potentiometer during free-swinging pendulum movement in a) orientation A (pitch), b) orientation B (roll), and c) orientation C (yaw).

Correlation values were calculated for potentiometer and processed smartphone data for each of the five trials of free swing movement of the pendulum (table 4.3) in all three attachment orientations of the smartphone to the pendulum. All correlation

values are greater than +0.9, indicating a strong linear relationship between the smartphone and the potentiometer data. The high mean correlation values and low standard deviation values (0.051, 0.0012, and 0.014) suggest that the smartphone data is highly repeatable.

Table 4. 3 Correlation values between potentiometer and smartphone data for free-swing pendulum movement.

<u>Trial</u>	<u>Pitch</u>	<u>Roll</u>	<u>Yaw</u>
1	0.997	0.960	0.998
2	0.954	0.972	0.981
3	0.968	0.982	0.964
4	0.941	0.991	0.996
5	0.989	0.983	0.991
Mean	0.950	0.978	0.986
SD	0.051	0.012	0.014

4.4.2.1 Out-of-plane rotation sensitivity

Table 4.4 (a) shows the correlation values for data recorded in orientation A in the sensitive axis (A) and the two non –sensitive axes (B and C).

Table 4.4 (b) shows the correlation values for data recorded in orientation B from the sensitive axis (B) and the two non –sensitive axes (A and C).

Table 4.4 (c) shows the correlation values for data recorded in orientation C from the sensitive axis (c) and the two non –sensitive axes (A and B).

Table 4. 4 (a) correlation values for non-sensitive axes in orientation A, (b) orientation B, (c) orientation C.

A) Pitch			B) Roll			C) Yaw		
Trial	Yaw	Roll	Trial	Pitch	Yaw	Trial	Pitch	Roll
1	0.385	0.155	1	-0.158	0.208	1	-0.346	-0.216
2	0.275	0.273	2	-0.342	0.300	2	-0.009	-0.128
3	0.030	0.265	3	-0.117	0.201	3	-0.007	-0.159
4	0.140	0.378	4	-0.080	0.117	4	-0.358	-0.534
5	0.011	-0.255	5	-0.098	0.124	5	0.200	-0.222
Mean	0.168	0.163	Mean	-0.159	0.190	Mean	-0.180	-0.252
SD	0.161	0.247	SD	0.106	0.075	SD	0.172	0.163

Table 4.4 shows that in each orientation, smartphone data for the non-sensitive axes have mean correlation values that are much lower than for the sensitive axis shown in table 4.3. For orientation A, rotation around the pitch axis, the yaw and roll axes have mean correlation values of 0.168 and 0.163 respectively. In orientation B, rotation around the roll axis, the mean correlations of the pitch and yaw axes are - 0.159 and 0.19 respectively. And for orientation C, rotation around the yaw axis, the pitch axis had a mean correlation of -0.18 and the roll axis had a mean correlation of -0.252. This indicates that the smartphone data is not strongly associated with the potentiometer data recorded from rotations about the non-sensitive axes.

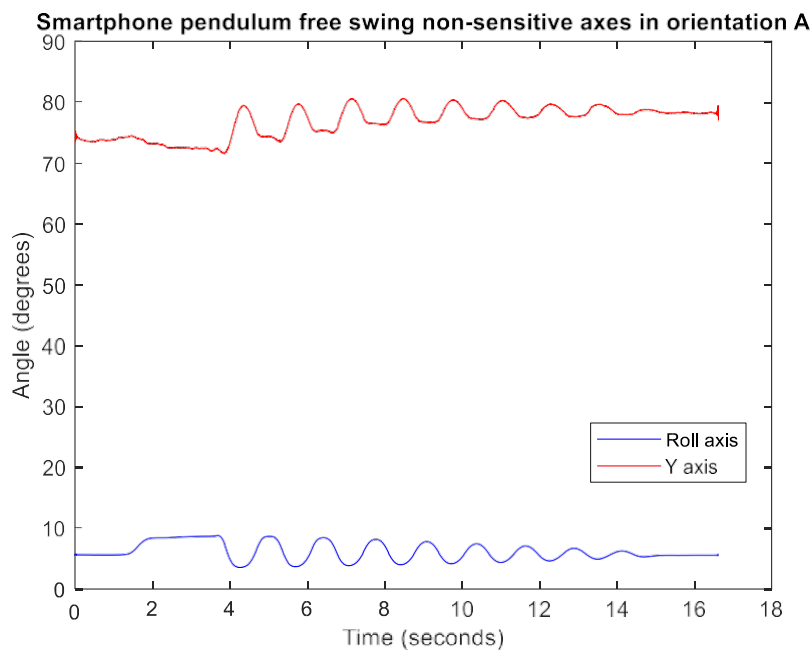


Figure 4. 10 Non-sensitive (roll and yaw) axes during free-swing of pendulum with smartphone in orientation A

Figure 4.10 shows a graph of angles ($^{\circ}$) against time (seconds) for the non-sensitive axes during free swing movement of the pendulum when the smartphone was attached at orientation A. It is shown that in the non-sensitive axes, the smartphone

data shows an angular output that oscillates slightly (less than 5° amplitude for each axis) during the free swing movement and this was also seen when recording in orientations B and C. This is most likely caused by slight physical movement of the smartphone itself in the two planes other than the principal rotation plane during the fast swinging movement of the pendulum arm.

4.4.3 Servo-powered gimbal system

4.4.3.1 Frequency response

4.4.3.1.1 Smartphone

Figure 4.11 shows amplitude Bode plots of the average frequency response of the smartphone during the velocity test on the servo-powered system in both the pitch and roll axes across all 10 trials. The 3dB cut-off frequencies were determined as $\sim 6\text{Hz}$ for the pitch axis and $\sim 10\text{Hz}$ for the roll axis. This cut-off point for the smartphone is equivalent to an angular velocity of $377^\circ/\text{s}$ and $628.3^\circ/\text{s}$ respectively.

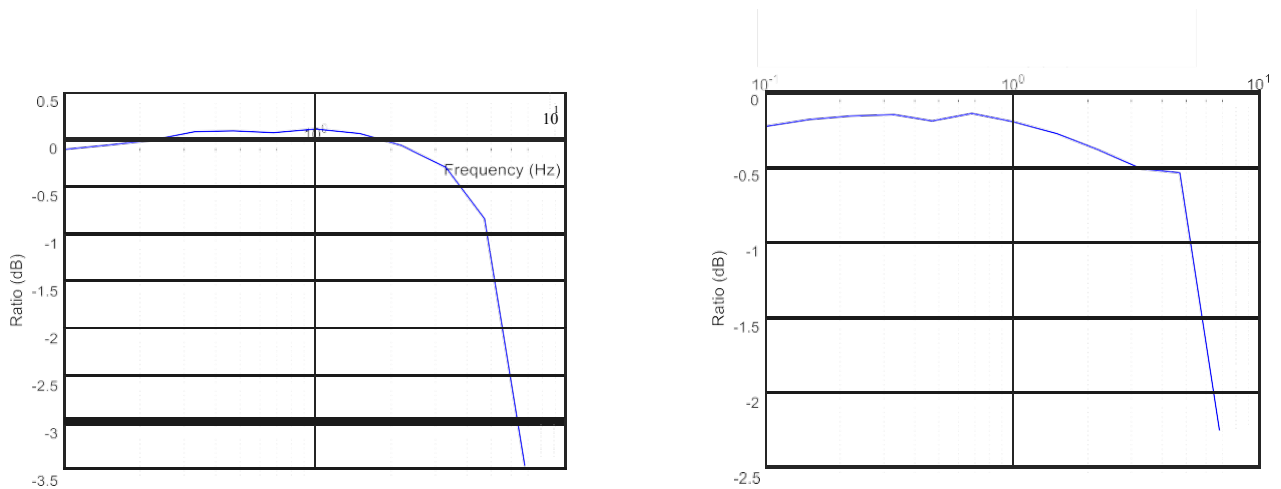


Figure 4. 11 Frequency response of smartphone in a) pitch axis and b) roll axis.

Table 4.5 further shows the average amplitude recorded by the smartphone in both the pitch and roll axes. The low standard deviations (less than 0.9°) indicate that the frequency response of the device is highly repeatable both within and between

recording days. Furthermore, for within-day trials, an intra-class correlation coefficient (ICC) of .982 (95% confidence interval (CI) .832 – .972) was calculated, supporting a high degree of repeatability. The ICC of inter-day trials was .99 (95% CI .888-.983), indicating a high degree of repeatability when the trial was repeated on different days. ICC estimates and their 95% confident intervals were calculated using SPSS statistical package version 24 (SPSS Inc, Chicago, IL) based on an absolute-agreement, 2-way mixed-effects model.

Table 4. 5 Average amplitude and standard deviations of amplitude (°) recorded by smartphone in pitch and roll axes at each frequency tested.

Freq (Hz)	PITCH AXIS		ROLL AXIS	
	Amp (°)	StDev	Amp(°)	StDev
0.1	9.862	0.22691	9.703	0.058
0.15	9.933	0.041847	10.056	0.238
0.22	9.394	0.215235	9.906	0.067
0.33	10.028	0.009542	9.985	0.106
0.47	9.566	0.084409	9.995	0.113
0.68	9.812	0.151261	10.071	0.260
1	9.740	0.12439	9.964	0.260
1.5	9.760	0.021234	10.017	0.264
2.2	9.810	0.023516	9.797	0.325
3.3	9.562	0.042	9.761	0.507
4.7	8.977	0.137746	9.794	0.350
6.8	5.468	1.202106	7.607	0.862

4.4.3.1.2 Smartwatch

Figure 4.12 shows similar amplitude Bode plots of the average frequency response of the smartwatch during the velocity test on the servo-powered system in both the pitch and roll axes across all 10 trials. A cut-off ratio of 3dB was again used. The 3dB cut-off frequencies were determined as ~5.7Hz for the pitch axis and ~9Hz for the roll axis. This cut-off point for the smartwatch is equivalent to an angular velocity of

358.1°/s and 565.5 °/s respectively. Table 3.6 further shows the average amplitude recorded by the smartwatch in both the pitch and roll axes. The smartwatch performed similarly to the smartphone. The low standard deviations (less than 1.3°) indicate that the frequency response of the device is highly repeatable both within and between recording days. The intraclass correlation coefficient of .982 (95% CI .905-.986) for within-day trials further indicates a high degree of repeatability comparable to the smartphone performance. The ICC of inter-day trials was .981 (95% CI .956-.994), indicating a high degree of repeatability when the trial was repeated on different days.

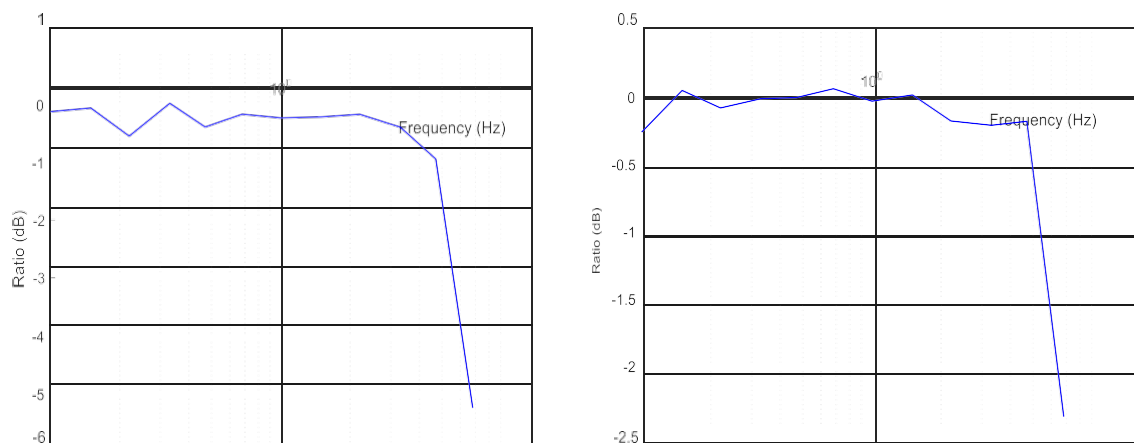


Figure 4. 12 Frequency response of smartphone in a) pitch axis and b) roll axis

Table 4. 6 Average amplitude and standard deviations of amplitude (°) recorded by smartwatch in pitch and roll axes at each frequency tested.

Freq (Hz)	PITCH AXIS		ROLL AXIS	
	Amp (°)	StDev	Amp(°)	StDev
0.1	9.862	0.227	9.703	0.058
0.15	9.933	0.0418	10.056	0.238
0.22	9.394	0.215	9.906	0.067
0.33	10.028	0.009	9.985	0.106
0.47	9.566	0.084	9.995	0.113

0.68	9.812	0.151	10.071	0.260
1	9.740	0.124	9.964	0.260
1.5	9.760	0.021	10.017	0.264
2.2	9.810	0.024	9.797	0.325
3.3	9.562	0.042	9.761	0.507
4.7	8.977	0.138	9.794	0.350
6.8	5.468	1.202	7.607	0.862

4.4.3.1 Continuous Measurement

Table 4.7 shows the mean value in degrees of both frequencies in each axis for both the smartphone and the smartwatch. The low standard deviations (less than 0.25) indicate a high repeatability between each 15-minute interval of the 3-hour test period. The intraclass correlation coefficient was determined for each device across all time-points. For the smartphone, the ICC was .99 (95%CI .736-.966), and for the smartwatch was .889 (95%CI .637-992). These high correlation coefficients further indicate the high repeatability of the measures and the ability of both devices to reliably record accurate rotation data over a prolonged period of continuous measurement.

Table 4. 7 Mean amplitude and standard deviations of smartphone and smartwatch for both frequencies across all 12 sampled time-points.

Phone				
Freq (Hz)	Pitch(°)		Roll (°)	
	Mean	StDev	Mean	StDev
0.68	9.9	0.074	9.682	0.070
1	9.876	0.018	9.58	0.150
Watch				
Freq (Hz)	Pitch(°)		Roll (°)	
	Mean	StDev	Mean	StDev
0.68	9.6	0.169	9.75	0.106
1	9.64	0.236	9.79	0.21

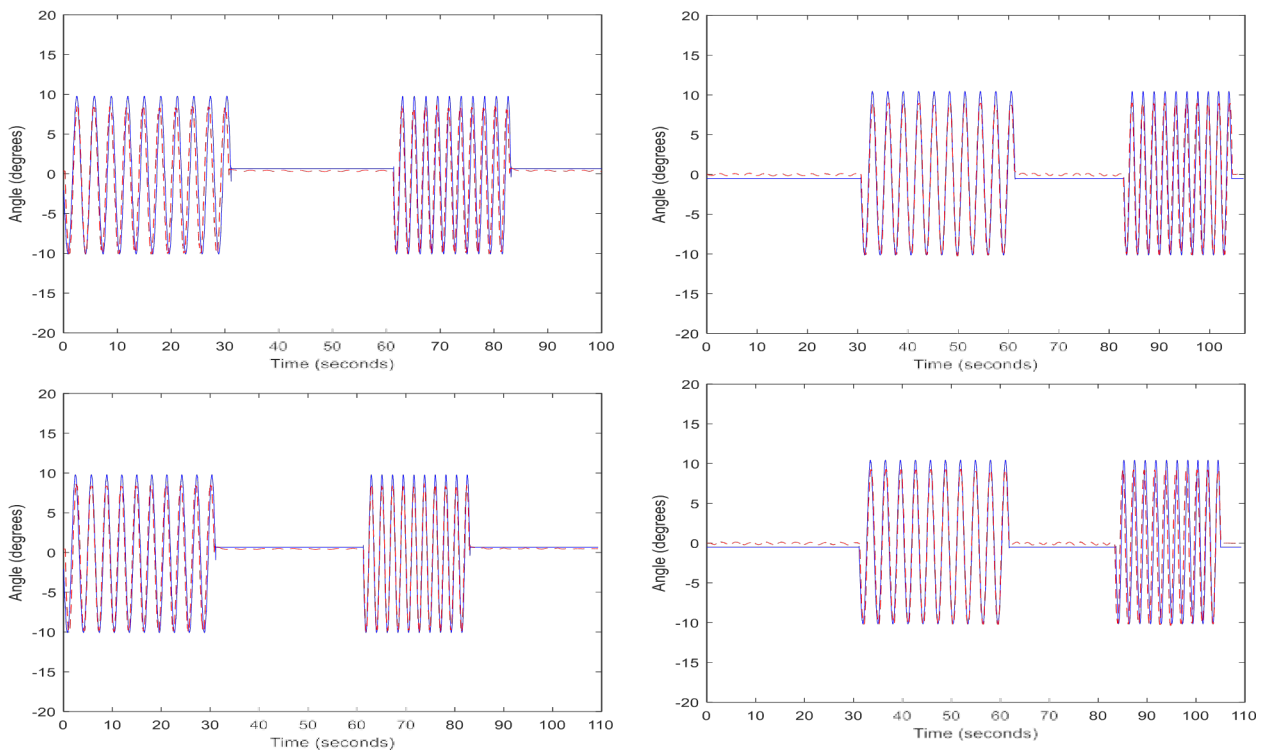


Figure 4. 13 Smartphone angular data compared to servo-feedback at 0.68 and 1Hz sinusoidal wave frequency in the a) pitch and b) roll axes at (i) time point 1 and (ii) time point 12.

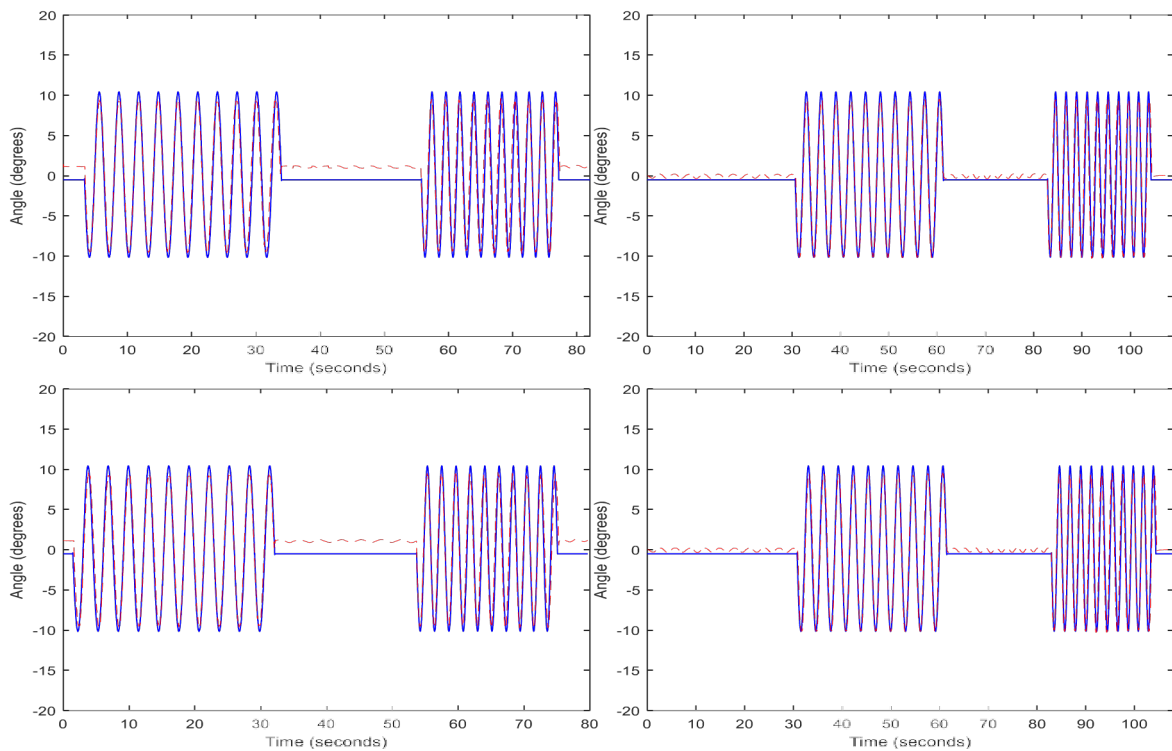


Figure 4. 14 Smartwatch angular data compared to servo-feedback at 0.68 and 1Hz sinusoidal wave frequency in the a) pitch and b) roll axes at (i) time point 1 and (ii) time point 12.

Figures 4.13 and 4.14 show the angle reported by the smartphone and smartwatch at time points 1 and 12 compared to the servo feedback. Both devices performed very well with respect to time-phase and amplitude reported at both time points, further suggesting their stability over time.

4.5 Discussion

The overall purpose of the conducted tests was to investigate the suitability of the developed application and the Android devices for use in 3-dimensional human upper limb motion analysis both for clinical goniometry and for measurement of shoulder joint angle during activities of daily living.

4.5.1 Static measurements

Static tests were performed to establish the accuracy, precision and repeatability of held positions, such as would be required in a standard goniometer measurement of joint angle. The reference system used was a commercially available inclinometer tool with a reported accuracy of $\pm 0.1^\circ$. Static tests were performed for multiple devices of the same model (Sony Xperia Z3 Compact) to establish if a significant offset was present between individual devices. In addition, a smartphone of a different model and manufacturer (Samsung SIII) and a smartwatch (LG Urbane), were tested to evaluate any inter-model discrepancies in the measurement of static angles. The main findings from the static tests conclude that there is a statistically significant offset in absolute angle estimation is present both within the same model and between different models and that this offset was highly repeatable on an individual phone basis. This suggests that characterisation of absolute angular data reported by a device should be done at an individual device level rather than at a manufacturer and model level, to account for any offset from the reference, absolute orientation. However, the relative angle between each 20° increment was accurately recorded with strong agreement and repeatability between each tested device, regardless of make and model, suggesting that although absolute angle measurements should be considered with respect to the calculated offset of the individual device, relative angle measurements between the different devices are comparable and repeatable. These results support the intended use of the application for joint goniometry, where the relative angle between the anatomical neutral position to the maximum range of motion performed by the subject is measured.

When evaluating the angular difference between steps in the yaw axis, the initial position was 20° . This approach was taken due to inaccuracies in the calibration of a rotation around a vertical direction as the phone coordinate system (calibrated on the axis of the gravity acceleration) is rotation –degenerate when the axis of rotation coincides with the reference, world axes. For human joint goniometry, it is unlikely that the device would be in absolute alignment with the world axes such that this degeneration would occur, and is indeed physically avoidable during such measurements. It is apparent in figure 3.8(c), that the initial angle reported by the smartphone and the smartwatch differs substantially from both the known angle (20°) and each other (68° and 158° respectively), given the difficulties in obtaining a reference ‘zero’ position. However, the relative orientation between successive 20° steps showed strong agreement and repeatability between the devices, similarly to the other pitch and roll axes.

The ability of the devices to accurately and repeatedly measure static relative angles within $\pm 1.1^\circ$, supports their potential use in goniometry-based shoulder ROM measurements for which the accepted minimal clinically important difference are 11° to 16° for a single evaluator (Muir et al., 2010).

4.5.2 Free-swinging Pendulum

Preliminary dynamic movement tests were conducted using a free-swinging pendulum with an inbuilt accurately calibrated potentiometer for one Sony Xperia Z3 Compact. The smartphone data was strongly correlated to the pendulum's potentiometer in each axis over repeated trials, indicating that the smartphone data was highly accurate and repeatable. During each trial of a single axis rotation, the out-

of-plane rotation in the non-sensitive axes was weakly correlated to the pendulum potentiometer, suggesting that there is minimal crosstalk between the sensitive and non-sensitive axes. It is shown that in the non-sensitive axes, the smartphone data shows an angular output that oscillates slightly (less than 5° amplitude for each axis) during the free swing movement and this was seen in each orientation. This is most likely caused by slight physical movement of the smartphone itself in the two planes other than the principal rotation plane during the fast swinging movement of the pendulum arm.

This preliminary data merited further investigation of the device and application capabilities under dynamic conditions relating to 3-dimensional human joint motion.

4.5.3 Servo-powered Gimbal

Both a smartphone (Sony Xperia Z3 Compact) and a smartwatch (LG Urbane) were characterised during dynamic movement of increasing angular frequency using a custom-made servo powered system. The range of frequencies used was determined by both the range equivalent to upper limb velocities during activities of daily living reported in the literature, and the specifications of the servo motors used. The pitch and roll axes were evaluated in this protocol. Due to system design limitations, it was not possible to evaluate the yaw axis. Based on the results of the previous pendulum study, in which rotation around the yaw axis was found to be of comparable accuracy and repeatability to the pitch and roll axes, it was assumed that it would perform similarly during the frequency response tests.

The data was highly repeatable for both within and between recording days in both the smartphone and the smartwatch for each axis. The frequencies at which the

smartphone no longer optimally performed for the pitch and roll axes were determined as equivalent to an angular velocity of $377^{\circ}/s$ and $628.3^{\circ}/s$ respectively. For the smartwatch this was $358.1^{\circ}/s$ and $565.5^{\circ}/s$ for the pitch and roll axes respectively.

For the purpose of the developed application, these results are well within the optimal responsiveness range compliant with angular velocity of the humerus when performing activities of daily living such as reaching for an object from a shelf (Rosen et al., 2005). In a study by Rosen (2003), the maximum angular velocity required to perform a common daily life task such as move an object at waist level and reach arm up to head height was between $49^{\circ}/second$ and $174^{\circ}/second$. Whilst the optimal responsiveness range of the smartwatch is slightly lower than the smartphone, it is still compliant with angular velocity of the humerus when performing activities of daily living (Rosen et al., 2005). The application on both devices may be limited for larger angular velocity humerus movements such as those associated with a tennis serve or volleyball spike which can be in excess of $590^{\circ}/s$ and $920^{\circ}/s$ respectively (Wagner et al., 2012).

4.5.4 Continuous Measurement

A mid-range frequency repetitive oscillation in the pitch and roll axes for a 3-hour period was used to evaluate the devices under conditions relating to the continuous measurement of human joint angles in daily life. Both devices produced accurate and repeatable data throughout the prolonged measurement period. This suggests their stability over time and indicates their potential use in continuous measurements of human upper limb joint angles during activities of daily living.

The characterisation protocol of the developed application run on different Android devices has a few limitations. The effect of gross acceleration applied to the devices on the angle measurements was not investigated. Magnetic interference from external sources was also not evaluated in the characterisation. The developed application obtains the data reported by the software Rotation Vector Sensor, a result of sensor fusion algorithms incorporating the hardware accelerometer, gyroscope and magnetometer. It was therefore assumed that the internal sensor fusion algorithms of the devices could adequately compensate for such external influences. Furthermore, the algorithms used are not open source and as such are hidden from the developer, making it difficult to correct for any identified effects of external influences.

Due to limitations in available resources, only two smartphone models and one smartwatch model were evaluated. Different manufacturers and models of smartphones and smartwatches employ different models of hardware sensors, which may result in discrepancies in accuracy between devices and, as shown in the results of this study, a significant offset in absolute orientation measurements. For the purpose of this thesis, only the devices characterised in this chapter were used in subsequent studies. If devices of another manufacturer and model are to be used, accuracy and repeatability should not be assumed and the device model should be individually characterised accordingly.

Further studies evaluating the developed application and Android devices compared to existing clinical tools for human joint goniometry will be discussed in Chapter 5.

Chapter 5: Concurrent Validity and Repeatability compared to a Universal Goniometer for Clinical Range of Motion Measurements

Chapter 5

5 Concurrent Validity and Repeatability compared to a Universal Goniometer for Clinical Range of Motion Measurements

5.1 Introduction

In order for the developed application to be considered as an acceptable or favourable alternative to tradition methods in routine clinical range of motion assessments, it must be validated by comparison to the gold standard. Validation is the process of assessing the psychometric characteristics of a measurement modality, specifically the validity and reliability. Validity indicates the extent to which a tool measures what it is intended to measure whilst reliability is the degree of stability of data recorded between two or more trials (Milani et al., 2014).

This chapter describes the validation procedure of the smartwatch application when compared to a universal goniometer in both healthy and impaired shoulder movement assessment by a single observer at two measurement intervals. The results are then discussed in relation to the accepted agreement and reliability for clinical use as outlined in the literature to date.

5.2 Materials and Methods

5.2.1 Ethics

Ethical approval from the Department of biomedical Engineering Ethics Committee was obtained for the experimental work detailed in this chapter.

5.2.2 Subjects

Twenty healthy participants, with no known musculoskeletal, neurological or sensory deficit affecting upper limb were recruited from within the Department of Biomedical Engineering, University of Strathclyde.

Table 5. 1 Subject demographic data

Sex	Age	Height (cm)	Mass (kg)
F	26	166	70
F	27	171.5	83
F	25	170.5	65
F	22	169.6	61.5
F	25	161	56
F	24	178	81
F	23	181.5	76
F	27	161.5	63
F	28	163.5	58
M	28	177	66
M	23	186	72
M	29	179	72
M	26	175.5	72
M	34	173.5	76
M	23	180	75
M	27	185.5	69
M	28	177.5	83
M	26	182.6	71
M	25	172	69
M	23	176	72

Written informed consent was obtained from all subjects prior to data collection and subjects were excluded from the study if they fell under any of the following exclusion criteria:

- Musculoskeletal, neurological or sensory deficit affecting upper limb
- Under the age of 18 or over the age of 65
- Pregnant
- Fitted with a pacemaker, neural stimulator, implantable cardioverter-defibrillator, cochlear implant or other implantable electronics
- Known allergy to sticking plasters or zinc oxide sticky tape

These exclusion criteria were rechecked immediately prior to testing.

Once informed consent was obtained, all subjects were asked to complete the Oxford Shoulder Score (OSS) Questionnaire (appendix 3). This questionnaire is routinely used during both pre- and post-operative clinical upper limb functional assessment to evaluate the degree of pain and disability caused by shoulder pathology (Dawson et al., 2009). It is a validated, 12-item patient reported questionnaire, which assesses the impact of shoulder pathology on the patients' perceived ability to carry out eight

activities of daily living and assesses the pain related to the individuals' shoulder pathology. For each question, a score of 0-4 is assigned where 4 represents no pain or impairment and 0 represents unbearable pain and an inability to perform the task. The resultant overall score ranges from 0-48, with 48 representing the best possible outcome. A score of below 40 is indicative of potential shoulder impairment (Dawson et al., 1996) and participants scoring less than 40 would be excluded from the study and advised to contact their GP for an assessment. The mean OSS scores from the volunteer subjects in this study are presented in table 2.2 below:

Table 5. 2 Mean Oxford Shoulder Scores for the study cohort

Mean male scores	Mean female score
47.7 (range 46-48)	47.3 (range 44-48)

The results of the questionnaire indicated that all subjects recruited for this study were healthy at the time of testing.

5.2.3 Materials

One LG Urbane smartwatch (SW) was attached to the lateral aspect of middle third of upper arm by a custom-made holder and elasticated strap as shown in figure 5.1. The holder was designed in Rhinoceros 3D computer-aided design software (McNeel, Spain) and 3D-printed in 1.75mm red PLA filament, and had a flat level surface to aid mounting of the smartwatch to the upper limb. The orientation of the mounted smartwatch was such that the Y axis of the coordinate system of the smartwatch (defined in section 3.3.1) was coincident with the corresponding Y axis of the humeral anatomical coordinate system (defined in Chapter 2, figure 2.9) and the Z axis of the smartwatch was co-aligned to the X axis of the humerus (figure 5.1).

The goniometer (UG) used in this study was a plastic double-arm goniometer with 360° marked in 1° increments. Each arm was 30cm long (figure 5.2).

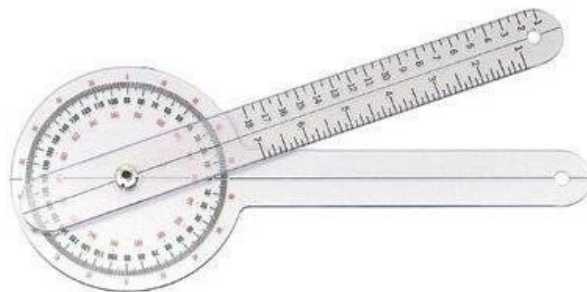


Figure 5. 2 Universal goniometer

Raters

One trained rater measured shoulder range of motion with both the smartwatch and the goniometer of the twenty subjects in single sessions. Ten of the subjects were then assessed on a separate occasion within a 4-week period to assess between-day, intra-rater reliability of the goniometer and the smartwatch in the assessment of healthy shoulder range of motion.

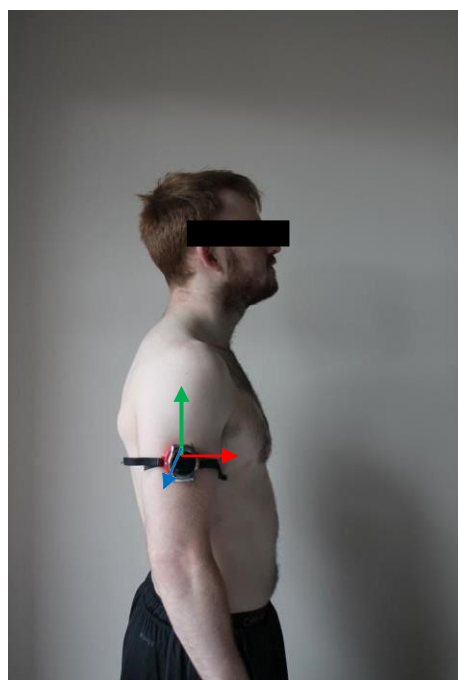


Figure 5. 1 Subject resting, neutral position with smartwatch attached showing a) the humerus anatomical coordinate system b) the smartwatch local coordinate system.

5.2.4 Planar movements in clinical examination

Routine clinical examination of shoulder function commonly assesses range of motion through the following planar movements:

1a. Maximal flexion

With palm of hand facing the midline of the body, keeping elbow and wrist straight, raise upper limb in front of body, parallel to sagittal plane (figure 5.3(a)).

1b. Maximal extension

With palm of hand facing the midline of the body, keeping elbow and wrist straight, extend upper limb behind body, parallel to sagittal plane (figure 5.3(b)).

1c. Maximal abduction

With palm of hand facing midline of the body in the neutral resting position, keeping elbow and wrist straight, raise arm out to side of body, parallel to the coronal plane (figure 5.3(c)).

1d. Maximal internal rotation

From the neutral resting position with palm of hand facing midline of the body, first raise the upper arm to 90° abduction in the coronal plane such that the elbow is parallel to the shoulder in the transverse plane. Keeping wrist straight, rotate the forearm towards the floor (figure 5.3(e)).

1e. Maximal external rotation

From the neutral resting position with palm of hand facing midline of the body, first raise the upper arm to 90° abduction in the coronal plane such that the elbow is parallel to the shoulder in the transverse plane. Keeping wrist straight, rotate the forearm towards the ceiling (figure 5.3(f)).

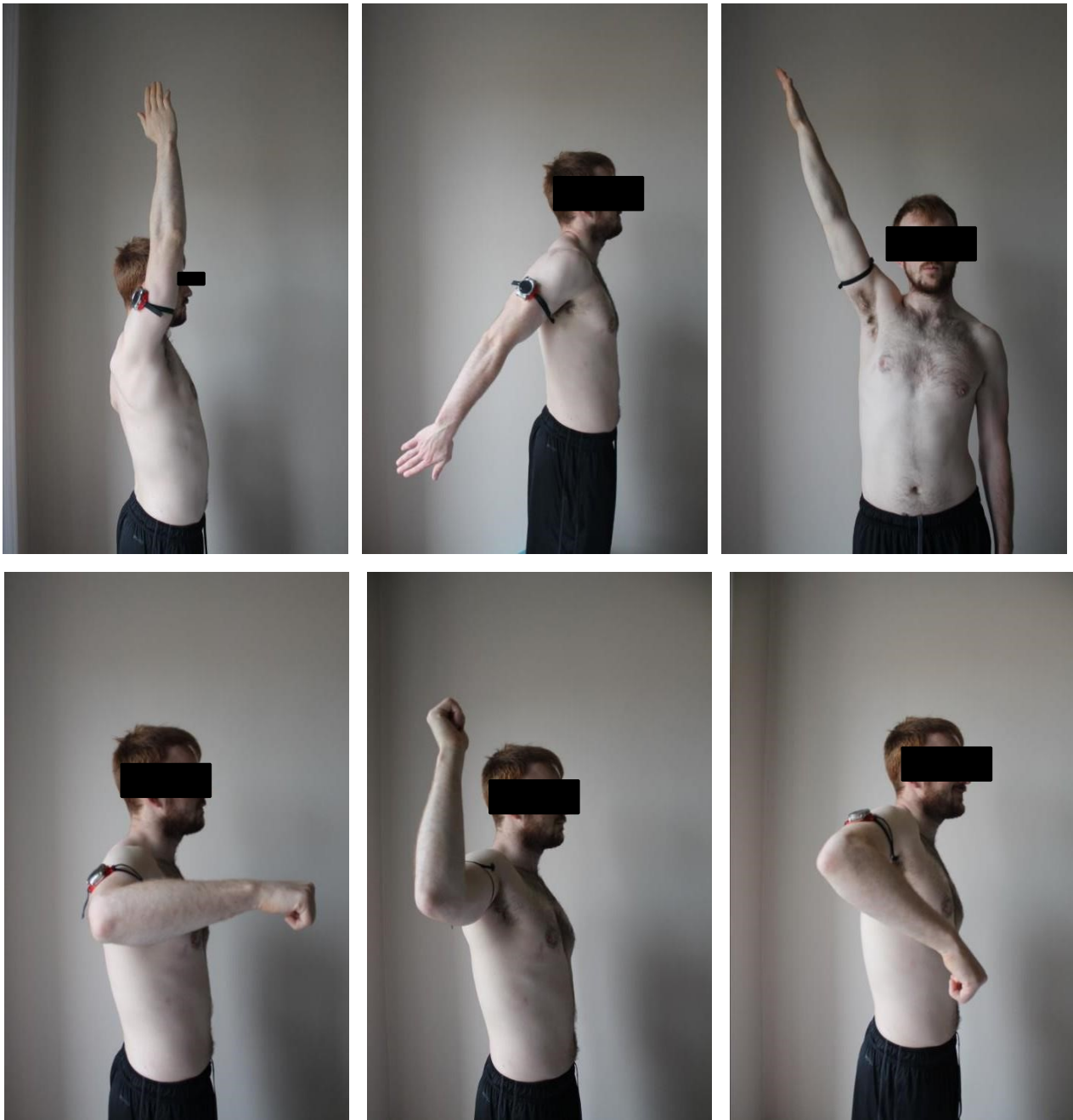


Figure 5. 3 Planar movements measured a) Flexion b) Extension c) Abduction d) Start position for rotation measurements e) External Rotation f) Internal Rotation

In this study, active range of motion was assessed with the subject in a standing upright posture through each of the above planar movements. Each movement was performed by the subject's dominant arm only. For flexion, extension and abduction, the subject began with the upper arm, forearm and hand placed comfortably at the side of the trunk in the neutral resting position (figure 5.1). For internal and external rotation, the subject began with the upper arm abducted to 90° and the forearm flexed to 90° such that it is parallel to the floor in the sagittal plane, wrist straight and palm facing the floor (figure 5.3(d)).

The rater first initiated the smartwatch application to start recording and aligned the axis and stationary arm of the goniometer to anatomical landmarks accordingly to the movement being assessed (table 5.3).

Table 5. 3 Alignment of goniometer to anatomical landmarks for each planar movement assessed

Movement assessed	UG Axis position	UG Stationary arm alignment
Flexion, Extension	Centre of the humeral head, near the acromion process	Mid-axillary line of the trunk
Abduction	Centre of the humeral head, near the acromion process	Parallel to the sternum
Internal/External Rotation	Olecranon process of the ulna	Horizontal with start position of forearm

A verbal signal was then given to the subject to commence each arm movement. Subjects were instructed to perform each movement to the maximal range they could achieve at a self-selected speed. Once the maximal range was reached, subjects were asked to hold this position and the rater rotated the moveable arm of the goniometer to measure the change in angle from the resting position.

Following each measurement, the arm was returned to the resting position and the smartwatch recording was stopped.

5.2.5 Data acquisition and pre-processing

The change in angle measured by the goniometer during each movement assessment was noted down by the rater. Smartwatch 3D-rotation data were captured by the Android application as detailed in chapter 3 and stored in the internal storage of the watch. This data was transferred to a PC for post-processing to obtain the angles measured during each assessment once all data collection was complete. Since the rater was not able to view the angle measured by the smartwatch at the time of the assessment, the rater was sufficiently blinded to the smartwatch measurement, and the potential for bias was greatly reduced.

5.2.6 Sensitivity to change in an impaired condition

Whilst the above protocol aims to investigate the concurrent validity of the smartwatch application to a gold standard clinical tool, the universal goniometer, in measuring range of motion of healthy shoulders, such assessments are usually performed in clinics on patients with a shoulder impairment. To better evaluate the validity of the smartwatch in a clinical setting, an impaired shoulder condition was simulated by applying kinesiology tape across the shoulder girdle of each healthy subject (figure 5.4). The subject was asked to sit with their elbow resting on a table, upper arm close to their body and their shoulder slightly elevated and protracted forward. Strapping was then applied tightly from the scapula to the anterior of the axilla. Further strapping was applied across the deltoid muscle to the lateral aspect of the upper arm. The slightly elevated and protracted shoulder position was maintained by the applied strapping and as a result, the subjects shoulder movement was subtly restricted.



Figure 5.4 Strapping with kinesiology tape applied across the shoulder girdle.

The above protocol of measuring shoulder range of motion in each of the planar movements was then repeated with the strapping in place and the subjects shoulder movement restricted. The subjects were instructed in exactly the same manner with additional instructions to allow the strapping to restrict their movement and not to resist it.

5.3 Data Analysis

A detailed account of the techniques for the description of humero-thoracic 3D kinematics used in this study is given in Chapter 2. This section gives a brief description of the specific steps taken to compute clinically relevant goniometric data of the shoulder joint from the smartwatch application. The statistical techniques used for the comparison of the smartwatch and universal goniometer are subsequently described. All data processing was carried out in Matlab (Mathworks Inc., MA) using custom written scripts and statistical analysis was performed using SPSS statistical software package version 24 (SPSS Inc., Chicago, IL, USA).

5.3.1 Computation of shoulder goniometric data

The single smartwatch attached to the subject's dominant humerus was used to calculate the humero-thoracic range of motion during each planar movement assessed. During each movement, the subject's trunk remained rigid and upright and the upper limb was moved in isolation. The joint angle was calculated on the assumption of static trunk motion and tracking the motion of the humerus only.

Successive unit quaternions were derived from the frame-by-frame change in smartwatch orientation. The resulting unit quaternion, Q_n , therefore described the orientation of the smartwatch coordinate system with respect to its orientation in the previous time frame, Q_{n-1} , with the first orientation, Q_1 , relating to the orientation of the smartwatch at the start of the movement cycle, Q_0 , at $t=0$ with the upper limb in the neutral resting position.

Each frame-by-frame unit quaternion, Q_n , was therefore transformed to a common reference orientation for the smartwatch, which was taken to be Q_0 , at $t=0$. Transformation of each frame-by-frame unit quaternion to the common reference quaternion was achieved through successive multiplication of the quaternions as described below:

The description of the orientation of any local frame relative to another was given by the following equation:

$${}^0_2Q = {}^1_2Q \cdot {}^1_0Q^{-1} \quad (28)$$

Where 0_2Q is the unit quaternion representing the orientation of the smartwatch at t=2 relative to the reference orientation 1_0Q at t=0.

The orientation of the smartwatch at t=3, 0_3Q , relative to the reference orientation was then determined as:

$${}^0_3Q = {}^2_3Q \cdot {}^2_0Q^{-1} \quad (29)$$

It follows that each frame-by-frame unit quaternion was transformed to a common reference orientation, 1_0Q , through successive multiplication of the orientation matrices:

$${}^0_nQ = {}^{n-1}_nQ \cdot {}^{n-1}_{n-2}Q^{-1} \dots \dots \dots {}^1_2Q \cdot {}^1_0Q^{-1} \quad (30)$$

Where n = number of frames.

Following this transformation, each frame-by-frame unit quaternion therefore gave the orientation of the smartwatch coordinate system relative to its orientation at the start of the movement cycle at t=0. Thus, each transformed frame-by-frame unit quaternion gave the change in orientation relative to its starting orientation, Q_0 , at t=0 and not a measure of its absolute orientation in space.

The orientation of the smartwatch unit relative to the corresponding anatomical coordinate system of the humerus was determined by aligning the axes of the smartwatch coordinate system to the underlying bony anatomy of the humerus as described in chapter 2. During each frame of the measurement, the smartwatch position remained fixed on the humerus and the corresponding anatomical coordinate system was therefore known at each instant in time.

Following calculation of the shoulder joint rotation angle as a unit quaternion, further analysis of this data was required in order to compare the clinical range of motion measurements of the universal goniometer and the smartwatch. The resultant frame-by-frame unit quaternions relative to the starting orientation were converted to latitude and longitude as described in Chapter 2, section 2.4.2.6, with the reference unit vector, V_l , coincident with the negative Y-axis of the humerus in the resting position.

For flexion, extension and abduction movements, the latitude represented the degree of humeral elevation from the resting neutral position to the maximum position reached and was used for comparison to the angle measured by the goniometer during these movements. For internal and external rotation, the latitude represented the degree of forearm elevation and depression relative to the starting horizontal flexed position of the forearm from the abducted humerus.

5.4 Statistical Analysis

The major aim of this study was to establish the concurrent validity and reliability of the smartwatch application for the clinical measurement of shoulder ROM in healthy and impaired conditions when compared to a gold standard universal goniometer. This section describes the statistical methods used to compare the shoulder range of motion goniometric data calculated from the universal goniometer and the smartwatch.

5.4.1 Concurrent Validity

The concurrent validity of the smartwatch application measurements compared with the gold-standard universal goniometer measurement for the assessment of shoulder range of motion was determined. To achieve this, the smartwatch measurement was compared to the goniometer measurement for each ROM measurement (flexion, extension, abduction, internal and external rotation) in each subject for both the healthy and impaired conditions independently.

Statistical comparison of the two measurement modalities in both the healthy and impaired states was made using Intraclass Correlation Co-efficient (ICC(2,1)), Bland-Altman mean differences and 95% limits of agreement (LOAs), and standard error of measurement (SEM).

An intraclass correlation coefficient [ICC(2,1)] and a 2-way-mixed-effects model with average measures and absolute agreement among measurements methods for each movement. The ICC was calculated for each movement measured and expressed as an ICC with 95% confidence interval (CI).

The ICC was interpreted according to the definitions given by Landis and Koch in which: 0.00 to 0.20, slight correlation; 0.21 to 0.40, fair correlation; 0.41 to 0.60, moderate correlation; 0.61 to 0.80, substantial correlation; and 0.81 to 1.00, strong correlation (Landis and Koch, 1977). The average ICC of each measurement device was calculated from the individual ICCs for each movement measured. These were then compared using a 1-way analysis of variance (ANOVA) with a Tukey post hoc test for statistical significant ($\alpha=.05$).

The average ICC of each measurement device was calculated from the individual ICCs for each movement measured in each of the subject states (healthy and impaired). These were then compared using a 1-way analysis of variance (ANOVA)

with a Tukey post hoc test for statistical significant ($\alpha=.05$) to compare the strength of measurement validity in the healthy and impaired conditions.

Whilst correlation studies are frequently employed to assess the agreement between two quantitative methods of measurement, they are limited to an examination of the relationship between variables and omit analysis of the absolute agreement between two the measurement techniques.

The Bland-Altman plot was first proposed in 1983 as an alternative analysis to quantify the agreement of two measurement methods by calculating the mean difference and constructing limits of agreement (LOA).

In this study, Bland-Altman mean differences were calculated as the differences between the smartwatch measurements and the associated gold-standard average standard goniometer measurements for each ROM measurement in each subject.

The 95% LOA was calculated as $1.96 \times SD_{\mu D}$, in which $SD_{\mu D}$ is the standard deviation of the differences for that particular ROM measurement.

The standard error of measurement (SEM) was also calculated for each measurement method as an additional measure of validity. This was calculated as $SEM = SD \sqrt{1 - ICC}$, in which SD is the standard deviation and the resulting SEM value is expressed in degrees.

5.4.2 Between day intra-rater reliability

Between day intra-rater reliability was calculated for each measurement method (universal goniometer and smartwatch). This was evaluated using an intraclass correlation coefficient [ICC(2,1)] and a 2-way-mixed-effects model with a single measure and consistency among measurement time-points for each movement. The

ICC was calculated for each movement measurement and expressed as an ICC with 95% confidence interval (CI) and interpreted as in the previous section.

The average ICC of each measurement device was calculated from the individual ICCs for each movement measured. These were then compared using a 1-way analysis of variance (ANOVA) with a Tukey post hoc test for statistical significant ($\alpha=.05$).

5.5 Results

5.5.1 Concurrent Validity

5.5.1.1 Healthy condition

A comparison of the day 1 smartwatch measurements with the day 1 universal goniometer measurements to determine the concurrent validity of the smartwatch application in healthy subjects is presented in table 5.4. Substantial to strong agreement with the gold standard was found with average ICC values just greater than 0.8. Measurement of abduction had the greatest agreement with the goniometer measurements with an ICC of 0.9. The other movement ICC values were as follows: Flexion, 0.744; Extension, 0.657; Internal rotation, 0.882; External rotation, 0.858. The average value of the mean difference between the two measurement modalities was 8.53°. Mean differences were highest for abduction (10.19°) and extension (10.58°) measurements and lowest in external rotation measurements. The average limits of agreement calculated was 19.04°.

SEM calculations reveal that the highest SEM was for measurements of Flexion (12.92°) indicating that the absolute validity of the smartwatch was worst for this movement plane. SEM for the remaining movement planes were: Extension, 7.75°; Abduction, 6.24°; Internal rotation, 6.66°, and External rotation, 9.59°.

Table 5. 4 Comparison of SW and UG measurements in the Healthy condition

Measurement	ICC	95% CI	Mean Diff 95% LOA (°)	± SEM (°)
Flexion	0.744	0.31-0.9	8.99±29.36	12.92
Extension	0.657	0.15-0.89	10.58±18.75	7.75
Abduction	0.9	0.04-0.98	10.19±12.89	6.24
Internal Rotation	0.882	0.21-0.97	7.78±13.9	6.66
External Rotation	0.858	0.62-0.945	5.11±20.28	9.59
Mean	0.81		8.53±19.04	8.63

5.5.1.2 Impaired Condition

A comparison of the smartwatch measurements in the impaired condition with goniometer measurements to determine the concurrent validity in impaired conditions is presented in table 5.5. The agreement with the gold standard goniometer is strong in all movements measured with a mean ICC of 0.88. Measurements of Flexion and Extension had the greatest agreement with ICCs of 0.928 and 0.905 respectively and lowest in External rotation with an ICC of 0.84. The average of the mean difference values was 8.68°, the greatest mean difference being in Abduction (15.36°) and the lowest in Flexion (4.17°). The average 95% LOA was 18.06°. SEM values averaged at 8.67° with a highest value of 14.42° for Flexion. The SEM for the other movements measures were: Extension, 7.66°; Abduction, 8.05°; Internal rotation, 6.09°, and External rotation, 7.13°.

Table 5. 5 Comparison of SW and UG measurements in impaired condition

Measurement	ICC	95% CI	Mean Diff 95% LOA (°)	± SEM (°)
Flexion	0.928	0.82-0.97	4.17±29.33	14.42
Extension	0.905	0.53-0.97	6.9±15.79	7.66
Abduction	0.846	0.16-0.96	15.36±17.15	8.05
Internal Rotation	0.874	0.06-0.97	8.13±12.77	6.09
External Rotation	0.84	0.06-0.95	8.84±15.25	7.13
Mean	0.88		8.68±18.06	8.67

ICC values were on average, higher in the impaired condition compared to the healthy condition. The one-way ANOVA test did not show a statistically significant difference between these groups ($p=0.211$).

5.5.2 Reliability

5.5.2.1 Healthy Condition (between day)

The between day, intra-rater reliability for both of the measurement methods by a single observer is reported in table 5.6. Both the smartwatch and the universal goniometer had very strong correlation between measurements taken on two separate test days with average ICC values greater than 0.9 and almost identical (0.9 and 0.92 respectively). The lowest ICC for each method of measurements was in Extension, at 0.84 for the goniometer and 0.835 for the smartwatch. A one-way ANOVA test comparing the average ICCs did not show any statistically significant difference between the two methods ($p=0.565$).

The smartwatch had the highest (worst) average SEM of 9.52° compared to the average SEM of the goniometer was 7.12°.

Table 5. 6 Between day reliability for UG and SW measurements.

	Measurement	ICC	95% Confidence interval	SEM (°)
Goniometer	Flexion	0.908	0.68-0.97	9.18
	Extension	0.84	0.85-0.94	7.21
	Abduction	0.979	0.92-0.99	4.80

	Internal Rotation	0.94	0.79-0.98	6.25
	External Rotation	0.917	0.51-0.98	8.18
	Mean	0.92		7.12
Smartwatch	Flexion	0.886	0.62-0.97	7.08
	Extension	0.835	0.42-0.95	6.47
	Abduction	0.979	0.93-0.99	4.05
	Internal Rotation	0.929	0.75-0.98	6.30
	External Rotation	0.881	0.59-0.97	9.52
	Mean	0.9		6.69

5.6 Discussion

This study showed good to excellent agreement of the smartwatch application compared with gold-standard goniometry for healthy subjects with ICC ranging from 0.66 to 0.9 over all ROM movements and an average of 0.8. It was lowest in extension. In the simulated impaired condition where strapping was applied to restrict movement of the shoulder joint, the agreement between the two measurement modalities was similarly strong with ICC ranging from 0.84 to 0.93 (average ICC 0.88). Previous studies using smartphone inclinometer applications show comparable agreement (Shin et al., 2012; Werner et al., 2014; Jenny et al., 2013; Milani et al., 2014).

Mean differences between the smartwatch application and universal goniometer in healthy testing ranged from 5.11° to 10.58°, within the minimal clinically important difference for shoulder ROM which is estimated as 11° to 16° for a single observer (Muir et al., 2010). However, mean limits of agreement for all movements was 19.04°, an unacceptable margin for clinical purposes. On closer inspection of the planar movements, the mean limits of agreement indicates that the difference between the smartwatch and the goniometer for a flexion measurement could be as high as 29.36°, and therefore the results indicate that the new method cannot be accepted for clinical use based solely on this study. For extension and external rotation the LOA was also out with the acceptable range (18.75° and 20.28°

respectively). The LOA of abduction and internal rotation fall within the acceptable limits at 12.89° and 13.9° however these are in the high range and lower limits would be preferable in all cases. These results are likely due to small sample size, the variability of manual goniometry and between method differences. Further studies with a larger sample size are required to fully ascertain the agreement of the two methods. Since preliminary accuracy and repeatability studies of the smartwatch to measure known angles showed excellent absolute agreement, the discrepancies in this study may be due to inaccuracy of the goniometer methods. Again, further study is needed to either confirm or deny which of the methods is most accurate. Comparison to 3-dimensional motion capture would appear to be warranted.

In the impaired condition, the mean differences ranged from 4.17° to 15.36° , with the highest difference found in abduction. Whilst this is higher than for healthy movement, it is still within the minimal important difference for clinical goniometry of the shoulder. However, similar to the healthy movements, the limits of agreement in the impaired condition were unacceptably high in all movements (average LOA was 18.06°) to suggest the two measurement modalities can be used interchangeably. Between day inter-rater repeatability of the smartwatch was very strong with an average ICC of 0.9 and comparable to the universal goniometer average ICC of 0.92). Indeed no statistically significant difference was shown between the two modalities in the repeatability test, thus repeatability did not appear to be a negative influence on agreement between the two methods. These results are similar to those reported in the literature (Jenny et al 2013; Werner et al., 2014; Mejia-Hernandez et al., 2018). Shin et al (2012) reported an average ICC of 0.9 for repeated smartphone inclinometer measurements whilst Mitchell et al (2014) found the intra-rater reliability of a novice, non-clinical user ranging from ICC 0.79 to 0.81.

Previous studies have also found good repeatability for the universal goniometer used by a single observer for healthy and patient groups (Kolber et al., 2012; Muir et al., 2010; Riddle, 1987). Other studies report lower but fair-good repeatability such as Hayes et al (2001) who found ICC of 0.53 to 0.65 for repeated goniometer assessment by a single observer. The between day measurement repeatability shows promise to the practical use of the developed system in monitoring impairment progression or evaluating treatment interventions.

Chapter 6: Discussion and Future Work

Chapter 6

6 Discussion

6.1 Methods of Describing Shoulder Kinematics

The methodology outlined in chapter 3 for describing 3-dimensional shoulder rotation derives a spherical coordinate-based system of altitude and azimuth from a unit quaternion. It gives a coherent and meaningful means of describing the orientation of the humerus relative to the thorax during different movement tasks in terms of the plane of movement and degree of elevation from the anatomical position. It is free from the problems of gimbal lock and more intuitive and clinically meaningful than a unit quaternion. However, the degree of axial rotation (position of the forearm) cannot be defined in this method and the use of Cardan/Euler angles remains the principal method of obtaining this information. The spherical coordinate-based system suffers from further mathematical issues that were brought to light during preliminary testing of known rotations. The elevation angle calculated was highly comparable to the known angle. However, the plane of movement magnitude inconsistently reflected the true plane. It was speculated that this was due to mathematical malalignment of the spherical coordinate axes with the anatomical axes producing out of plane axis crosstalk as the humerus vector rotates relative to the thorax vector.

Despite attempts to add a correctional step using the T-pose position of the upper body to define the abduction plane as a reference, this study was unable to overcome the issue within the available timeframe. Thus further work is required to develop a robust mathematical method for aligning the spherical coordinate axes with the anatomical axes of the humero-thoracic joint.

Since the elevation angle was consistent with the true angle in initial investigations, this method could be used in the goniometry study where the single plane of movement is clearly defined and recorded during the measurement by the observer.

6.2 System Development

6.2.1 Devices

One Sony Xperia Z3 smartphone and one LG Urbane smartwatch were used, both of which ran the Android operating system. These devices were chosen due to their cost-effectiveness and physical sensing capabilities (namely, MEMS inertial sensors) whilst the Android operating system is an open platform allowing applications to be adapted for different devices open source and, freely deployed onto the market.

6.2.2 Validation Protocol

A number of previous smartphone applications which utilise the embedded MEMS inertial sensors have been developed to assess joint goniometry, providing accurate, immediately available and easily interpretable, real-time measurements (Cuesta-Vargas et al., 2016; Kos et al., 2016). Such applications exploit the native sensor fusion software to estimate orientation from the physical sensors. Whilst it is well known that the phones' low power consumption, small size and conservative production costs merit their use, their sensors are prone to errors such as offset instabilities, inappropriately low bandwidth, incorrect sensor fusion software implementation or unsuitable calibration, e.g. not referenced to a well-defined direction. Accumulation of these inaccuracies can thus cause significant discrepancies in the measurements reported by the device with respect to the physical measurements on the patient, especially in dynamic conditions, where bandwidth and

dynamic calibration considerations apply. Mourcou et al (2015) reported on the performance of different smartphones and sensor fusion approaches compared to a robotic arm during both static and dynamic movement at two different speeds and found comparable results. The performance of the iPhone 4 position sensors was evaluated by Kos (2016), highlighting the importance of gaining an understanding of the capabilities of individual smartphones.

As the data reported by the phone undergoes heavy fusion, we cannot rely on the nominal specifications of the native sensors and should evaluate the data output by the Rotation Vector software sensor.

Thus, Chapter 3 details a thorough validation process for a potential inertial sensor-based technology intended for use in clinical goniometry. The Rotation Vector Sensor performance during static, dynamic and continuous measurement conditions can be evaluated through this protocol. By comparison with an industry standard inclinometer tool (reported accuracy of $\pm 0.1^\circ$), the accuracy and repeatability of sensor system to perform stationary angular measurements in a single plane can be tested.

Difficulties arose evaluating the zero position at 20° of the Yaw axis which large fluctuations from the physical angle being reported (68° and 158° for the phone and watch respectively). We speculate that this may be due to the algorithm used to calibrate the rotation sensors working on assumptions on gravity direction. When the local coordinate system of the embedded sensors of the smartphone is aligned with the world axes, the yaw axis of the smartphone lies parallel to the vector of gravity. In this orientation the IMU is rotation-degenerate and thus prevented from obtaining a reference for calibration from the accelerometer resulting in an indeterminate

orientation output around the Yaw axis. However the relative orientation recorded between successive 20° steps showed strong agreement and repeatability between devices.

A free-swinging pendulum can test the accuracy and repeatability of the device to record sinusoidal oscillations (similar to planar movements of the upper arm) and, compare its performance at differing distances from the fulcrum.

The development of the novel servo-powered gimbal allows controlled movements of the centrally-mounted device at increasing angular velocities to determine the appropriate frequency range for accurate angular measurement during dynamic movement. It also allows for assessment of axis crosstalk during planar rotation and for accumulation of drift in continuous measurement.

Validation of the inertial sensing technology of the smartphone and smartwatch showed that static angle measurements were highly correlated with a commercially available inclinometer tool (reported accuracy of $\pm 0.1^\circ$) for all three axes of rotation. This was investigated in multiple devices of the same model as well as in a different smartphone. The ability of the devices to accurately and repeatedly measure relative static angles within $\pm 1.1^\circ$, supports their use in goniometry-based shoulder ROM measurements for which the accepted minimal clinically important difference are 11° to 16° for a single evaluator (Muir et al., 2010).

It is important to note that this accuracy was only found for the relative angle between two known positions. The absolute angle measured by each of the smartphones tested was significantly different ($p < 0.05$). Whilst the standard deviation of these differences between tests was low suggesting the discrepancies are

repeatable, care should be taken to characterise any offsets in angular measurement when employing a device to measure absolute orientation.

Smartphone and smartwatch data was strongly correlated (>0.95) to the potentiometer during repeated dynamic measurement trials. During pendulum swing for single axis oscillations, the out of plane rotation in non-sensitive axes were weakly correlated (<0.19), demonstrating minimal crosstalk between axes.

Using a custom-designed servo-powered gimbal system, planar rotation of both the smartphone and smartwatch was characterised at increasing angular velocities. Data was highly repeatable for both within and between days in both devices for each axis. The frequencies at which the smartphone and smartwatch optimally performed ($377^\circ/\text{s}$ and $358.1^\circ/\text{s}$ respectively) are well within the optimal responsiveness range compliant with angular velocity of the humerus when performing activities of daily living such as reaching for an object from a shelf (Rosen et al., 2005). In a study by Rosen (2015), the maximum angular velocity required to perform a common daily life task such as move an object at waist level and reach arm up to head height was between $49^\circ/\text{second}$ and $174^\circ/\text{second}$. Whilst the optimal responsiveness range of the smartwatch is slightly lower than the smartphone, it is still compliant with angular velocity of the humerus when performing activities of daily living (Rosen et al., 2005). The application on both devices may be limited for larger angular velocity humerus movements such as those associated with tennis serve or volleyball spike which can be in excess of $590^\circ/\text{s}$ and $920^\circ/\text{s}$ respectively (Wagner et al., 2012). Repetitive oscillation tests with the gimbal system over a 3-hour period produced consistently accurate and repeatable data from both the smart devices thus

demonstrating stability over time and an adequate internal compensation of sensor drift over prolonged measurement periods. This is in contrast the use of accelerometers or gyroscopes in the absence of sensor fusion in which the accumulation of drift during integration of data renders their use for ambulatory measurements longer than a few seconds infeasible (Giansanti et al., 2003; Zhou and Hu, 2007).

The validation protocol has some limitations. Only planar movements were evaluated. Whilst this is reflective of some goniometry applications such as of the knee which is a hinge joint, it doesn't address the cross axis movement characteristics of the shoulder. However, the results indicate that each of the 3 axes perform comparably well and that crosstalk between them is minimal. As the inertial sensor unit is 3-dimensional and the data is output as a unit quaternion describing orientation in 3-dimensional space, an evaluation of the post-processing steps to decompose the quaternion into meaningful clinical angles rather than of the raw output from the rotation vector sensor is more appropriate.

The design of the servo-powered gimbal restricted the evaluation of the Yaw axis during dynamic conditions. However during the pendulum swing trials, this axis performed similarly well to the Roll and Pitch and thus was assumed to be of comparable performance during further testing.

The continuous measurement period was limited to 3 hours in this work. The battery consumption of the smartphone and smartwatch would allow for longer durations and therefore future studies should look at their performance over a longer time.

6.2.3 Application

The simple mobile application that has been developed to record goniometric measurements of the humero-thoracic joint consists of a single sensing unit (smartwatch or smartphone) that can be easily and quickly attached to the upper arm via elasticated Velcro straps. The mobile device is ideally attached to the lateral aspect of the upper arm at the site of least muscle mass to avoid slippage during arm movement. The distance of the attached sensor to the joint centre is negligible for the description of relative orientation of consecutive body segments (el-Zayat et al., 2011).

In contrast to conventional goniometry using goniometers and electrogoniometers, it does not require to be attached across a joint and therefore allows for natural and unrestricted movement. Following the validation of the accuracy of the devices to measure angular change during dynamic motion, the system can be used to record rotation of the shoulder joint during motion. Thus the patient is not required to maintain a static end of range position as in conventional goniometry. This is particularly beneficial for patients suffering from shoulder pain due to impingement or any other condition affecting the joint and the surrounding soft tissue. Some studies have shown that dynamic measurement is likely to be more reflecting of the patients' true ability to achieve maximum rotation, albeit momentarily during the angular movement of the humerus.

The developed mobile system is portable and does not require any other set up for obtaining measurements. The measurement data can be readily stored on the device itself and operated remotely in any location.

This study has shown that such a system can be developed within a cost-effective budget. The application can be made widely available to users of most modern Android smartphones, giving it a distinct advantage over other digital inclinometers and more complex measurement tools. Not all providers outside of those specializing in musculoskeletal medicine have routine access to a conventional double-armed goniometer, whereas most have a smartphone, giving the smartphone goniometer an availability advantage in this regard.

After data collection, Bluetooth or Wi-Fi connectivity facilitates transmission of the recorded measurements to a PC or laptop for analysis.

Development of real-time output within the mobile application itself could provide instantaneous results to the clinician and patient during the clinical examination, and eliminate the requirement of wireless transmission to a computer for time-consuming offline processing.

6.3 Concurrent Validity and Repeatability for Clinical Goniometry

The strong agreement between the smartwatch application and the universal goniometer in both healthy (ICC 0.8) and impaired (ICC 0.88) conditions indicated the potential for the smartwatch to be an alternative measurement tool for clinical shoulder ROM measurements. This is comparable to the results of previous studies comparing smartphone inclinometry to a traditional goniometer (Shin et al., 2012; Werner et al., 2014; Jenny et al., 2013; Milani et al., 2014).

The mean differences between the angles recorded by the smartwatch and the goniometer fell within the minimal clinically important range of 11° to 16° for a

single observer in all movements in both the healthy and impaired conditions. However, upon further inspection using Bland Altman plot analysis, the LOA in both the healthy and impaired conditions were unacceptably high for most of the movements measured. The LOA for internal rotation was the only movement for which the values fell within the acceptable clinical range in both conditions, and even so, was towards the high limit (13.9° and 12.77°). As discussed in Chapter 5, the unfavourable results may be due to the small sample size and large variation in measurement differences and further study is required to ascertain whether the two methods can be used interchangeably. Since preliminary accuracy and repeatability studies of the smartwatch to measure known angles showed excellent absolute agreement, the discrepancies in this study may be due to inaccuracy of the goniometer methods. Again, further study is needed to either confirm or deny which of the methods is most accurate.

The strong between day inter-rater repeatability ($ICC > 0.9$) of the smartwatch shows promise to the practical use of the developed system in monitoring impairment progression or evaluating treatment interventions. The agreement was statistically comparable to the goniometer repeatability ($ICC 0.92$). This relationship was comparable to the existing literature of smartphone applications (Mitchell et al., 2014; Mejia-Hernandez et al., 2018) .

Whilst the application of kinesiology tape across the shoulder girdle gives some insight into the reliability and repeatability of the measurement modalities when movement is impaired, further investigation in different patient populations and impairment severity is needed to validate the developed system for clinical use.

In this study, the smartwatch was attached to the lateral aspect of the upper arm via an elasticated strap. Due to its small size, it did not restrict normal movement and subject feedback confirmed it was not uncomfortable to wear for the period of measurement. The exact distance from the shoulder joint centre was not considered since for description of relative orientation of consecutive body segments, the distance of the attached sensor to the joint centre is negligible (el-Zayat et al., 2011). Shin et al (2012) used a smartphone inclinometer tool with the device attached to the distal forearm to measure active and passive shoulder ROM in 41 patients. This achieved acceptable inter and intra-observer reliability compared to classical goniometry. Furthermore, Mourcou (2015) found an error of less than 0.12° when varying the position of a smartphone on a robotic arm during inclinometer application testing. Since the smartwatch is fundamentally designed to be worn on the wrist, future tests should establish whether the application can produce results of similar reliability and repeatability when worn on the forearm rather than the primary consecutive body segment. During flexion, extension and abduction, the observer should be extra vigilant that the elbow is maintained in a fixed, extended position throughout the movement so that pure shoulder rotation can be assessed. This may also improve measurements of internal and external rotation of the shoulder since these movement control the position of forearm relative to humerus when the elbow is flexed.

Due to limitations in resources there was only one observer during the trials.

Evaluation of inter-observer reliability, particularly at different levels of expertise (for example, orthopaedic surgeon, physiotherapist, medical student and family

member) would further inform the potential application of the developed system in clinical and remote goniometry. Whilst the between day repeatability of traditional goniometry is strong for a single observer, when measurements are taken on consecutive days by different observers, the repeatability is often low (Riddle, 1987). In busy clinics ROM measurement may be recorded by a different clinician between one appointment and the next. Thus the ability to communicate effectively and consistently between peers regarding patient improvement is of significant value. In addition, with increasing demands on clinics and waiting times, researchers are turning their attention to tele-rehabilitation and remote monitoring as a solution (Ongvisatepaiboon et al., 2015; Hoffmann et al., 2007). For this, patients and their family members could record their shoulder ROM at home and submit the results electronically or via video call to their clinician for review, without requiring attendance at the clinic. Furthermore, this could increase access to physiotherapy services for patients living in remote, rural locations or, patients who are unable to travel to clinic for regular appointments.

An accurate and consistent measurement of shoulder ROM is important in the physical examination and functional evaluation of the shoulder. Considering convenience, cost-effectiveness and its validity compared to the current clinical gold standard for goniometry, this new method could be widely used for measuring the shoulder ROM, although the inter-observer reliability needs to be established first.

6.4 Future Work

This thesis has described the development and initial validation of a mobile technology for the purpose of clinical goniometry of the shoulder. The overall aim of

the system was to provide a cost-effective and accurate quantitative measure of shoulder range of motion that could be used in a clinical or home environment. The system is portable, with the potential to be operated from the clinician or patients own smart device and can be used in a non-specialised space.

The inclusion of a within-application data analysis step to calculate range of motion in real-time, would eliminate the need for connectivity and transfer to a PC or laptop thus allowing the clinician to view results immediately. This would further increase the usability of the system in efficient clinical assessment. The system was developed within a limited budget and can be operated on the majority of modern Android smartphones or smartwatches.

Due to their small size the use of the smartphone and smartwatch as a goniometric tool could be expanded past the shoulder and used to measure ROM of other joints of the body such as the elbow or knee. A similar comparison to conventional goniometry or optical motion tracking of these joints would be required to validate this.

Whilst this work focuses on planar measurements of the shoulder akin to conventional goniometry, the 3D inertial sensor technology of the devices provides potential for measuring 3D kinematics of the shoulder during multi-planar movement tasks of daily living. Initial testing of accuracy and repeatability for angular velocities within the range associated with most daily living activities of the upper limb show promise in the system for measuring the functional range of motion of the shoulder. Further testing compared to gold standard techniques such as optical motion capture is required to validate the technology for this purpose. The main barrier to this currently is a lack of standardised analysis to obtain clinically

meaningful joint angle data from the angular data collected, as discussed in Chapter 2. There is a need to develop an algorithm that is able to interpret raw unit quaternion data from the mobile device into 3-dimensional angles in the absence of both gimbal lock and singularities. Alternatively, an algorithm that can reliably convert the raw data into latitude (elevation) or longitude (plane) corrected to the anatomical plane of the humero-thoracic joint would facilitate this application. The mathematical solution for this remains to be established.

The ability to quantify dynamic range of motion in this way would facilitate the incorporation of functional tasks and ADL movements into routine clinical assessment, which more accurately reflects the effect of treatment interventions on the daily lives of patients.

Furthermore, continuous monitoring of shoulder range of motion during daily life would be greatly beneficial for increasing our knowledge of joint characteristics in both healthy and pathological populations. During preliminary tests the system showed stability in accurately recording angular change over prolonged periods of measurement on the servo-powered gimbal. In addition, the smart devices have internal storage space capable of storing large amounts of data on the devices themselves. In the future this technology could be tested for use as a powerful wearable system to collect ambulatory data of the shoulder over a period of a day. Continuous remote monitoring would greatly help to inform clinical assessment, diagnosis, risk factors, prosthesis design and, treatment planning and evaluation of interventions to ensure patients are able to carry out their normal lives and achieve an optimal quality of life.

References

- Alizadehkhayat, O., Roebuck, M.M., Makki, A.T. and Frostick, S.P., 2017. Pain, functional disability, psychological status, and health-related quality of life in patients with subacromial impingement syndrome. *Cogent Medicine*, 4(1), p.1406631.
- Aminian, K., Najafi, B., Büla, C., Leyvraz, P.F. and Robert, P., 2002. Spatio-temporal parameters of gait measured by an ambulatory system using miniature gyroscopes. *Journal of biomechanics*, 35(5), pp.689-699.
- Anglin, C. and Wyss, U.P., 2000. Arm motion and load analysis of sit-to-stand, stand-to-sit, cane walking and lifting. *Clinical biomechanics*, 15(6), pp.441-448.
- Angst, F., Goldhahn, J., Drerup, S., Aeschlimann, A., Schwyzer, H.K. and Simmen, B.R., 2008. Responsiveness of six outcome assessment instruments in total shoulder arthroplasty. *Arthritis Care & Research*, 59(3), pp.391-398.
- Antos, S.A., Albert, M.V. and Kording, K.P., 2014. Hand, belt, pocket or bag: Practical activity tracking with mobile phones. *Journal of neuroscience methods*, 231, pp.22-30.
- Bachmann, E.R., McGhee, R.B., Yun, X. and Zyda, M.J., 2001, November. Inertial and magnetic posture tracking for inserting humans into networked virtual environments. In *Proceedings of the ACM symposium on Virtual reality software and technology* (pp. 9-16). ACM.
- Bai, L., Pepper, M.G., Yana, Y., Spurgeon, S.K. and Sakel, M., 2012, May. Application of low cost inertial sensors to human motion analysis. In *Instrumentation and Measurement Technology Conference (I2MTC), 2012 IEEE International* (pp. 1280-1285). IEEE.
- Baker, M.J., 2017. <http://www.euclideanspace.com/maths/algebra/realNormedAlgebra/quaternions/> (Accessed February 2019).
- Barker, T.M., Nicol, A.C., Kelly, I.G. and Paul, J.P., 1996. Three-dimensional joint co-ordination strategies of the upper limb during functional activities. *Proceedings of the Institution of Mechanical Engineers, Part H: Journal of Engineering in Medicine*, 210(1), pp.17-26.
- Bartlett, R., Wheat, J. and Robins, M., 2007. Is movement variability important for sports biomechanists?. *Sports biomechanics*, 6(2), pp.224-243.

- Bernmark, E. and Wiktorin, C., 2002. A triaxial accelerometer for measuring arm movements. *Applied ergonomics*, 33(6), pp.541-547.
- Bland, J.M. and Altman, D., 1986. Statistical methods for assessing agreement between two methods of clinical measurement. *The lancet*, 327(8476), pp.307-310.
- Bonnechère B, Jansen B, Salvia P, et al. 2014. Validity and reliability of the Kinect within functional assessment activities: comparison with standard stereophotogrammetry. *Gait Posture*;39:593–598.
- Boone, D.C., Azen, S.P., Lin, C.M., Spence, C., Baron, C. and Lee, L., 1978. Reliability of goniometric measurements. *Physical therapy*, 58(11), pp.1355-1360.
- Bourne, D.A., Choo, A.M., Regan, W.D., MacIntyre, D.L. and Oxland, T.R., 2007. Three-dimensional rotation of the scapula during functional movements: an in vivo study in healthy volunteers. *Journal of Shoulder and Elbow surgery*, 16(2), pp.150-162.
- Borstad, J.D. and Ludewig, P.M., 2002. Comparison of scapular kinematics between elevation and lowering of the arm in the scapular plane. *Clinical Biomechanics*, 17(9-10), pp.650-659.
- Bouten, C.V., Koekkoek, K.T., Verduin, M., Kodde, R. and Janssen, J.D., 1997. A triaxial accelerometer and portable data processing unit for the assessment of daily physical activity. *IEEE transactions on biomedical engineering*, 44(3), pp.136-147.
- Buckley, M.A., Yardley, A., Johnson, G.R. and Cams, D.A., 1996. Dynamics of the upper limb during performance of the tasks of everyday living—a review of the current knowledge base. *Proceedings of the Institution of Mechanical Engineers, Part H: Journal of Engineering in Medicine*, 210(4), pp.241-247.
- Cancela J, Arredondo MT, Hurtado O. Proposal of a Kinect(TM)-based system for gait assessment and rehabilitation in Parkinson's disease. *Conf Proc IEEE Eng Med Biol Soc.* 2014;2014:4519–4522.
- Charry, E., Lai, D.T., Begg, R.K. and Palaniswami, M., 2009. A study on band-pass filtering for calculating foot displacements from accelerometer and gyroscope sensors. *IMU*, 1, p.0.
- Clark RA, Pua YH, Fortin K, et al. Validity of the Microsoft Kinect for assessment of postural control. *Gait Posture*. 2012;36:372–377.
- Coley, B., Jolles, B.M., Farron, A. and Aminian, K., 2008. Arm position during daily activity. *Gait & posture*, 28(4), pp.581-587.

- Coley, B., Jolles, B.M., Farron, A. and Aminian, K., 2009. Detection of the movement of the humerus during daily activity. *Medical & biological engineering & computing*, 47(5), pp.467-474.
- Corazza, S., Mündermann, L. and Andriacchi, T., 2006, June. Markerless motion capture methods for the estimation of human body kinematics. In 9th International Symposium on the 3D Analysis of Human Movement, Valenciennes, France, June (pp. 28-30).
- Cuesta-Vargas, A.I., Galán-Mercant, A. and Williams, J.M., 2010. The use of inertial sensors system for human motion analysis. *Physical Therapy Reviews*, 15(6), pp.462-473.
- Cutti, A.G., Giovanardi, A., Rocchi, L., Davalli, A. and Sacchetti, R., 2008. Ambulatory measurement of shoulder and elbow kinematics through inertial and magnetic sensors. *Medical & biological engineering & computing*, 46(2), pp.169-178.
- Dawson, J., Rogers, K., Fitzpatrick, R. and Carr, A., 2009. The Oxford shoulder score revisited. *Archives of orthopaedic and trauma surgery*, 129(1), pp.119-123.
- De Vries, W.H.K., Veeger, H.E.J., Cutti, A.G., Baten, C. and Van Der Helm, F.C.T., 2010. Functionally interpretable local coordinate systems for the upper extremity using inertial & magnetic measurement systems. *Journal of biomechanics*, 43(10), pp.1983-1988.
- De Winter, A.F., Heemskerk, M.A., Terwee, C.B., Jans, M.P., Devillé, W., Van Schaardenburg, D.J., Scholten, R.J. and Bouter, L.M., 2004. Inter-observer reproducibility of measurements of range of motion in patients with shoulder pain using a digital inclinometer. *BMC musculoskeletal disorders*, 5(1), p.18.
- Diebel, J., 2006. Representing attitude: Euler angles, unit quaternions, and rotation vectors. *Matrix*, 58(15-16), pp.1-35.
- Del Rosario, M.B., Redmond, S.J. and Lovell, N.H., 2015. Tracking the evolution of smartphone sensing for monitoring human movement. *Sensors*, 15(8), pp.18901-18933.
- Doorenbosch, C.A., Veeger, H.E.J. and Harlaar, J., 2003. The globe system: an unambiguous description of shoulder positions in daily life movements.
- Duc, C., Farron, A., Pichonnaz, C., Jolles, B.M., Bassin, J.P. and Aminian, K., 2013. Distribution of arm velocity and frequency of arm usage during daily activity: objective outcome evaluation after shoulder surgery. *Gait & posture*, 38(2), pp.247-252.

- El-Zayat, B.F., Efe, T., Heidrich, A., Wolf, U., Timmesfeld, N., Heyse, T.J., Lakemeier, S., Fuchs-Winkelmann, S. and Schofer, M.D., 2011. Objective assessment of shoulder mobility with a new 3D gyroscope-a validation study. *BMC musculoskeletal disorders*, 12(1), p.168.
- Faber HvH, H., van Ipenburg, S. and van Lummel, R.C., 2006. Measurement of the Elevation and Rotation of the Humerus using a 3D Accelerometer. In *Congress of the Dutch Society of Arthroscopy*.
- Fayad, F., Lefevre-Colau, M.M., Gautheron, V., Macé, Y., Fermanian, J., Mayoux-Benhamou, A., Roren, A., Rannou, F., Roby-Brami, A., Revel, M. and Poiraudreau, S., 2009. Reliability, validity and responsiveness of the French version of the questionnaire Quick Disability of the Arm, Shoulder and Hand in shoulder disorders. *Manual therapy*, 14(2), pp.206-212.
- Ferriero, G., Vercelli, S., Sartorio, F., Lasa, S.M., Ilieva, E., Brigatti, E., Ruella, C. and Foti, C., 2013. Reliability of a smartphone-based goniometer for knee joint goniometry. *International journal of rehabilitation research*, 36(2), pp.146-151.
- Fern'ndez-Baena, A., Susín, A. and Lligadas, X., 2012, September. Biomechanical validation of upper-body and lower-body joint movements of kinect motion capture data for rehabilitation treatments. In *Intelligent networking and collaborative systems (INCoS), 2012 4th international conference on* (pp. 656-661). IEEE.
- Foxlin, E., 1996, March. Inertial head-tracker sensor fusion by a complementary separate-bias Kalman filter. In *Virtual Reality Annual International Symposium, 1996.*, Proceedings of the IEEE 1996 (pp. 185-194). IEEE.
- Gates, D.H., Walters, L.S., Cowley, J., Wilken, J.M. and Resnik, L., 2016. Range of motion requirements for upper-limb activities of daily living. *American Journal of Occupational Therapy*, 70(1), pp.7001350010p1-7001350010p10.
- Gajdosik, R.L. and Bohannon, R.W., 1987. Clinical measurement of range of motion: review of goniometry emphasizing reliability and validity. *Physical therapy*, 67(12), pp.1867-1872.
- Galinski, D. and Dehez, B., 2012, June. Evaluation of initialization procedures for estimating upper limb kinematics with MARG sensors. In *Proceedings of 4th IEEE RAS & EMBS International Conference, Roma, Italy* (pp. 24-27).
- Giansanti, D., Maccioni, G. and Macellari, V., 2005. The development and test of a device for the reconstruction of 3-D position and orientation by means of a kinematic sensor assembly with rate gyroscopes and accelerometers. *IEEE transactions on biomedical engineering*, 52(7), pp.1271-1277.

- Giansanti, D., Macellari, V., Maccioni, G. and Cappozzo, A., 2003. Is it feasible to reconstruct body segment 3-D position and orientation using accelerometric data?. *IEEE transactions on biomedical engineering*, 50(4), pp.476-483.
- Godfrey, A.C.R.M.D.O.G., Conway, R., Meagher, D. and ÓLaighin, G., 2008. Direct measurement of human movement by accelerometry. *Medical engineering & physics*, 30(10), pp.1364-1386.
- Haering, D., Raison, M., Arndt, A. and Begon, M., 2014. Kinematic model and elbow flexion interaction on shoulder range of motion. *Computer methods in biomechanics and biomedical engineering*, 17(sup1), pp.84-85.
- Hambly, K., Sibley, R. and Ockendon, M., 2012. Level of agreement between a novel smartphone application and a long arm goniometer for the assessment of maximum active knee flexion by an inexperienced tester. *International Journal of Physiotherapy & Rehabilitation*, 2.
- Hanson, A.J., 2005, July. Visualizing quaternions. In *ACM SIGGRAPH 2005 Courses* (p. 1). ACM.
- Hayes, K., Walton, J.R., Szomor, Z.L. and Murrell, G.A., 2001. Reliability of five methods for assessing shoulder range of motion. *Australian Journal of Physiotherapy*, 47(4), pp.289-294.
- He, Y. and Li, Y., 2013. Physical activity recognition utilizing the built-in kinematic sensors of a smartphone. *International Journal of Distributed Sensor Networks*, 9(4), p.481580.
- Hebert, L.J., Moffet, H., McFadyen, B.J. and St-Vincent, G., 2000. A method of measuring three-dimensional scapular attitudes using the optotrak probing system. *Clinical Biomechanics*, 15(1), pp.1-8.
- Henmi, S., Yonenobu, K., Masatomi, T. and Oda, K., 2006. A biomechanical study of activities of daily living using neck and upper limbs with an optical three-dimensional motion analysis system. *Modern rheumatology*, 16(5), pp.289-293.
- Herda, L., Urtasun, R., Fua, P. and Hanson, A., 2003. Automatic determination of shoulder joint limits using quaternion field boundaries. *The International Journal of Robotics Research*, 22(6), pp.419-436.
- Hoffmann, T., Russell, T. and Cooke, H., 2007. Remote measurement via the Internet of upper limb range of motion in people who have had a stroke. *Journal of telemedicine and telecare*, 13(8), pp.401-405.

- Hurd, W.J., Morrow, M.M., Miller, E.J., Adams, R.A., Sperling, J.W. and Kaufman, K.R., 2014. Novel approaches to objectively assess shoulder function. *Journal of shoulder and elbow surgery*, 23(10), pp.e251-e255.
- Jenny, J.Y., 2013. Measurement of the knee flexion angle with a smartphone-application is precise and accurate. *The Journal of arthroplasty*, 28(5), pp.784-787.
- Johnson, P.W., Jonsson, P. and Hagberg, M., 2002. Comparison of measurement accuracy between two wrist goniometer systems during pronation and supination. *Journal of Electromyography and Kinesiology*, 12(5), pp.413-420.
- Johnson, L.B., Sumner, S., Duong, T., Yan, P., Bajcsy, R., Abresch, R.T., de Bie, E. and Han, J.J., 2015. Validity and reliability of smartphone magnetometer-based goniometer evaluation of shoulder abduction—A pilot study. *Manual therapy*, 20(6), pp.777-782.
- Jordan, K., Dziedzic, K., Mullis, R., Dawes, P. T., & Jones, P. W. (2001). The development of three-dimensional range of motion measurement systems for clinical practice. *Rheumatology*, 40, 1081–1088.
- Karduna, A.R., McClure, P.W. and Michener, L.A., 2000. Scapular kinematics: effects of altering the Euler angle sequence of rotations. *Journal of Biomechanics*, 33(9), pp.1063-1068.
- Kirking, B., El-Gohary, M. and Kwon, Y., 2016. The feasibility of shoulder motion tracking during activities of daily living using inertial measurement units. *Gait & posture*, 49, pp.47-53.
- Kirkley, A., Griffin, S., McLintock, H. and Ng, L., 1998. The development and evaluation of a disease-specific quality of life measurement tool for shoulder instability. *The American Journal of Sports Medicine*, 26(6), pp.764-772.
- Kocher, M.S., Horan, M.P., Briggs, K.K., Richardson, T.R., O'holleran, J. and Hawkins, R.J., 2005. Reliability, validity, and responsiveness of the American Shoulder and Elbow Surgeons subjective shoulder scale in patients with shoulder instability, rotator cuff disease, and glenohumeral arthritis. *JBJS*, 87(9), pp.2006-2011.
- Kolber, M.J. and Hanney, W.J., 2012. The reliability and concurrent validity of shoulder mobility measurements using a digital inclinometer and goniometer: a technical report. *International journal of sports physical therapy*, 7(3), p.306.
- Kos, A., Tomažič, S. and Umek, A., 2016. Suitability of smartphone inertial sensors for real-time biofeedback applications. *Sensors*, 16(3), p.301.

- Kuipers, J.B., 1999. Quaternions and rotation sequences (Vol. 66, pp. 127-143). Princeton: Princeton university press.
- Lang, C.E., Wagner, J.M., Edwards, D.F. and Dromerick, A.W., 2007. Upper extremity use in people with hemiparesis in the first few weeks after stroke. *Journal of Neurologic Physical Therapy*, 31(2), pp.56-63.
- Lee, W.W., Yen, S.C., Tay, E.B.A., Zhao, Z., Xu, T.M., Ling, K.K.M., Ng, Y.S., Chew, E., Cheong, A.L.K. and Huat, G.K.C., 2014. A smartphone-centric system for the range of motion assessment in stroke patients. *IEEE journal of biomedical and health informatics*, 18(6), pp.1839-1847.
- Levanon, Y., Gefen, A., Lerman, Y., Givon, U. and Ratzon, N.Z., 2010. Validity and reliability of upper extremity three-dimensional kinematics during a typing task. *Gait & posture*, 32(4), pp.469-474.
- Li S, Pathirana PN, Caelli T. Multi-kinect skeleton fusion for physical rehabilitation monitoring. *Conf Proc IEEE Eng Med Biol Soc*. 2014;2014:5060–5063.
- Liu, T., Inoue, Y. and Shibata, K., 2009. Development of a wearable sensor system for quantitative gait analysis. *Measurement*, 42(7), pp.978-988.
- Ludewig, P.M., Phadke, V., Braman, J.P., Hassett, D.R., Cieminski, C.J. and LaPrade, R.F., 2009. Motion of the shoulder complex during multiplanar humeral elevation. *The Journal of Bone and Joint Surgery. American volume.*, 91(2), p.378.
- Luinge, H.J., 2002. Inertial sensing of human movement (pp. 2079-2089). Enschede: Twente University Press.
- Luinge, H.J. and Veltink, P.H., 2004. Inclination measurement of human movement using a 3-D accelerometer with autocalibration. *IEEE Transactions on neural systems and rehabilitation engineering*, 12(1), pp.112-121.
- Luinge, H.J., Veltink, P.H. and Baten, C.T., 2007. Ambulatory measurement of arm orientation. *Journal of biomechanics*, 40(1), pp.78-85.
- MacDermid, J.C., Solomon, P. and Prkachin, K., 2006. The Shoulder Pain and Disability Index demonstrates factor, construct and longitudinal validity. *BMC musculoskeletal disorders*, 7(1), p.12.
- Magermans, D.J., Chadwick, E.K.J., Veeger, H.E.J. and Van Der Helm, F.C.T., 2005. Requirements for upper extremity motions during activities of daily living. *Clinical biomechanics*, 20(6), pp.591-599.
- Mathie, M.J., Coster, A.C.F., Lovell, N.H. and Celler, B.G., 2003. Detection of daily physical activities using a triaxial accelerometer. *Medical and Biological Engineering and Computing*, 41(3), pp.296-301.

- Matsen III, F.A., Tang, A., Russ, S.M. and Hsu, J.E., 2017. Relationship between patient-reported assessment of shoulder function and objective range-of-motion measurements. *JBJS*, 99(5), pp.417-426.
- Mayagoitia, R.E., Nene, A.V. and Veltink, P.H., 2002. Accelerometer and rate gyroscope measurement of kinematics: an inexpensive alternative to optical motion analysis systems. *Journal of biomechanics*, 35(4), pp.537-542.
- MacDermid, J.C., Ramos, J., Drosdowech, D., Faber, K. and Patterson, S., 2004. The impact of rotator cuff pathology on isometric and isokinetic strength, function, and quality of life. *Journal of Shoulder and Elbow Surgery*, 13(6), pp.593-598.
- Mejia-Hernandez, K., Chang, A., Eardley-Harris, N., Jaarsma, R., Gill, T.K. and McLean, J.M., 2018. Smartphone applications for the evaluation of pathologic shoulder range of motion and shoulder scores—a comparative study. *JSES Open Access*, 2(1), pp.109-114.
- Merriaux, P., Dupuis, Y., Boutteau, R., Vasseur, P. and Savatier, X., 2017. A study of Vicon system positioning performance. *Sensors*, 17(7), p.1591.
- Micallef, N., Baillie, L. and Uzor, S., 2016, September. Time to exercise!: an aide-memoire stroke app for post-stroke arm rehabilitation. In *Proceedings of the 18th international conference on Human-computer interaction with mobile devices and services* (pp. 112-123). ACM.
- Milani, P., Coccetta, C.A., Rabini, A., Sciarra, T., Massazza, G. and Ferriero, G., 2014. Mobile smartphone applications for body position measurement in rehabilitation: a review of goniometric tools. *PM&R*, 6(11), pp.1038-1043.
- Mitchell, E., Monaghan, D. and O'Connor, N.E., 2013. Classification of sporting activities using smartphone accelerometers. *Sensors*, 13(4), pp.5317-5337.
- Mitchell, K., Gutierrez, S.B., Sutton, S., Morton, S. and Morgenthaler, A., 2014. Reliability and validity of goniometric iPhone applications for the assessment of active shoulder external rotation. *Physiotherapy Theory and Practice*, 30(7), pp.521-525.
- Morris, J.R.W., 1973. Accelerometry—A technique for the measurement of human body movements. *Journal of biomechanics*, 6(6), pp.729-736.
- Mortazavi, B., Nemat, E., VanderWall, K., Flores-Rodriguez, H.G., Cai, J.Y.J., Lucier, J., Naeim, A. and Sarrafzadeh, M., 2015. Can smartwatches replace smartphones for posture tracking?. *Sensors*, 15(10), pp.26783-26800.

- Mourcou, Q., Fleury, A., Franco, C., Klopčič, F. and Vuillerme, N., 2015. Performance evaluation of smartphone inertial sensors measurement for range of motion. *Sensors*, 15(9), pp.23168-23187.
- Mullaney, M.J., McHugh, M.P., Johnson, C.P. and Tyler, T.F., 2010. Reliability of shoulder range of motion comparing a goniometer to a digital level. *Physiotherapy Theory and Practice*, 26(5), pp.327-333.
- Muir, S.W., Corea, C.L. and Beaupre, L., 2010. Evaluating change in clinical status: reliability and measures of agreement for the assessment of glenohumeral range of motion. *North American journal of sports physical therapy: NAJSPT*, 5(3), p.98.
- Mündermann, L., Corazza, S., Chaudhari, A.M., Andriacchi, T.P., Sundaresan, A. and Chellappa, R., 2006, January. Measuring human movement for biomechanical applications using markerless motion capture. In *Three-dimensional image capture and applications VII* (Vol. 6056, p. 60560R). International Society for Optics and Photonics.
- Murray, I. A. (1999). Determining upper limb kinematics and dynamics during everyday tasks. Ph.D Thesis, Centre for Rehabilitation and Engineering Studies, Newcastle University. Newcastle upon Tyne, UK.
- Murray, I.A. and Johnson, G.R., 2004. A study of the external forces and moments at the shoulder and elbow while performing every day tasks. *Clinical biomechanics*, 19(6), pp.586-594.
- Namdari, S., Yagnik, G., Ebaugh, D.D., Nagda, S., Ramsey, M.L., Williams Jr, G.R. and Mehta, S., 2012. Defining functional shoulder range of motion for activities of daily living. *Journal of shoulder and elbow surgery*, 21(9), pp.1177-1183.
- O'Donovan, K.J., Kamnik, R., O'Keefe, D.T. and Lyons, G.M., 2007. An inertial and magnetic sensor based technique for joint angle measurement. *Journal of biomechanics*, 40(12), pp.2604-2611.
- Oihénart, L., Duc, C. and Aminian, K., 2012. iShould: Functional evaluation of the shoulder using a Smartphone. *Gait & Posture*, 36, pp.S61-S62.
- Ongvisatepaiboon, K., Vanijja, V. and Chan, J.H., 2015. Smartphone-based Tele-Rehabilitation Framework for Patient with Frozen Shoulder. *ICADIWT*, 2015, pp.158-169.
- Phadke, V., Braman, J.P., LaPrade, R.F. and Ludewig, P.M., 2011. Comparison of glenohumeral motion using different rotation sequences. *Journal of biomechanics*, 44(4), pp.700-705.

- Phan, D., Siong, L.Y., Pathirana, P.N. and Seneviratne, A., 2015, October. Smartwatch: Performance evaluation for long-term heart rate monitoring. In *Bioelectronics and Bioinformatics (ISBB), 2015 International Symposium on* (pp. 144-147). IEEE.
- Pérez, R., Costa, Ú., Torrent, M., Solana, J., Opisso, E., Cáceres, C., Tormos, J.M., Medina, J. and Gómez, E.J., 2010. Upper limb portable motion analysis system based on inertial technology for neurorehabilitation purposes. *Sensors*, 10(12), pp.10733-10751.
- Peterson, B. and Palmerud, G., 1996. Measurement of upper extremity orientation by video stereometry system. *Medical and Biological Engineering and Computing*, 34(2), pp.149-154.
- Picerno, P., Cereatti, A. and Cappozzo, A., 2008. Joint kinematics estimate using wearable inertial and magnetic sensing modules. *Gait & posture*, 28(4), pp.588-595.
- Pichonnaz, C., Aminian, K., Ancey, C., Jaccard, H., Lécureux, E., Duc, C., Farron, A., Jolles, B.M. and Gleeson, N., 2017. Heightened clinical utility of smartphone versus body-worn inertial system for shoulder function BB score. *PloS one*, 12(3), p.e0174365.
- Pichonnaz, C., Duc, C., Jaccard, H., Ancey, C., Lécureux, E., Aminian, K., Farron, A., Jolles, B.M. and Gleeson, N., 2015. Comparison of a dedicated body-worn inertial system and a smartphone for shoulder function and arm elevation evaluation. *Physiotherapy*, 101, pp.e1205-e1206.
- Rawassizadeh, R., Price, B.A. and Petre, M., 2015. Wearables: Has the age of smartwatches finally arrived?. *Communications of the ACM*, 58(1), pp.45-47.
- Reither, L.R., Foreman, M.H., Migotsky, N., Haddix, C. and Engsberg, J.R., 2018. Upper extremity movement reliability and validity of the Kinect version 2. *Disability and Rehabilitation: Assistive Technology*, 13(1), pp.54-59.
- Riddle, D.L., Rothstein, J.M. and Lamb, R.L., 1987. Goniometric reliability in a clinical setting: shoulder measurements. *Physical therapy*, 67(5), pp.668-673.
- Robertson, G., et al. (2014) *Research Methods in Biomechanics*. 2nd Edition, Human Kinetics, USA, 92.
- Roldan-Jimenez, C., Cuesta-Vargas, A. and Bennett, P., 2015. Studying upper-limb kinematics using inertial sensors embedded in mobile phones. *JMIR rehabilitation and assistive technologies*, 2(1).

- Roren, A., Lefevre-Colau, M.M., Roby-Brami, A., Revel, M., Fermanian, J., Gautheron, V., Poiraudau, S. and Fayad, F., 2012. Modified 3D scapular kinematic patterns for activities of daily living in painful shoulders with restricted mobility: a comparison with contralateral unaffected shoulders. *Journal of biomechanics*, 45(7), pp.1305-1311.
- Rosen, J., Perry, J.C., Manning, N., Burns, S. and Hannaford, B., 2005, July. The human arm kinematics and dynamics during daily activities-toward a 7 DOF upper limb powered exoskeleton. In *Advanced Robotics, 2005. ICAR'05. Proceedings. 12th International Conference on* (pp. 532-539). IEEE.
- Roetenberg, D., Luinge, H.J., Baten, C.T. and Veltink, P.H., 2005. Compensation of magnetic disturbances improves inertial and magnetic sensing of human body segment orientation. *IEEE Transactions on neural systems and rehabilitation engineering*, 13(3), pp.395-405.
- Roetenberg, D., Baten, C.T. and Veltink, P.H., 2007. Estimating body segment orientation by applying inertial and magnetic sensing near ferromagnetic materials. *IEEE Transactions on Neural Systems and Rehabilitation Engineering*, 15(3), pp.469-471.
- Roy, J.S., MacDermid, J.C. and Woodhouse, L.J., 2009. Measuring shoulder function: a systematic review of four questionnaires. *Arthritis Care & Research: Official Journal of the American College of Rheumatology*, 61(5), pp.623-632.
- Rundquist, P.J., Anderson, D.D., Guanche, C.A. and Ludewig, P.M., 2003. Shoulder kinematics in subjects with frozen shoulder1. *Archives of physical medicine and rehabilitation*, 84(10), pp.1473-1479.
- Schepers, H.M., Roetenberg, D. and Veltink, P.H., 2010. Ambulatory human motion tracking by fusion of inertial and magnetic sensing with adaptive actuation. *Medical & biological engineering & computing*, 48(1), p.27.
- Schiefer, C., Ellegast, R.P., Hermanns, I., Kraus, T., Ochsmann, E., Larue, C. and Plamondon, A., 2014. Optimization of inertial sensor-based motion capturing for magnetically distorted field applications. *Journal of biomechanical engineering*, 136(12), p.121008.
- Schutz, Y., Weinsier, R.L. and Hunter, G.R., 2001. Assessment of free-living physical activity in humans: an overview of currently available and proposed new measures. *Obesity Research*, 9(6), pp.368-379.
- Šenk, M. and Cheze, L., 2006. Rotation sequence as an important factor in shoulder kinematics. *Clinical biomechanics*, 21, pp.S3-S8.

- Shin, S.H., Lee, O.S., Oh, J.H. and Kim, S.H., 2012. Within-day reliability of shoulder range of motion measurement with a smartphone. *Manual therapy*, 17(4), pp.298-304.
- Stenneberg, M.S., Busstra, H., Eskes, M., van Trijffel, E., Cattrysse, E., Scholten-Peeters, G.G. and de Bie, R.A., 2018. Concurrent validity and interrater reliability of a new smartphone application to assess 3D active cervical range of motion in patients with neck pain. *Musculoskeletal Science and Practice*, 34, pp.59-65.
- Stokdijk, M., Nagels, J. and Rozing, P.M., 2000. The glenohumeral joint rotation centre in vivo. *Journal of Biomechanics*, 33(12), pp.1629-1636.
- Terwee, C.B., de Winter, A.F., Scholten, R.J., Jans, M.P., Devillé, W., van Schaardenburg, D. and Bouter, L.M., 2005. Interobserver reproducibility of the visual estimation of range of motion of the shoulder. *Archives of physical medicine and rehabilitation*, 86(7), pp.1356-1361.
- Uswatte, G., Foo, W.L., Olmstead, H., Lopez, K., Holand, A. and Simms, L.B., 2005. Ambulatory monitoring of arm movement using accelerometry: an objective measure of upper-extremity rehabilitation in persons with chronic stroke. *Archives of physical medicine and rehabilitation*, 86(7), pp.1498-1501.
- Vaish, P., Bharath, R. and Rajalakshmi, P., 2017, July. Smartphone based automatic organ validation in ultrasound video. In *Engineering in Medicine and Biology Society (EMBC), 2017 39th Annual International Conference of the IEEE* (pp. 4289-4292). IEEE.
- Van Andel, C.J., Wolterbeek, N., Doorenbosch, C.A., Veeger, D.H. and Harlaar, J., 2008. Complete 3D kinematics of upper extremity functional tasks. *Gait & posture*, 27(1), pp.120-127.
- Van den Noort, J.C., Wiertsema, S.H., Hekman, K.M., Schönhuth, C.P., Dekker, J. and Harlaar, J., 2014. Reliability and precision of 3D wireless measurement of scapular kinematics. *Medical & biological engineering & computing*, 52(11), pp.921-931.
- Van Herp, G., Rowe, P., Salter, P. and Paul, J.P., 2000. Three-dimensional lumbar spinal kinematics: a study of range of movement in 100 healthy subjects aged 20 to 60+ years. *Rheumatology*, 39(12), pp.1337-1340.
- Veeger, H.E.J., 2000. The position of the rotation center of the glenohumeral joint. *Journal of biomechanics*, 33(12), pp.1711-1715.
- Veltink, P.H., Bussmann, H.J., De Vries, W., Martens, W.J. and Van Lummel, R.C., 1996. Detection of static and dynamic activities using uniaxial accelerometers. *IEEE Transactions on Rehabilitation Engineering*, 4(4), pp.375-385.

- Wagner, H., Pfusterschmied, J., Tilp, M., Landlinger, J., Von Duvillard, S.P. and Müller, E., 2014. Upper-body kinematics in team-handball throw, tennis serve, and volleyball spike. *Scandinavian journal of medicine & science in sports*, 24(2), pp.345-354.
- Wang, X., Maurin, M., Mazet, F., Maia, N.D.C., Voinot, K., Verriest, J.P. and Fayet, M., 1998. Three-dimensional modelling of the motion range of axial rotation of the upper arm. *Journal of biomechanics*, 31(10), pp.899-908.
- Wang, A., Chen, G., Yang, J., Zhao, S. and Chang, C.Y., 2016. A comparative study on human activity recognition using inertial sensors in a smartphone. *IEEE Sensors Journal*, 16(11), pp.4566-4578.
- Wei, S.H., McQuade, K.J. and Smidt, G.L., 1993. Three-dimensional joint range of motion measurements from skeletal coordinate data. *Journal of Orthopaedic & Sports Physical Therapy*, 18(6), pp.687-691.
- Werner, B.C., Holzgrefe, R.E., Griffin, J.W., Lyons, M.L., Cosgrove, C.T., Hart, J.M. and Brockmeier, S.F., 2014. Validation of an innovative method of shoulder range-of-motion measurement using a smartphone clinometer application. *Journal of shoulder and elbow surgery*, 23(11), pp.e275-e282.
- Welch, G. and Foxlin, E., 2002. Motion tracking: No silver bullet, but a respectable arsenal. *IEEE Computer graphics and Applications*, 22(6), pp.24-38.
- Williams, J.G. and Callaghan, M., 1990. Comparison of visual estimation and goniometry in determination of a shoulder joint angle. *Physiotherapy*, 76(10), pp.655-657.
- Wong, C., Zhang, Z.Q., Lo, B. and Yang, G.Z., 2015. Wearable sensing for solid biomechanics: A review. *IEEE Sensors Journal*, 15(5), pp.2747-2760.
- Wong WY, Wong MS, Lo KH. Clinical application of sensors for human posture and movement analysis: a review. *Prosthet Orthot Int* 2007;31:62–75.
- Woltring, H.J., 1991. Representation and calculation of 3-D joint movement. *Human Movement Science*, 10(5), pp.603-616.
- Woltring, H.J., 1994. 3-D attitude representation of human joints: a standardization proposal. *Journal of Biomechanics*, 27(12), pp.1399-1414.
- Wu, G., Van der Helm, F.C., Veeger, H.D., Makhsous, M., Van Roy, P., Anglin, C., Nagels, J., Karduna, A.R., McQuade, K., Wang, X. and Werner, F.W., 2005. ISB recommendation on definitions of joint coordinate systems of various joints for the reporting of human joint motion—Part II: shoulder, elbow, wrist and hand. *Journal of biomechanics*, 38(5), pp.981-992.

Zhou, H., Hu, H. and Tao, Y., 2006. Inertial measurements of upper limb motion. *Medical and Biological Engineering and Computing*, 44(6), pp.479-487.

Zhou, H. and Hu, H., 2007. Inertial sensors for motion detection of human upper limbs. *Sensor Review*, 27(2), pp.151-158.

Zheng, H., Black, N. D., & Harris, N. D. (2005). Position-sensing technologies for movement analysis in stroke rehabilitation. *Medical & Biological Engineering & Computing*, 43(4), 413–20.

Appendix 1

Android Application Code (C#)

```
using System; using
Android.App; using
Android.Content; using
Android.Runtime; using
Android.Views; using
Android.Widget; using
Android.OS; using
Android.Util;
using Android.Support.V4.Content; using
Android.Hardware;
using Android.Support.Wearable.Views;
using Android.Support.V4.App; using
Android.Support.V4.View;
using Java.IO; using Java.Util; using
Android.Content.PM; using
Android.Views.Animations; using
System.Numerics; using
System.Timers; using
Android.Gms.Common.Apis; using
Android.Gms.Wearable; using
System.Linq; using Android; using
Android.Graphics;

namespace ROM
{
    [Activity(Label = "ROM", MainLauncher = true, Icon = "@drawable/icon")] public
    class MainActivity : Activity, ISensorEventListener {

        static readonly object _syncLock = new object(); private static
        object newobject()
        { throw new NotImplementedException(); }

        public StreamStatus streaming = StreamStatus.DISABLED;
        private SensorManager _sensorManager; private Sensor
        mSensor;

        private float qx;
        private float qy;
        private float qz;
        private float q0;
        private float qw;
        const string _syncPath = "/ROM/Data";
```

```
protected override void OnCreate(Bundle bundle)
{
    base.OnCreate(bundle);

    this.Window.SetFlags(WindowManagerFlags.KeepScreenOn,
    WindowManagerFlags.KeepScreenOn);

    SetContentView(Resource.Layout.MainWear); AttachHandlers();

    _sensorManager =
    (SensorManager)GetSystemService(Context.SensorService); mSensor =
    _sensorManager.GetDefaultSensor(SensorType.RotationVector);

    _sensorManager.RegisterListener(this, mSensor,
    SensorDelay.Fastest);
}

protected override void OnResume()
{
    base.OnResume();
    _sensorManager.RegisterListener(this, mSensor,
    SensorDelay.Fastest);
}

protected override void OnPause()
{
    base.OnPause();
    _sensorManager.UnregisterListener(this);
}

public void OnAccuracyChanged(Sensor sensor, SensorStatus accuracy) {
}

private string DIRECTORY = Android.OS.Environment.DirectoryPictures; public
File dir;
```

```

public File file;
    public System.IO.StreamWriter streamWriter;

    public void StartRecording()
    { dir = getAlbumStorageDir("/ROM");

        Int32 unixTimestamp = (Int32)(DateTime.UtcNow.Subtract(new
DateTime(1970, 1, 1))).TotalSeconds; file = new File(dir, "Arm_" +
        unixTimestamp.ToString() + ".csv"); streamWriter = new
        System.IO.StreamWriter(file.AbsolutePath);
    }

    public void StopRecording() {

        streamWriter.Flush();
        streamWriter.Close();
    }

    public void RecordLine(string msg)
    {
        streamWriter.WriteLine(msg);
    } public void OnSensorChanged(SensorEvent evt) {

        lock (_syncLock)
        {

            if (streaming == StreamStatus.ENABLED) {

                Quaternion q = new Quaternion(); qx
                = evt.Values[0]; qy = evt.Values[1];
                qz = evt.Values[2];

                qw = (float)(Math.Sqrt(1 - (qx * qx + qy * qy + qz * q0
qz)));
                = (float)(-2.0 * Math.Asin(Math.Sqrt(evt.Values[0] *
evt.Values[0] + evt.Values[1] * evt.Values[1] + evt.Values[2] * evt.Values[2]));

                DateTimeOffset dto = new DateTimeOffset(1970, 1, 1, 0, 0,
0, TimeSpan.Zero);
                Int64 unixTimestamp = (Int64)(DateTime.UtcNow.Subtract(new
DateTime(1970, 1, 1))).TotalMilliseconds; string line = String.Format(@"{0:s}", {1:s},
                {2:s},
                {3:s}, {4:s}, {5:s}, {6:s}", unixTimestamp.ToString(),
                evt.Timestamp.ToString(), qx.ToString(), qy.ToString(), qz.ToString(), qw.ToString(),
                q0.ToString());
                RecordLine(line);
            }
        }
    }
}

```

```
    }  
}  
  
public void AttachHandlers()  
{  
    Spinner placementSelect =  
FindViewById<Spinner>(Resource.Id.spinner1);  
  
    ToggleButton On = FindViewById<ToggleButton>(Resource.Id.Onbtn);  
  
    On.Click += delegate  
    {  
        toggleStreamStatus();  
    };  
}  
  
public void updateStatus(string msg) {  
  
    TextView status = FindViewById<TextView>(Resource.Id.status); status.Text  
    = msg;  
}  
  
public void toggleStreamStatus()  
{  
    Spinner placementSelect =  
FindViewById<Spinner>(Resource.Id.spinner1);  
    ToggleButton On = FindViewById<ToggleButton>(Resource.Id.Onbtn);  
  
    if (streaming == StreamStatus.DISABLED)  
    {  
        setStreamStatus(StreamStatus.ENABLED); placementSelect.Enabled =  
false; On.SetBackgroundColor(Color.Blue);  
  
        StartRecording();  
  
        {  
            setStreamStatus(StreamStatus.DISABLED); placementSelect.Enabled  
            = true; On.SetBackgroundColor(Color.Gray);  
  
            StopRecording();  
        }  
    }  
}  
  
private void setStreamStatus(StreamStatus status)  
{ streaming = status;  
  
}
```

```
        public File getAlbumStorageDir(String albumName)
        {
            string directory =
System.IO.Path.Combine(Android.OS.Environment.ExternalStorageDirectory.AbsolutePath,
Android.OS.Environment.DirectoryPictures);
            File file = new
File(Android.OS.Environment.ExternalStorageDirectory, albumName);

            file.SetReadable(true);

            if (!file.Mkdirs())
            {
                Log.Error("ROM", "Directory not created");
            }
            return file;
        }
    }
    public enum StreamStatus
    {
        ENABLED,
        DISABLED
    }
}
}
```

Appendix 2



DEPARTMENT OF BIOMEDICAL ENGINEERING

Consent Form for Participants

Name of department: Biomedical Engineering

Title of the study: A validity study of a smartphone system and a wearable sensor system for the assessment of shoulder range of motion

- I confirm that I have read and understood the information sheet for the above project and the researcher has answered any queries to my satisfaction.
- I understand that my participation is voluntary and that I am free to withdraw from the project at any time, up to the point of completion, without having to give a reason and without any consequences.
- I understand that anonymised data (i.e. data which do not identify me personally) cannot be withdrawn once they have been included in the study.
- I understand that any information recorded in the investigation will remain confidential and no information that identifies me will be made publicly available.
- I understand that participating or not participating in this study will in no way influence my standing or relationship within the University
- I am not wearing a pacemaker, an implanted defibrillator-cardioverter, a cochlear implant, a neurostimulator, or another device for which I should not hold mobile phones close to my body
- I consent to having markers placed on body and strapping applied
- I am aware that this study involves mild/ moderate levels of activity/ exercise.
- I have no known allergic reaction to either sticking plasters/ strapping.
- I consent to being a participant in the project.

(PRINT NAME)

Signature of Participant:	Date:
---------------------------	-------

The place of useful learning

The University of Strathclyde is a charitable body, registered in Scotland, number SC015263

REF UK TOP 20 RESEARCH-INTENSIVE UNIVERSITY

THE UK UNIVERSITY OF THE YEAR WINNER

THE UK ENTREPRENEURIAL UNIVERSITY OF THE YEAR WINNER

Appendix 3

Oxford Shoulder Score Questionnaire

Shoulder Surgery Questionnaire – Before / after your operation

PROBLEMS WITH YOUR SHOULDER

Tick (✓) one box for every question.

1. During the past 4 weeks...

How would you describe the **worst** pain you had from your shoulder?

None	Mild	Moderate	Severe	Unbearable
<input type="checkbox"/>				

2. During the past 4 weeks...

Have you had any trouble dressing yourself because of your shoulder?

No trouble at all	A little bit of trouble	Moderate trouble	Extreme difficulty	Impossible to do
<input type="checkbox"/>				

3. During the past 4 weeks...

Have you had any trouble getting in and out of a car or using public transport because of your shoulder?

No trouble at all	A little bit of trouble	Moderate trouble	Extreme difficulty	Impossible to do
<input type="checkbox"/>				

4. During the past 4 weeks...

Have you been able to use a knife and fork - at the same time?

Yes, easily	With little difficulty	With moderate difficulty	With extreme difficulty	No, impossible
<input type="checkbox"/>				

5. During the past 4 weeks...

Could you do the household shopping on your own?

Yes, easily	With little difficulty	With moderate difficulty	With extreme difficulty	No, impossible
<input type="checkbox"/>				

6. During the past 4 weeks...

Could you carry a tray containing a plate of food across a room?

Yes, easily	With little difficulty	With moderate difficulty	With extreme difficulty	No, impossible
<input type="checkbox"/>				

7. During the past 4 weeks...Could you brush/comb your hair with the affected arm?Yes,
easilyWith little
difficultyWith
moderate
difficultyWith extreme
difficultyNo,
impossible**8. During the past 4 weeks...**How would you describe the pain you usually had from your shoulder?

None

Very mild

Mild

Moderate

Severe

9. During the past 4 weeks...Could you hang your clothes up in a wardrobe, using the affected arm?Yes,
easilyWith little
difficultyWith
moderate
difficultyWith great
difficultyNo,
impossible**10. During the past 4 weeks...**

Have you been able to wash and dry yourself under both arms?

Yes,
easilyWith little
difficultyWith
moderate
difficultyWith extreme
difficultyNo,
impossible**11. During the past 4 weeks...**How much has pain from your shoulder interfered with your usual work (including housework)?

Not at all

A little bit

Moderately

Greatly

Totally

12. During the past 4 weeks...Have you been troubled by pain from your shoulder in bed at night?No
nightsOnly 1 or 2
nightsSome
nightsMost
nightsEvery
night

**Finally, please check back that you have answered each question.
Thank you very much.**

Appendix 4

MATLAB Code for Goniometer application data processing

To obtain plane and elevation :

```
clear all

OQUAT = xlsread('OQUAT');
MOVEQUAT = xlsread('MOVEQUAT');
UV(1,:) = [0 0 1 0];
n = size(MOVEQUAT,1);
for i = 1:n

    InvOQUAT(1,:) = [OQUAT(1,1), (OQUAT(1,2)*-1), (OQUAT(1,3)*-1),
(OQUAT(1,4)*-1)];

    TESTQUAT(i,1) = (InvOQUAT(1,1) .* MOVEQUAT(i,1)) -
(InvOQUAT(1,2) .* MOVEQUAT(i,2)) - (InvOQUAT(1,3) .*
MOVEQUAT(i,3)) - (InvOQUAT(1,4) .* MOVEQUAT(i,4));
    TESTQUAT(i,2) = (InvOQUAT(1,2) .* MOVEQUAT(i,1)) +
(InvOQUAT(1,1) .* MOVEQUAT(i,2)) + (InvOQUAT(1,4) .*
MOVEQUAT(i,3)) - (InvOQUAT(1,3) .* MOVEQUAT(i,4));
    TESTQUAT(i,3) = (InvOQUAT(1,3) .* MOVEQUAT(i,1)) -
(InvOQUAT(1,4) .* MOVEQUAT(i,2)) + (InvOQUAT(1,1) .*
MOVEQUAT(i,3)) + (InvOQUAT(1,2) .* MOVEQUAT(i,4));
    TESTQUAT(i,4) = (InvOQUAT(1,4) .* MOVEQUAT(i,1)) +
(InvOQUAT(1,3) .* MOVEQUAT(i,2)) - (InvOQUAT(1,2) .*
MOVEQUAT(i,3)) + (InvOQUAT(1,1) .* MOVEQUAT(i,4));

    InvTESTQUAT(i,:) = [TESTQUAT(i,1), (TESTQUAT(i,2)*-1),
(TESTQUAT(i,3)*-1), (TESTQUAT(i,4)*-1)];

    RESQUAT1(i,1) = (UV(1,1) .* TESTQUAT(i,1)) - (UV(1,2) .*
TESTQUAT(i,2)) - (UV(1,3) .* TESTQUAT(i,3)) - (UV(1,4) .*
TESTQUAT(i,4));
    RESQUAT1(i,2) = (TESTQUAT(i,2) .* UV(1,1)) + (TESTQUAT(i,1)
.* UV(1,2)) + (TESTQUAT(i,4) .* UV(1,3)) - (TESTQUAT(i,3) .*
UV(1,4));
    RESQUAT1(i,3) = (TESTQUAT(i,3) .* UV(1,1)) - (TESTQUAT(i,4)
.* UV(1,2)) + (TESTQUAT(i,1) .* UV(1,3)) + (TESTQUAT(i,2) .*
UV(1,4));
    RESQUAT1(i,4) = (TESTQUAT(i,4) .* UV(1,1)) + (TESTQUAT(i,3)
.* UV(1,2)) - (TESTQUAT(i,2) .* UV(1,3)) + (TESTQUAT(i,1) .*
UV(1,4));
```

```

RESQUAT2(i,1) = (InvTESTQUAT(i,1) .* RESQUAT1(i,1)) -
(InvTESTQUAT(i,2) .* RESQUAT1(i,2)) - (InvTESTQUAT(i,3) .*
RESQUAT1(i,3)) - (InvTESTQUAT(i,4) .* RESQUAT1(i,4));

RESQUAT2(i,2) = (RESQUAT1(i,2) .* InvTESTQUAT(i,1)) +
(RESQUAT1(i,1) .* InvTESTQUAT(i,2)) + (RESQUAT1(i,4) .*
InvTESTQUAT(i,3)) - (RESQUAT1(i,3) .* InvTESTQUAT(i,4));
RESQUAT2(i,3) = (RESQUAT1(i,3) .* InvTESTQUAT(i,1)) -
(RESQUAT1(i,4) .* InvTESTQUAT(i,2)) + (RESQUAT1(i,1) .*
InvTESTQUAT(i,3)) + (RESQUAT1(i,2) .* InvTESTQUAT(i,4));
RESQUAT2(i,4) = (RESQUAT1(i,4) .* InvTESTQUAT(i,1)) +
(RESQUAT1(i,3) .* InvTESTQUAT(i,2)) - (RESQUAT1(i,2) .*
InvTESTQUAT(i,3)) + (RESQUAT1(i,1) .* InvTESTQUAT(i,4));

XYZYZ(i,:) = [RESQUAT2(i,2), RESQUAT2(i,3), RESQUAT2(i,2),
RESQUAT2(i,4), RESQUAT2(i,3), RESQUAT2(i,4)];

XSq(i,:) = RESQUAT2(i,2)*RESQUAT2(i,2);
YSq(i,:) = RESQUAT2(i,3)*RESQUAT2(i,3);

Azmith(i,:) = (atan2(RESQUAT2(i,4), (sqrt(XSq(i,1) +
YSq(i,1)))));
Altitude(i,:) = (atan2(RESQUAT2(i,3), RESQUAT2(i,2)));

end

```

To obtain axial rotation :

```

clear all

QuatO = xlsread('OQUAT');
QuatM = xlsread('MOVEQUAT');
n = size(QuatM, 1);

for i = 1:n
    InvQO(1,:) = [QuatO(1,1), (QuatO(1,2)*-1), (QuatO(1,3)*-
1), (QuatO(1,4)*-1)];

RelQuat(i,1) = (QuatM(i,1) .* InvQO(1,1)) - (QuatM(i,2) .*
InvQO(1,2)) - (QuatM(i,3) .* InvQO(1,3)) - (QuatM(i,4) .*
InvQO(1,4));
RelQuat(i,2) = (QuatM(i,1) .* InvQO(1,2)) + (QuatM(i,2) .*
InvQO(1,1)) + (QuatM(i,3) .* InvQO(1,4)) - (QuatM(i,4) .*
InvQO(1,3));

```

```

RelQuat(i,3) = (QuatM(i,1) .* InvQO(1,3)) - (QuatM(i,2) .*
InvQO(1,4)) + (QuatM(i,3) .* InvQO(1,1)) + (QuatM(i,4) .*
InvQO(1,2));

RelQuat(i,4) = (QuatM(i,1) .* InvQO(1,4)) + (QuatM(i,2) .*
InvQO(1,3)) - (QuatM(i,3) .* InvQO(1,2)) + (QuatM(i,4) .*
InvQO(1,1));

RA(i,1) = 1-(2*((RelQuat(i,3).^2)-(2*((RelQuat(i,2)).^2)))));
RA(i,2) =
(2*(RelQuat(i,1)).*(RelQuat(i,2)))+(2*(RelQuat(i,3)).*(RelQuat(i,
4)));
RA(i,3) = (2*(RelQuat(i,1)).*(RelQuat(i,3)))-
(2*(RelQuat(i,2)).*(RelQuat(i,4)));
RA(i,4) = (2*(RelQuat(i,1)).*(RelQuat(i,2)))-
(2*(RelQuat(i,3)).*(RelQuat(i,4)));
RA(i,5) = (1-(2*((RelQuat(i,1)).^2)-(2*((RelQuat(i,3)).^2)))));
RA(i,6) =
(2*(RelQuat(i,2)).*(RelQuat(i,3)))+(2*(RelQuat(i,1)).*(RelQuat(i,
4)));
RA(i,7) =
(2*(RelQuat(i,1)).*(RelQuat(i,3)))+(2*(RelQuat(i,2)).*(RelQuat(i,
4)));
RA(i,8) = (2*(RelQuat(i,2)).*(RelQuat(i,3)))-
(2*(RelQuat(i,1)).*(RelQuat(i,4)));
RA(i,9) = 1-(2*((RelQuat(i,1)).^2)-(2*((RelQuat(i,2)).^2)));

RA(i,:) = [RA(i,1),RA(i,2),RA(i,3),RA(i,4),RA(i,5),RA(i,
6),RA(i,7),RA(i,8),RA(i,9)];
RAc{i,:} = [RA(i,1:3); RA(i,4:6); RA(i,7:9)];

[a{i},b{i}] =RotMatToCardanicAngles(RAc{i},[2 1 2]); a_new(i,:)
= [a{i}];

Rot(i,1) =rad2deg(a_new(i,3));

Angles(i,:) = [Elev(i), Abd(i),Rot(i)]; end

```